2004-02-13

Effects of Friction Stir Welding on Polymer Microstructure

Seth R. Strand
Brigham Young University - Provo

EFFECTS OF FRICTION STIR WELDING ON POLYMER MICROSTRUCTURE

by

Seth R. Strand

A thesis submitted to the faculty of

Brigham Young University

in partial fulfillment of the requirements for the degree of

Master of Science

Department of Mechanical Engineering

Brigham Young University

April 2004

BRIGHAM YOUNG UNIVERSITY

GRADUATE COMMITTEE APPROVAL

of a thesis submitted by

Seth R. Strand

This thesis has been read by each member of the following graduate committee and by majority vote has been found to be satisfactory.

_____	_____
Date	Carl D. Sorensen, Chair
_____	_____
Date	Tracy W. Nelson
_____	_____
Date	A. Brent Strong

BRIGHAM YOUNG UNIVERSITY

As chair of the candidate's graduate committee, I have read the thesis of Seth R. Strand in its final form and have found that (1) its format, citations, and bibliographical style are consistent and acceptable and fulfill university and department style requirements; (2) its illustrative materials including figures, tables, and charts are in place; and (3) the final manuscript is satisfactory to the graduate committee and is ready for submission to the university library.

_____ _____

Date

Carl. D. Sorensen
Chair, Graduate Committee

Accepted for the Department

_____

Brent L. Adams
Graduate Coordinator

Accepted for the College

_____

Douglas M. Chabries
Dean, College of Engineering and Technology

ABSTRACT

EFFECTS OF FRICTION STIR WELDING ON POLYMER MICROSTRUCTURE

Seth R. Strand

Department of Mechanical Engineering

Master of Science

This work establishes the relationships between several key Friction Stir Welding process parameters and the resulting microstructural and flexural properties of the welded joint. A series of four single parameter experiments were run. The parameters investigated were pin diameter, feedrate, shoe temperature, and pressure time. Butt welds were made in 6 mm thick stress-relieved extruded polypropylene sheet. Three-point bend tests were used to determine the ultimate flexural strength and coincident strain. The maximum bend angle before failure was used to label the welds as "good or bad." An optical microscope capable of cross polarization was used to examine and photograph the weld microstructure. Welds were evaluated according to 1) DVS bend angle, 2) flexural properties, and 3) weld microstructure.

All welds made surpassed the DVS requirements for classification as a "good weld" established for hot-gas, extrusion, and laser welding processes. Most welds met the bend angle requirement for hot-plate welds.

Welds created for this work maintained 80-92% of base material flexural strength. In the majority of the welds, the strength was between 85 and 90% of base material. The

FSW joints showed a flexural strength of 10500 psi, compared to a base material strength of 12400 psi.

Four microstructural zones were found to exist in the FSW joints. These were: 1) advancing interface, 2) retreating interface, 3) bottom disturbance, and 4) central zone. Several common microstructure types and defects were found to exist in the welds. These were: 1) spherulites, 2) voids, 3) root defects, 4) flow lines, and 5) onion skin.

A distinct correlation was observed between weld microstructure and flexural properties. Those welds whose microstructure most nearly resembled the base material demonstrated the best flexural properties. This can be accomplished by operating with a low feedrate, a high shoe temperature, and a large pin.

ACKNOWLEDGMENTS

This work would not have been possible without the assistance of many individuals. I am grateful for the support of my dear wife– she never wavered in her faith that I could finish this research. I thank the members of my committee for their assistance in developing the technologies necessary for this work, and for their patient help in preparing this manuscript. I wish to thank Dr. Erik Christiansen for loaning me his microscope and Spencer for teaching me to use it effectively. I am also indebted to Mike Standing for his help in developing the sectioning technique used.

TABLE OF CONTENTS

List of Tables

List of Figures

Glossary of Terms

Shoe	Rectangular block having holes for the heater and pin, it holds the weld under pressure during initial cooling.
Pin	Rotating body which is plunged into the joint, stirs the material, and produces high frictional forces to soften the material for welding.
Anvil	Metal plate used to hold the workpieces during welding.
Pressure time	The length of time during which the shoe applies forging pressure to the weld as it cools.
Advancing	The side of the weld where the rotation of the pin coincides with the feed direction of the pin.
Retreating	The side of the weld where the rotation of the pin opposes the feed direction of the pin.
Spherulite	The basic microstructural organization of polypropylene. Spherulites appear as small spheroids, having both crystalline (light) and amorphous (dark) areas.
Weld Zone	Region within the weld where the local microstructure is the same.
Bottom Disturbance	Region of the weld extending upward from the bottom of the joined material. It is identified by a difference in flow line morphology and density from the surrounding weld.
Interface	Region of the weld extending laterally from the base material into the weld. It is identified by a difference in material morphology from the central region of the weld.

Central Zone	Region of the weld bounded on the sides by the advancing/ retreating interfaces, on the bottom by the bottom disturbance, by the top of the joined material.
Root defect	An unwelded region of the joint extending upward from the bottom of the material.
Flow Line	An area of alternating light and dark bands. These bands appear to show the pattern of material flow, be it laminar or turbulent.
Flow line severity	A measure of the flow line pattern, considering the density of flow lines (the number of lines crossing a 1mm line), the area covered by flow lines, the contrast between light and dark flow lines, and the ease of visibly detecting the presence of flow lines.
Onion ring	A special case of flow lines, wherein the flow lines have closed on themselves to form a ring or loop of concentric flow lines, usually centered about the center-point of the weld.
Onion ring severity	A measure of the onion ring pattern, analogous to flow line severity.

CHAPTER 1
Introduction

1.1 Introduction to Friction Stir Welding

Friction Stir Welding is a new process for joining polymeric materials. Since 1998, major research assessing the feasibility of the process has been ongoing at Brigham Young University. Several polymers have been successfully welded, retaining over 90% of base material tensile strength. However, very little has been known regarding the effect of the process on the polymer microstructure. This research was carried out with the primary goal of setting forth the relationships between several key operational parameters, the resulting weld microstructure, and flexural properties of the welded joint.

Friction Stir Welding (FSW) is a relatively new joining process, being first demonstrated successfully on aluminum alloys in 1991 at The Welding Institute (TWI) in England. Quickly becoming widely accepted in the metals manufacturing realm, extensive research has been performed on tool designs, joint geometries, process parameters, and weldable materials.

Meanwhile, the process is still in its infancy among polymer processors. Relatively little is known about the process when applied to polymers, including the effects of FSW on the material microstructure. Very few groups have reported research on FSW of polymeric materials. Of the thousands of polymers in existence, a mere half dozen have been investigated for compatibility with FSW technology. An entire manufacturing method is waiting to be developed.

FSW utilizes the friction between a rotating tool and the workpiece to generate the necessary heat for fusion of the joint. The tool consists of a rotating pin, a large shoulder, and a heater. The pin is primarily responsible for the frictional heating of the workpiece and stirring of material within the joint. The shoulder's main purposes are to trap the

material displaced by the pin and to apply forging pressure to the joint as the weld cools. The heater supplies additional thermal energy when the frictional heating is not sufficient

The tool shoulder used to contain the displaced material and to hold pressure on the weld while it cools is much larger than that used for FSW of metals and is called a "shoe." As the polymer cools, it is very important to promote a uniform cooling rate throughout the weld volume. If the outer material cools much quicker than the inner, a hard shell is formed. As the inner layers then cool, the material contracts and pulls away from the shell. Large voids are formed which detract greatly from the mechanical performance of the welded joint. Increasing the shoe length allows pressure to be maintained for a longer time as the weld cools. Because more cooling and solidification of the weld occur under pressure, material shrinkage is more uniform, and void formation is reduced.

The shoe is stationary relative to the pin, whereas in FSW of metals the shoulder rotates with the pin. It has been found that rather than holding the displaced material within the weld as with metals, a rotating shoulder pushes the polymer out of the weld volume. This reduction in material is responsible for very poor weld formation and performance. By holding the shoe stationary relative to the pin, the displaced material is effectively trapped. The non-rotating shoe also acts to smooth the weld surface.

FSW is performed in a few simple steps. First, the spinning pin is plunged into the joint between the pieces to be welded and allowed to heat up. As the tool rotates there is very high friction, evidenced by a release of thermal energy. The process is made more efficient when the majority of the energy goes into the workpieces rather than the tool.

The tool then advances along the joint, removing material from in front of the tool and depositing it behind the trailing edge of the tool. FSW of polymers is not strictly a solid state process. Because polymers consist of molecules of different lengths, and thus of different molecular weights, the materials do not have single melting points, but melting ranges. During FSW processing, some shorter chains reach their melting point while longer chains do not. Thus bits of solid material are suspended in enough molten material to render the mixture easy to move and form.

As the tool moves along the joint, the shoe maintains pressure on the weld as it cools. Once the pin reaches the end of the weld, the pin is stopped and the weld is allowed to cool somewhat before the pin is retracted and the shoe raised.

1.2 Industrialization of FSW

In order for FSW of polymers to become viable on an industrial scale, several key technologies need to be improved. Tooling durability and longevity must be improved, a larger pool of joinable materials needs to be created, and weld properties need to be proven. However, before any of these areas can be fully understood and developed, a fundamental knowledge of the process and its effect on the material must be gained.

An enormous effort is needed to understand the effects of FSW processes on the structure and properties of polymers. Both on a micro- and macro-structural basis, there is no knowledge of what happens to the material during and after the welding process. Without such knowledge, critical process and product design issues cannot be addressed. Many applications are therefore rendered impossible. With an understanding of the structural effects of the process on the material, standard weld procedures and post treatments can be developed. This thesis is intended to address the fundamental issue of what effect FSW processing has on the structure of the polymer. The basic theory of this research is that the weld whose microstructure most closely resembles that of the base material will have the best properties and performance.

1.3 Thesis Statement

There exists some relationship between the microstructure of the polymer within the weld zone and the mechanical properties and performance of the welded joint. This relationship is affected by key processing parameters including the pin diameter, pin rpm, feedrate, and the length of cooling time under pressure. The purposes of this work are to establish the effects of the FSW process on the structure of polypropylene, and put forth the relationship between weld properties and characteristic microstructure.

This research answers several underlying questions. These include:

1. What is the typical microstructure of a FSW weld in PP?
2. Is there a relationship between process parameters and the weld microstructure? If so, what is that relationship?
3. Does the weld microstructure affect the flexural properties of the weld?
4. Does the weld with the highest performance most resemble the base material structure?

1.4 Delimitations

This work is very concentrated in scope. Only one resin is investigated– polypropylene. This is further limited to 6 mm thick stress-relieved extruded sheet. Pin diameter is changed as a factor in the experiment, but other aspects of pin geometry (material, thread style and pitch, taper, etc.) Are not considered. Material thickness is not considered, nor is any aging response of the resin. Aging is herein defined so as to include heat treatments, annealing, natural aging, etc. Because of their importance to most PP applications, only flexural properties are analyzed, disregarding all others (tensile, impact, chemical, thermal, etc.).

1.5 Document Organization

This thesis is designed for dual functionality. Herein are contained both a detailed presentation of the research carried out and a shorter paper intended for publication. The detailed presentation will satisfy the requirements for a Masters thesis submitted to the Mechanical Engineering Department of Brigham Young University (BYU). The publishable paper (to be published in a peer reviewed journal) will give others ready access to the knowledge gained through this research. This thesis has the following organization:

Chapter 1 is an introduction to this document, containing a brief discussion of the purpose and organization of this thesis. The friction stir welding (FSW) process is introduced. A brief history of the process and a discussion of how the process works is given. The differences between FSW of metals and polymers are discussed.

Chapter 2 contains an in-depth review of published literature concerning FSW of polymeric materials. Also included is an overview of other common polymer joining processes, serving as a basis for comparison. Other literature dealing with analytical methods of polymer welds is also reviewed.

Chapter 3 gives information about the experimental procedure employed in this research. The experimental design, method, and analysis are discussed. Procedures for welding, specimen preparation, and testing are explained.

Chapter 4 is the stand-alone portion of this thesis. It contains a brief version of the literature review, experimental procedures, and a discussion of the experimental results. The conclusions for the current work are presented here. This chapter will be submitted for peer reviewed publication.

Chapter 5 presents recommendations for future work, along with brief discussions of important technological issues.

Several Appendices contain detailed records of tool geometries, mechanical testing results, and statistical analyses too lengthy to be included in the body. Also found in the appendices is a full collection of weld micrographs.

CHAPTER 2
Literature Review

2.1 Introduction

As very little formal research has been performed on friction stir welding of polymers, it is important to establish the state of the art. A careful search revealed that the few published reports on the subject focus only on the successful joining of polymers with the process. Essentially no work has been reported regarding the mechanics of the process or the effects of the process on the microstructure of the polymer itself.

This literature review provides background information vital to each step of the research. Section 2.2 contains a review of the common practices of joining polymers. Their methods, advantages, and disadvantages are discussed. In section 2.3 a description and discussion of the friction stir welding process (both of metals and polymers) is found. Readers will be familiarized with the process; its terminology, history, and anticipated comparison with the common practices discussed previously. A comparison of several common processes and FSW for a specific part is found in section 2.4. An outline of the testing of mechanical properties of the welds is found in section 2.5. The three-point bend test is described in some detail. Information regarding the governing standard for the test is given. Previous research on the microstructure of thermoplastic welds is reviewed in section 2.6.

2.2 Joining of Polymers

In developing FSW as a viable joining process for polymeric materials, it is important to compare it against existing processes. Several processes have come to dominate the field of joining polymeric parts. A brief review of the most common processes and their strengths and weaknesses follows.

Processes of securing polymer parts fall into two major categories- mechanical fastening and joining. Joining can be separated into bonding and welding. These in turn can be subdivided into solvents or adhesives and thermal or friction welding. The relationships and examples of processes are shown graphically in Figure 1. Before discussing individual processes, it is important to establish some key working definitions.

Fastening refers to the use of a foreign body to mechanically connect distinct parts. Mechanical fastening techniques make use of external fasteners to hold the pieces together. Screws, rivets, staples, bolts, clamps, brackets, and snap-fits are typical examples of mechanical fasteners. **Joining** secures the parts without foreign bodies. Glues, welding techniques, and solvents are common examples of joining processes. **Bonding** uses chemical reactions to create a permanent joint. Examples of bonding include one- or two-part adhesives and solvents. **Welding** fuses the two parts together by non-chemical means. This requires the melting of a small volume of the part at the joint. Hot gases, hot tools, ultrasonic vibrations, friction, and lasers are commonly used to cause the joints to fuse.

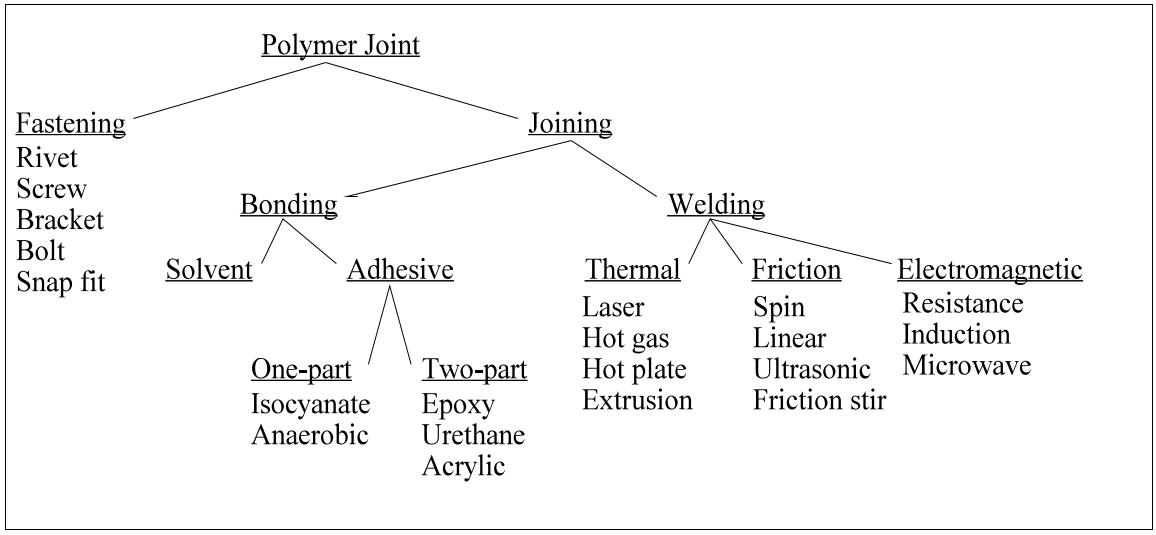

Figure1- Classification of polymer joining methods (Altered from Stokes 1989).

Mechanical fastening involves the joining together of assemblies with external parts. Fastened joints can be made to be permanently closed, or re-openable for maintenance purposes. While they are generally simple processes, they require external parts, and often a substantial labor input. Furthermore, considerable stress concentration occurs at and around the fastener locations. Because mechanical joints are generally not high performance, they will not be compared to friction stir welding in this research.

Many forms of welding have been developed, each with unique advantages. Welded joints can be made of a variety of materials, geometries, and sizes. Dissimilar materials can be joined if they are compatible. However, the mechanics of the welding process, along with its affects on the material structure are still greatly unknown.

All polymer welding techniques progress through three common stages. The first stage involves the formation of a melt on the surfaces to be joined. This melt does not need to be large in volume but must exist in order for the polymer chains to fuse across the joint. In the second stage, the parts are brought together under pressure. Exerting pressure on the melted volume helps ensure thorough mixing of the material across the joint line. During the third and final stage, the melt is allowed to cool. Pressure should be maintained in order to prevent voids from forming within the weld.

Following are discussions of the most common polymer joining techniques. For the welding techniques, brief process descriptions are given in terms of how the three stages of welding are approached. In the case of adhesive bonding, descriptions of how the joint is formed are given. The major advantages and limitations of each process are discussed.

2.2.1 Adhesives

Adhesive research has reached a state of maturity as a science. Bonding techniques have been developed to provide high quality, high perfomance joints in polymeric parts. The mechanics of the process have been studied in depth, and are well understood (Stokes 1989). Today's adhesives allow the joining of nearly any polymer. The properties of the adhesive joint can also be tailored to the application.

Adhesives can be broadly classified as one- or two-part systems. One-part adhesives require no mixing or stirring prior to use. Cyanoacrylates are common examples of one-part polymer adhesives. Bonding by means of one-part adhesives is simple. The adhesive is applied to one side of the joint. The parts are brought into contact, then held under pressure as the adhesive cures. Cure times for anaerobic adhesives range from seconds to hours at room temperature.

Two-part adhesives rely on a chemical reaction between their components to cure. Generally, the two parts must be mixed according to precise recipes prior to use. The strongest joints are usually achieved by applying the adhesive to both parts to be joined. After allowing the adhesive to cure slightly, the parts are brought together and held under pressure while the adhesive continues to cure. Epoxies are the most common in this class of adhesives that includes acrylics, urethanes, and others. Cure times are generally long (measured in hours) for high performance epoxies. Others can achieve a strong bond within minutes. The cure rate for epoxies can normally be increased with heat.

Adhesives have some very strong advantages over other joining processes. It is possible to bond nearly any polymer with the correct adhesive and surface preparation. Whereas many processes are only suitable for thermoplastic materials, adhesives work equally well with thermoset materials. Because of this, they are frequently the only choice of joining process. They are simple to use, even more so with the one-part systems. Cure times can be very short. Often multiple systems will be capable of creating a joint; hence the properties can be adjusted through adhesive selection. Little operator training is necessary, and joint strength can be very repeatable (Stokes 1989).

There are however, serious disadvantages to using adhesives. Many of them release toxic fumes during use and cure, requiring the use of protective apparatus. Surface preparation including a degreasing step is critical to achieving a good bond. Because of this, the repeatability of joint properties is dependent on worker skill. Another disadvantage of adhesives is the difference in behavior between the cured adhesive and the polymer which can introduce inherent weaknesses.

2.2.2 Solvents

If creating a bonded joint without introducing new material is important, a solvent bond may be the answer. Solvents soften a layer of the polymer around the joint and allow the polymer chains to fuse across the joint line. After acting to "open" the ends of the chains, the solvent evaporates, allowing the polymer chains to diffuse across the joint and bond, leaving a homogeneous joint. Because of the diffusion of polymer chains across the joint, the process is sometimes referred to as solvent welding.

A major advantage of solvent bonds is the intermingling of polymer chains. After the solvent evaporates, there is very little difference between the material within the joint and the base material. This results in a very smooth transition of loads from one side of the joint to the other.

Solvents have two major disadvantages. First and foremost are the environmental issues. Most solvents show very damaging effects on the environment as they evaporate. Serious dangers to personal health exist, and are made worse by frequent exposure. Second, solvents tend to be slow acting. This may be acceptable for one-of-a kind parts, but is not for large-scale production (Stokes 1989). Additionally, no reasonable solvent exists for some of the most common polymers.

2.2.3 Hot-Plate

In hot-tool or hot-plate welding, the surfaces to be joined are melted through forced contact with a heated tool. Once a thin molten layer is developed, the tool is removed and the surfaces brought together under pressure. While the joint fuses and cools, the pressure is maintained. The tool is metallic, and is generally heated internally. Complex geometries can be created, albeit at an increased cost.

Hot-plate welding offers several advantages. In theory, any thermoplastic material can be joined. Because the tool is in contact with the part, extremely high temperatures can be reached. Thermally sensitive materials benefit from the use of modern temperature control systems that reduce the danger of overheating the workpiece. The process lends itself very well to either highly automated or portable systems. Dissimilar

materials can easily be joined, on condition that both can be molten simultaneously without degrading one or the other (Stokes 1989).

There are limitations to hot-plate welding. Cycle times tend to be long; especially as part size increases. For example, a single weld of large pipe can require 30 minutes. The forced contact between part and tool also poses a problem. As the molten film is developed, the material tends to stick to the tool. This can be avoided by coating the tool with PTFE. However, this limits the working temperature range of the tool.

2.2.4 Hot-Gas

This process resembles oxy-fuel welding. A hot gas (air, nitrogen, CO_2, etc.) is directed at the joint. As the material softens, a filler rod is pushed into the joint. Also heated, the filler material fuses with the parent material, and a welded joint is created (Bauer1990). A v-groove joint design is commonly used to make the process more efficient and effective. Neither the substrate nor the filler is completely melted, only substantially softened.

The major advantage of hot-gas welding is its flexibility. Simple portable devices can easily be made. Hence, the process is very well suited for on-site repair work, or for fabrication of large, one-of-a-kind parts (Stokes 1989).

In spite of its simplicity, hot-gas welding is not well suited for large-scale manufacturing, nor where joint performance is critical. It is a very slow and difficult to control process. Over- or under-heating of the joint is common, and devastating to mechanical properties.

2.2.5 Extrusion

Extrusion welding is closely related to hot-gas welding. In this process the filler material is melted and extruded directly into the joint. A heated gas is still used to preheat the substrate material, enabling the fusion of the joint. As it is more readily controlled and more consistent than hot-gas welding, it is often preferred for the automatic welding of large assemblies (Stokes 1989).

2.2.6 Friction

Several variations of friction welding have been developed. All rely on the conversion of frictional energy into thermal energy to melt the joint. The surfaces to be fused rub against one another under controlled pressure. Once the desired amount of melting has occurred, the parts are held together under stationary pressure as the joint fuses and cools. Friction welding techniques have the major advantage of insensitivity to many surface irregularities. As the parts are rubbed against each other, the peaks simply melt away and any valleys are filled in.

Spin welding is used when at least one of the mating pieces has a circular cross-section. The joint must be planar, with no requirement of angular alignment between the two parts (Bauer 1990). This process can be performed on relatively simple machinery, and can form a joint in seconds. Because the angular velocity increases as the radius grows, there is a tendency to overheat and degrade the material in the outer regions of welds made on large diameter, solid parts. To achieve uniform melting, a thin-walled hollow part is best suited for this process.

Linear friction welding rubs the parts together in a linear fashion. Displacements are small, usually between .254 and .508 mm. Parts with flat seams are best suited for this process (Bauer 1990). Complex geometries and low modulus materials (i.e.- elastomers) cannot be joined.

2.2.7 Ultrasonic

By far the most widely used polymer welding process is ultrasonic welding (Stokes 1989). High frequency (20- 50 KHz), low amplitude (.0127- .0635 mm) mechanical vibrations are used to create highly localized welds. There are two major styles of joints welded ultrasonically. Butt joints, wherein the major vibrational energy is perpendicular to the joint, are the most common. In these joints, energy directors are needed to focus the vibrational energy exactly. Energy directors are cone shaped protrusions molded or machined into one side of the joint (see Figure 2). Exposed to the ultrasonic vibrations, these energy directors melt and flow- fusing the joint. The second type, shear joints, use a tight fit between to parts to create frictional energy. Because the

vibrations are mostly parallel to the joint, no energy directors are needed. As the ultrasonic vibrations oscillate the parts, they fuse much like a linear friction weld.

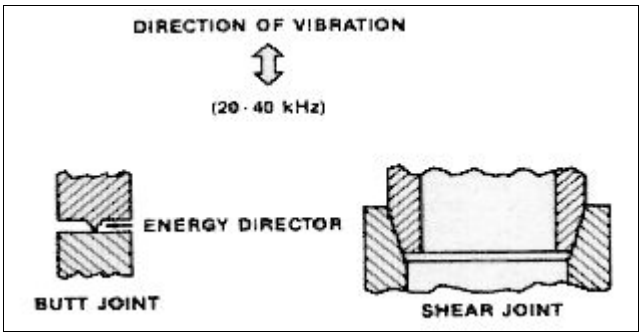

Figure 2- Standard joint types in ultrasonic welding (Stokes 1989).

Ultrasonic welding is further divided into near- and far-field operations. This classification is based simply on the distance from the ultrasonic horn and the actual weld site. The horn is the tip of the welding apparatus that serves to amplify the vibrations and transfer that energy to the workpiece. Near-field welding is generally taken to mean that the horn is less than 0.25" from the weld. Anything more distant than this is considered to be far-field welding. Far field welds are much less efficient, requiring much higher energy inputs because of the damping characteristics of polymeric materials.

Advantages of ultrasonic welding include speed, automation, and compactness of equipment. Typical cycle times for ultrasonic welding operations are between 1 and 2 seconds. The equipment is very compact, and can be portable. The process is highly automatable.

However, part and joint geometries are critical in ultrasonic welding. If the energy cannot be focused, cycle times will increase dramatically, while joint properties suffer. It is also unsuitable as a process for joining large seams, only spot welds are considered feasible with current technology. Furthermore, material choices are slightly limited by the fact that low modulus materials tend to damp the vibrations too quickly, and high quality welds cannot be formed.

2.2.8 Resistance (Implant)

Resistance welding can be used to form high quality welds for any joint geometry. In this process an electrically conductive material is placed at the joint interface and resistively heated. This can be a wire, braid, or other material. The hot wire causes the surrounding material to melt and create a weld when cooled under pressure. Cycle times are short, typically in the 15-25 second range for even the largest parts (Stokes 1989). It is an extremely simple process requiring very little surface preparation.

However, because the wire remains in the weld the joint properties are compromised, and can be difficult to repeat. Leaving the wire behind is costly, hence the process is used mostly when faced with a complex joint in a specialty part. The setup times for resistance welds tend to be very long. The implant wire must be laid along the centerline of the entire weld. If the joint geometry is complex the wire must also be "tacked" into place. Further care must be taken when bringing the workpieces into contact to avoid disturbing or displacing the implant.

2.3 FSW of Polymers

Because friction stir welding of polymers is so new, it is not surprising that little work has been published. Very few groups have reported performing research into the process as applied to polymers. The leading research groups are working at TWI and BYU. An extensive search revealed published results in three areas- tool design, process parameters, and weldable materials.

Noticeably absent from published literature was any study of the structure of the welded material. Nor was there any report of a study of the effect of the process on the structure of the polymer. To this point, all work on FSW of polymers has been to prove it works. Little attention has been given to how it works or what it does to the material.

2.3.1 Tool Design

Only preliminary work has been reported with regard to tooling issues. Johns (Johns 1999) describes several iterative attempts to create a functional FSW tool for polymers. A standard aluminum style tool (integral shoulder and pin) could form a weld,

but with very poor mechanical and visual properties. Rather than holding the material within the weld volume, it dragged it out, resulting in large voids throughout the weld.

A second tool design used a stationary cone mounted to the mill head to apply pressure to the weld and brace the pin against the cyclic loading experienced during the FSW process. This too failed to create high quality welds. The area of the cone was insufficient to apply pressure to the cooling weld, and the cyclic loading of the pin still caused catastrophic failure after a very limited number of welds.

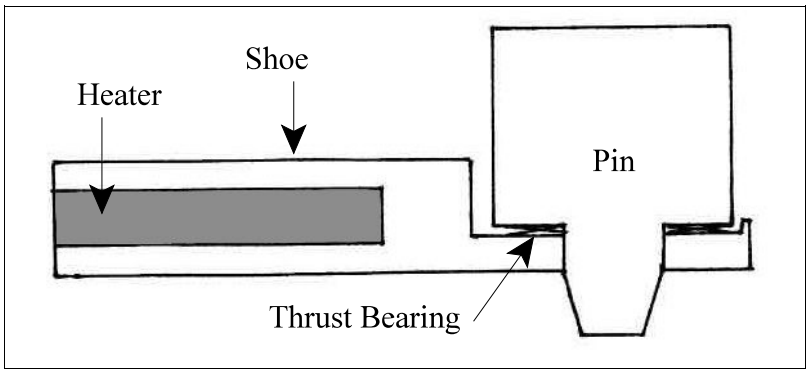

Figure 3- Final iteration of Johns' tool design (Sorensen 2001)

Johns' final tool iteration (Figure 3) proved much more successful, and is the model for the current tooling used at BYU. It consists of a rotating pin, a thrust bearing, and a stationary shoe. The shoe allows pressure to be applied over a large area of the weld as it cools, limiting the formation of voids. It can be heated if additional energy is needed for proper fusion of the joint. Johns concluded that in order to increase tool life, the pin needs to be kept as short as possible. This will minimize the moment acting on the tool, thus helping to overcome the effects of cyclic loading.

TWI has reported nothing of the design of their tooling, save the shape thereof. They have reported the successful welding of polypropylene with "an airfoil shaped reciprocating tool"(ASM International 2000).

2.3.2 Process Parameters

Researchers at BYU are the only group to have reported successful operating parameters. Various parameters including shoe temperature, spindle speed, weld feedrate, tool offset depth (distance from the bottom of the pin to the top of the anvil), and pin geometry were studied. The rotational speed of the tool was found to be very critical, as was the feedrate of the weld. In general, higher spindle speeds (1500- 1800 rpm) resulted in higher tensile strengths. Lower feedrates (10- 25.4 cpm) were found to yield superior properties (Nelson 2000).

2.3.3 Materials

To date, a mere half-dozen of the thousands of available polymers have been investigated for compatibility with FSW. Polymers investigated include various grades of polyethylene (PE), polypropylene (PP), polyamide (PA), polycarbonate (PC), polymethylmethacrylate (PMMA), and polytetrafluoroethylene (PTFE). While some niche markets can be entered with these materials, widespread acceptance and use of FSW will only occur when a greater selection of materials can be joined.

TWI reported success in joining PP, with tensile strength above 90% (Advanced Materials 2000). Johns reported that acrylonitrile butadiene styrene (ABS) could be readily joined by FSW, achieving 75% of the base material tensile strength (Johns 1999). He also found however, that PTFE was not weldable with FSW given the present state of technology.

BYU research has shown promising results in welding various materials. Most materials have undergone some optimization of operating parameters. Others have received only cursory attention thus far. Welded specimens have been tested under tensile loading, with the results shown in Table 1.

One noteworthy property not reported in any literature is the characteristic strain of the welded parts. It has been noted that while the tensile strength of the welds can be quite high, the strain at failure is very low. Whereas an unwelded specimen may reach a

strain of 100- 150%, a welded specimen attains only 10- 15%. The reason for this dramatic difference is unknown, but is evidence of a fundamental change in the material.

Table 1- Tensile test results for various polymers. (Sorensen 2001)

Material	Base Material	Friction Stir Welding Results	
	Ultimate Tensile Stress (MPa)	Ultimate Tensile Stress (psi)	% base material Ultimate Tensile Stress
ABS	34.1	32.7	96
HDPE	22.5	21.5	95
PA (nylon)	72.4	28.4	39
PC	68.3	57.1	83
PMMA	42.0	21.5	51
PP	31.3	30.6	98
UHMWPE	28.8	20.0	69

2.4 Brief Comparison of Polymer Joining Processes

As FSW will be competing with well established practices of joining polymers, a specific example comparing several processes for the production of a specific part has been created. We will consider ultrasonic, hot-plate, hot-gas, extrusion, and friction welding processes. FSW will also be compared to adhesive joining. Comparisons will be made on the basis of part preparation, process time, consumables, process repeatability, joint efficiency, and machine/ tool cost. The ability of the processes to produce continuous and discrete parts will also be compared. For this paper, the processes will be compared in producing a 12 in long butt weld in 0.25 in thick polypropylene. A summary of the process requirements is found in Table 2, with a comparison of the process capabilities is given in Table 3.

Table 2- Process requirement comparison of common polymer joining techniques for 12 in long butt weld in 0.25 in thick PP.

Process	Preparation	Process time	Total Time	Consumables	Machine/ Tool, consumable cost
Ultrasonic	energy directors	1-3 sec.	5-10 min.	none	$30,000
Hot-plate	none	30-40 sec.	60-90 sec.	none	$47,000
Hot-gas	v- groove	8-10 min.	15 min.	gas, filler	$3,500
Extrusion	v- groove	8- 10 min.	15 min.	gas, filler	$5,500
Friction	flatten face	10-15 sec.	6- 8 min.	none	$89,000
Adhesives	clean	3 min.	2-3 hours	cleaner, adhesive	$3,000
FSW	none	2 min.	3 min.	none	$11,000

Ultrasonic welding is the most widely used method of welding polymers. It is a very fast process, with weld times of 1-4 seconds. Joint efficiencies of above 75% are possible, and the process is very repeatable. However, machines and tools are expensive, and part preparation is time consuming. Only discrete parts can be produced, and only spot welding is performed. Thus for the example part, the properties will be inferior.

Hot-plate welding is also a widely used process. Very high joint efficiencies are possible, the weld time for the specified part is 30- 40 seconds. Little surface preparation is required, and the repeatability of the process is high. Machine and tooling costs are on the higher end of the spectrum, and again only discrete parts are produced. Complex joint geometries can be accommodated, but at great cost.

Table 3- Process capability comparison for common polymer joining techniques.

Process	Joint Efficiency	Repeatability	Continuous	Discrete
Ultrasonic	75 %	high	No	Yes
Hot-plate	90 %	high	No	Yes
Hot-gas	60 %	fair	Difficult	Yes
Extrusion	70 %	fair	Difficult	Yes
Friction	85 %	high	No	Yes
Adhesives	90 %	fair	No	Yes
FSW	95 %	high	Yes	Yes

Hot-gas and extrusion welds are very similar in process and performance. A v-groove is required for proper weld formation, which is performed at a very slow rate. Joint efficiencies for the processes are generally 60-70%, with fair repeatability. However, this is highly dependent on the operator's skill level. Consumables include gas and filler rod. The process can be used for continuous welding, but with difficulty. The machine costs are low, but the labor is quite high.

Several forms of friction welding are used. The two parts are either spun opposite one another, or linearly displaced relative to each other. Here, linear welding will be considered. Little preparation is required, generally a single step to flatten the surfaces and make them planar. Weld times are short, about 15-20 seconds, and efficiencies of 85% are achieved. No consumables are required, and the repeatability is quite high. Machine and tooling costs are moderate.

Adhesives offer a great variety of possibilities. Cure times can be very short (in minutes for anaerobics) or very long (several hours for high performance epoxies.) Little operator skill is needed, but often environmental issues prove costly. Joint strengths are adjustable by careful adhesive selection, and are often above 90%. Part preparation is required, to clean and ensure proper contact between the parts. A unique advantage of adhesives is the ability to join both thermoplastic and thermoset polymers.

Friction stir welding shows great capability in the current example. Machine and tooling costs are very low, and joint efficiencies are often in the 90-95% range for both tensile and flexural properties. Feedrates in PP have reached 6 ipm with 90% base material tensile strength. No part preparation or consumables are required. Discrete and continuous parts are readily produced on simple machines.

2.5 Mechanical Testing Standards

Two published standards were found to be applicable to this research. A set of standards developed by the Deutscher Werband für Schweissen und Verwandte Verfahren (DVS) governs the testing of welded thermoplastic polymers, specifically DVS Direction 2203-5 "Testing of welded joints of thermoplastic plates and tubes: Technological bend test." ASTM standard D 790-96a controls flexural testing of unreinforced plastics. Both tests use three-point bend tests. This work uses both standards to analyze the performance of the welded joint. The DVS standard uses a "bend angle" to assess the flexibility of the weld. The ASTM standard uses maximum fiber stress and strain to assess the strength of the material.

The fixtures prescribed by both standards were equivalent, with the exception of the support rollers. While the DVS direction called for a roller diameter of 50 mm, the ASTM standard specified a maximum of 36 mm. Because the primary goal was to assess the flexibility of the weld, the DVS dimension was used for the roller.

Detailed dimensional information for the test fixture used in this research is listed in Table 4. A typical test apparatus and setup with key dimensions labeled is shown in Figure 4. The standard requires the testing of six specimens from each weld. Three place the weld root in tension. The other three place the root in compression. The ram displacement and load at yield and rupture are recorded, and used to calculate key properties.

Table 4- Critical dimensions for three-point bending (DVS 1999).

Nominal thickness	Length (Lt)	Width (b)	Roller distance (Ls)	Roller diameter (d)	Ram tip diameter (a)
6.0 mm	200 mm	20 mm	90 mm	50 mm	8 mm

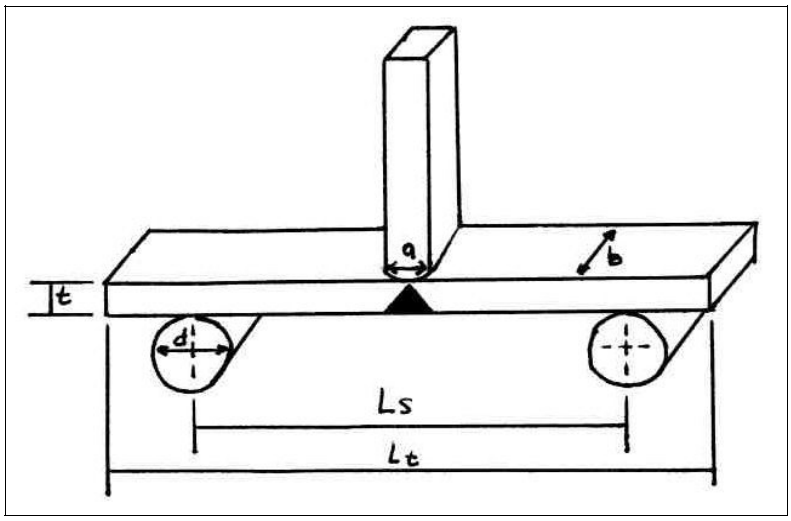

Figure 4- Typical three point bend test setup for welded polymers (DVS 1999).

DVS directions use the bend angle to classify welds as good or bad. The DVS bend angle is defined as the total angle bent through by the specimen during the test. That is, the bend angle is the difference between the initial and final included angles of the weld. The bend angle required for "good" classification vary by material, thickness, and joining process. For welds in 6 mm polypropylene a bend angle of 50° is required for hot-gas, extrusion, and laser welding processes. A bend angle of 85° is required for hot-plate welds.

ASTM standards report the engineering stress/ strain characteristics of the material, in this case a welded joint. The flexural properties and performances are related in terms of maximum fiber stress and strain. The maximum fiber (tensile) stress and strain occur at the bottom of the specimen. Given the ram displacement, load, and specimen thickness, the maximum fiber strain can be calculated by:

Equation 1 $$\varepsilon = \frac{6Dt}{L^2}$$

where: r = maximum fiber strain, (mm/mm),
D = midspan deflection (mm),
t = beam thickness (mm), and
L = support span (mm).

The maximum fiber tensile stress is calculated by:

Equation 2 $$\sigma = \frac{3PL}{2wt^2}$$

where: s = maximum fiber stress (MPa),
P = load (kg),
L = support span (mm),
w = beam width (mm), and
t = beam thickness (mm).

2.6 Microstructure

While no research has been reported regarding the microstructure of FSW joints in thermoplastic materials, several published reports were found regarding the microstructure of hot-plate butt welds. These reports identified not specific structure types but zones of common structure within a weld.

In 1967 Menges and Zohren identified four zones of common microstructure in HDPE hot-plate butt welds (Menges 1967). No details were given regarding the actual structures or their causes. Menges and Zohren only stated that the zones were caused by thermal affects during the welding process.

Barber concluded that five zones exist in the butt welds, rather than four (Figure 5). Observing differing rates of attack by chromic acid for each of the zones, he proposed that different crystal structures existed in each region (Barber 1972).

Work by Atkinson and DeCourcy gives perhaps the most detailed explanation of the formation of zones. They concluded that the zones represent areas of molecular orientation. (Atkinson 1981). The degree of orientation varies for each region, and the

rate of etchant attack depends on the degree of orientation. DeCourcy theorized that shear forces during the welding process formed these zones (DeCourcy 1976). As the weld is brought together under pressure, the molten material within the weld zone is forced to flow. The amount of flow determines the extent of orientation, most markedly when there is substantial flow of material having a low melt index. Near the center of the weld where the least amount of flow occurs, there is the least molecular alignment. Near the outer surface of the weld, the material flows furthest, and is aligned to a higher degree.

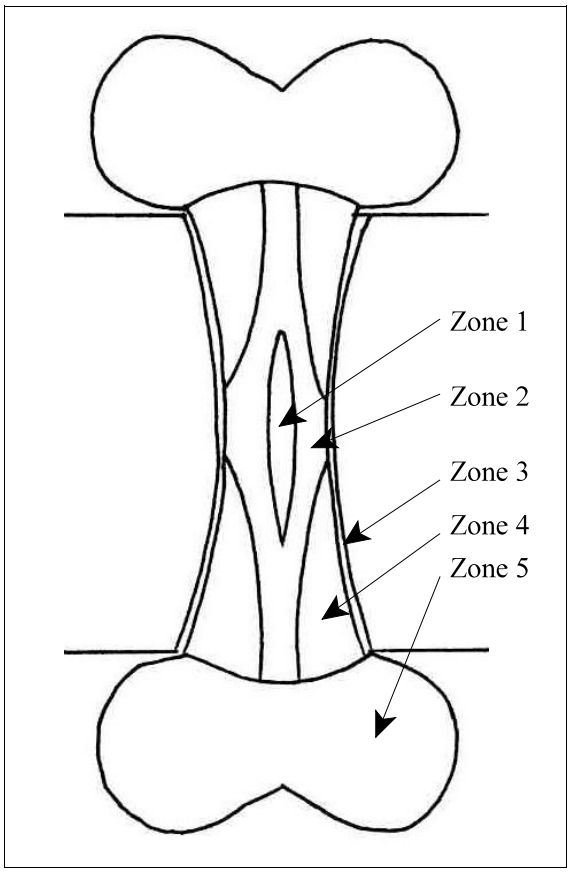

Figure 5- Microstructure zones in hot plate butt weld of HDPE (Barber 1972).

CHAPTER 3

Experimental Procedure

3.1 Introduction

This work proceeded in several stages. First, the parameters to be studied and their levels were selected. Next, a number of tools were created specifically for the various feedrates and pressure times. The welds were then made, and the three-point bend tests were performed. The microstructural study was the final major step in the research. This chapter describes and discusses the procedures used throughout the work.

3.2 Experimental Design

Preliminary research revealed several parameters which affect the quality of the weld. Weld performance was high over broad ranges of shoe temperatures and feedrates. However, weld performance was very sensitive to spindle rpm. In this microstructure study, the author included two parameters which had never been considered (pressure time and pin diameter) and two which had been examined in cursory fashion (feedrate and shoe temperature). Spindle speed was held constant because of the aforementioned sensitivity.

During this research each parameter was studied in a one-at-a-time fashion. Each parameter had multiple levels. Pin diameters were 6.4, 9.5, and 12.7 mm. Feedrates of 51, 102, 203, and 305 mm/min were investigated. Shoe temperatures of 110, 127, 143, 160, and 177 °C were examined. Pressure time had values of 30, 60, 90, and 120 seconds. The rotational speed of the pin was held constant at 1080 rpm. Welds were made at the parameter combinations listed in Table 5.

This one-at-a-time design was selected in place of a full factorial design for two major reasons. First, this was the first research of its kind. Because no previous work had been performed there no knowledge of how each parameter would affect the material

Table 5- Weld parameter levels and run order

Weld Number	Run Order	Spindle Speed	Pin Diameter	Feedrate	Pressure Time	Shoe Temp.
		RPM	mm	cpm	seconds	°C
P.D. 9a	19	1080	9.5	102	90	160
P.D. 9b	23	1080	9.5	102	90	160
P.D. 12a	9	1080	12.7	102	90	160
P.D. 12b	26	1080	12.7	102	90	160
P.D. 6a	16	1080	6.4	102	90	160
P.D. 6b	12	1080	6.4	102	90	160
F.R. 51a	7	1080	9.5	51	90	160
F.R. 51b	1	1080	9.5	51	90	160
F.R. 102a	22	1080	9.5	102	90	160
F.R. 102b	2	1080	9.5	102	90	160
F.R. 203a	11	1080	9.5	203	90	160
F.R. 203b	28	1080	9.5	203	90	160
F.R. 305a	21	1080	9.5	305	90	160
F.R. 305b	32	1080	9.5	305	90	160
P.T. 30a	8	1080	9.5	102	30	160
P.T. 30b	13	1080	9.5	102	30	160
P.T. 60a	10	1080	9.5	102	60	160
P.T. 60b	6	1080	9.5	102	60	160
P.T. 90a	30	1080	9.5	102	90	160
P.T. 90b	4	1080	9.5	102	90	160
P.T. 120a	25	1080	9.5	102	120	160
P.T. 120b	27	1080	9.5	102	120	160
S.T. 110a	17	1080	9.5	102	90	110
S.T. 110b	20	1080	9.5	102	90	110
S.T. 127a	18	1080	9.5	102	90	127
S.T. 127b	29	1080	9.5	102	90	127
S.T. 143a	5	1080	9.5	102	90	143
S.T. 143b	14	1080	9.5	102	90	143
S.T. 60a	3	1080	9.5	102	90	160
S.T. 160b	15	1080	9.5	102	90	160
S.T. 177a	24	1080	9.5	102	90	177
S.T. 177b	31	1080	9.5	102	90	177

microstructure. Weld parameter levels were selected to represent a wide range of possibilities. Second, the factorial design was rejected due to the large number of welds needed to fully populate the design. With repetition, the one-at-a-time design allowed us to explore the influences of 4 parameters with 32 welds. A full factorial design populated with the same number of parameters, levels, and repetitions, would require 480 welds.

In decreasing the number of welds, there were drawbacks. No interaction effects could be studied; only the individual effects of the parameters were determinable. Interaction effects will need to be explored in the future. This work helped determine the bounds for each parameter. If absolute optimization were desired, the results of this study would serve as a foundation upon which to build a factorial design of fewer parameters and levels.

3.3- Equipment

As mentioned earlier, one of the great advantages of FSW is the simple machinery and tooling required. At BYU, all polymer FSW is performed using a standard Lagun Model mill. The mill used is shown in Figure 6. Only three minor modifications were made to the mill in preparation for FSW use. First, a collar was clamped around the quill. This collar held the shoe stationary and applied forging pressure through the shoe. Second, a small temperature controller was bolted to the side of the mill head. The final modification was to replace the mill's vise with the anvil which secured the part during welding. This anvil will be discussed in detail later.

The tooling used for this research was very simple. As indicated in Figure 7, the tool consisted of a shoe, pin, heater, and thermocouple. The shoe was solid aluminum, with a hole for the heater drilled in front of the pin. The pins used for this work were turned from H13 tool steel. They were tapered at the tip, with a decrease in diameter of 3 mm over the last 6 mm of the pin. The pins were also threaded to a very coarse 4.2 mm pitch. Dimensioned drawings for the various pins and shoes used in this research are found in Appendix 1.

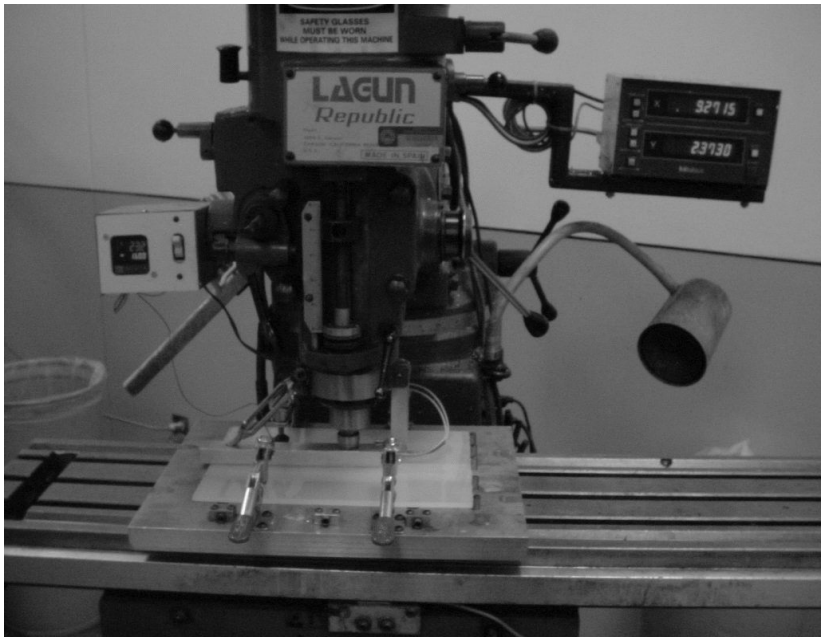

Figure 6- Milling machine used for FSW of polymers.

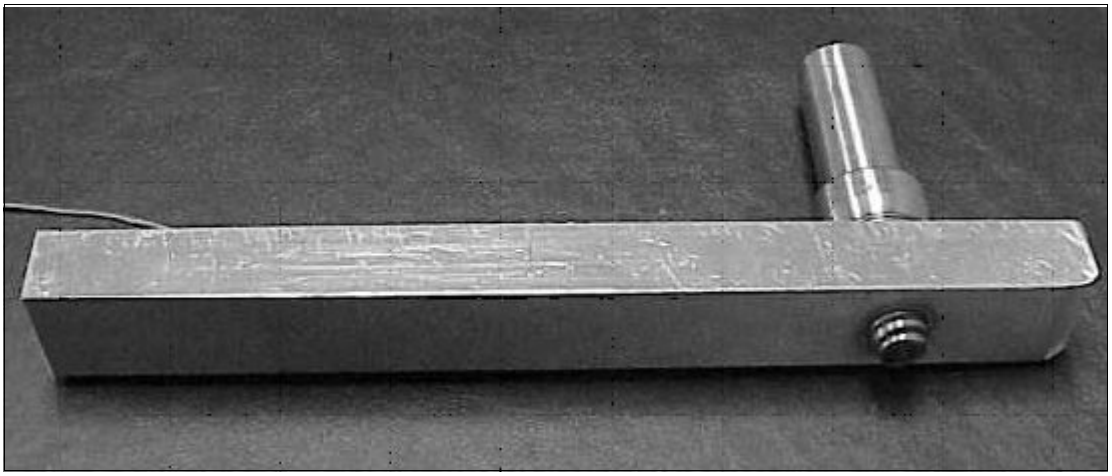
Figure 7- Typical FSW tool for polymers.

3.4 Welding

Friction stir welding of the PP plates was quite easily accomplished with the aid of a simple fixture. This fixture, commonly known as the anvil, provided a stiff backing against which the tool could apply forging pressure and securely held the plates together, as shown in Figure 8. The following simple steps were followed to make each weld.

First, the machine parameters were set. With the spindle stopped, the bed height was set such that the pin would run .08 mm above the anvil. The spindle speed and weld feedrate were set to the desired level. A closed-loop temperature controller was used to set and monitor the shoe temperature.

Second, the plates to be joined were fixtured. Clamps applied vertical holding force to both plates. Set screws were used to apply horizontal pressure to the joint. Once clamped tightly onto the anvil, the jointline was checked for parallelism to the bed of the mill. The pin was brought close to the surface of the plates and centered on the weld. The length of the joint was then traversed to verify that the pin was centered on the joint along the entire weld length.

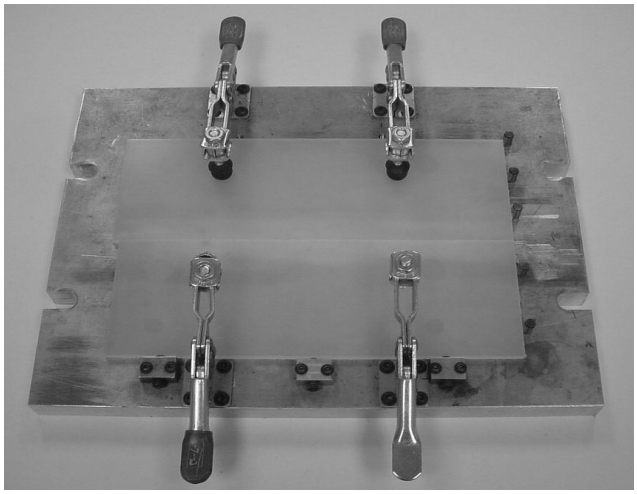

Figure 8- Anvil with PP sheets clamped for welding.

The third step was to plunge the pin into the joint and initiate the FSW process. With the spindle spinning at the desired speed, the pin was slowly plunged into the joint. Once full depth was achieved, the tool was allowed to heat the material, creating a pool of semi-molten material. This usually required 10-15 seconds. When the pin was plunged into the material, solid chunks of material were trapped under the shoe. As the tool and workpiece heated up, those solid chunks began to soften and melt. When sufficiently

heated, this material was extruded from under the shoe. Once this occurred, the tool could be advanced to form the weld.

Fourth, the bed feed was engaged, and the pin traversed the joint. The weld was formed and allowed to cool somewhat under pressure. After the rear of the shoe passed the end of the workpieces, the spindle and bed feed were stopped. The shoe was cooled with compressed air until it reached 37 °C. All welds were allowed to cool for 10 minutes while still clamped in the fixture.

3.5 Specimen preparation

The welds were allowed to cool for 24 hours before testing began. As there were two distinct types of testing carried out, the specimen preparation procedures will be given for each type. All specimens were taken from prescribed locations along the weld. To eliminate the effects of initiating and ending the FSW process, no specimens were taken from the first or last 30 mm of the weld. Microscopy specimens were staggered between the bend test specimens, so that microscopic data was directly related to the bend test data. A diagram of the specimen locations and typical identification numbers are found in Figure 9.

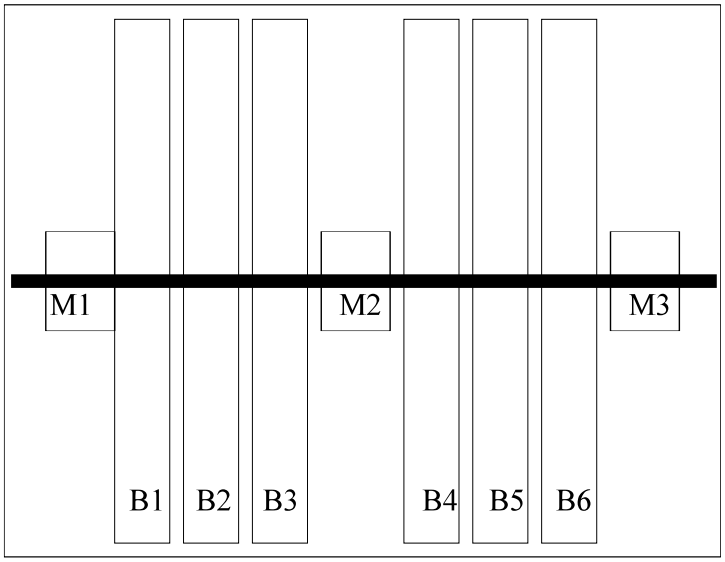

Figure 9- Layout and identification of specimens.

3.5.1 Bend Test Specimens

The preparation of three-point bend test specimens was governed by DVS 2203-5. As shown earlier, there are standard dimensions for the specimens (see section 2.4-Mechanical Testing Standards). Bend test specimens were rectangular, measuring 200 mm long by 20 mm wide The specimens were machined to ensure acceptable and consistent surface finish. Before machining, the specimens were marked for identification. This marking not only allowed easy recording of data, but also enhanced the analysis of data. By recording the location of the specimen along the weld, information regarding process trends could be gathered.

After machining, the specimen's width and thickness were measured to the nearest .01 mm. To ensure consistency and repeatability, the measurements were taken at the center of the weld, directly over the root. At this point the specimens were conditioned for a minimum of 8 hours. Conditioning required exposure to an ambient temperature of 18- 21 °C with not more than 50% relative humidity. The three-point bend testing was then carried out under identical ambient conditions.

3.5.2 Microscopy Sections

Preparation of the microscopic sections was much more involved. In order to acquire usable images, the sections had to be very thin, very flat, and properly mounted on microscope slides. Several steps were followed to create usable specimens.

The cut lines for the microscope specimen blocks were drawn directly onto the weld. At the same time, an indicator line was drawn parallel to the advancing side of the weld. This allowed the sections to later be aligned properly on the slides.

The blocks cut from the weld were mounted on a Sorvall JB-4 microtome, equipped with a Tungsten carbide knife. The surface to be sectioned was cut repeatedly. The first several cuts were intended to true the surface rather than create usable sections. Once a flat, straight surface was established, usable sections were cut. Each section was cut .008 mm thick. A total of nine sections were cut from each block.

Immediately after being cut the individual sections were placed on microscope slides. A drop of water on the slide served to hold each section in place. Each weld had a

separate slide, and all sections were placed on the slide such that the advancing side was on the right when viewed from above. The slides were placed in a 60 °C oven for 24 hours. During this time the water evaporated from the slide, and the sections relaxed. Sectioning the PP weld left residual stresses that occasionally caused the sections to curl. The warm oven allowed the sections to release the residual stresses.

Once the sections were dry and flat, a cover slip was applied to the slide with a sealing agent. In this research, Permount® (toluene solution) was used. It effectively sealed dust and other environmental contaminants out of the slide. Permount® was selected because it could do this without interfering with the optical observation of the sections under polarized light. Slight pressure was applied to the coverslip over a 24 hour period while the Permount® cured.

When the Permount® was dry, the sections were ready for microscopic examination. Care was taken to store the slides in a clean environment, and they were cleaned prior to use.

3.6 Three-Point Bending

For this research, all three-point bend testing was performed on an Instron model 4204 mechanical testing machine. Data acquisition was performed using National Instruments software and firmware. All data was collected at a frequency of 5 Hz. This frequency was shown to yield accurate results without taking excessive amounts of data.

A three-point bend fixture was constructed according to the dimensions given in DVS 2203-5 (see section 2.4). Namely, the support roller diameter was 50 mm, the rollers were spaced 90 mm on center, and the ram had a nose diameter of 8 mm. As shown in Figure 10, the specimen acted as a simply supported beam, with a single point load at its midpoint. The fixture was designed to apply the load directly to the welded joint. For each weld, three specimens were tested such that the weld root was in compression, and three such that the root was in tension. This was accomplished simply by placing three specimens in the fixture such that the ram contacted the top of the weld, and three such that the ram contacted the bottom of the weld.

Figure 10- Three-point bend test fixture.

The Instron machine allowed easy control of the test parameters and recording of key data points. The travel rate of the ram was set at the specified rate of 20 mm/min (DVS, 1999). As the welding process tends to leave a bend in the specimen, the start point differed for each specimen. For this work, the point of 0 deflection was defined as the point of contact between ram and specimen resulting in not more than .5 kg load. Displays on the machine recorded the loads and displacements of the ram at the yield and break points for the specimen. These points were used to calculate fiber stresses and strains.

Bend tests were run to either specimen rupture or crack initiation. If a crack were estimated to be 1.25 mm deep, the test was stopped. In the case that the specimen bent without crack initiation to a bend angle of 160°, "no failure" was entered as the break point of the specimen. In the case of rupture without previous yielding of the specimen, yield and break were labeled as the same point.

The most stringent DVS standard required a bend angle of 85° for classification as a good weld. For sake of simplicity, several bend angles were converted to ram displacements empirically. Five specimens were tested, and the ram displacement was recorded for observed bend angles of 0-160° in 5° increments. The first case was for a straight specimen– representative of non-welded material. The second specimen had a high positive initial angle, the third had a high negative initial angle; these represented the

welds with the highest initial angle. The fourth and fifth specimens had low initial angles– representing a welds with the lowest initial angle. This table of values was then used to determine the bend angle for each specimen tested during this research. The full table is included as Appendix 2.

Welding the PP plates caused them to deflect somewhat. As a result, the ram displacement necessary to achieve a bend angle of 85° was not the same for every weld. Furthermore, the specimens tested root-up required a different displacement than those tested root-down. The angle of deflection was measured for all welds before testing, and was found to be between 8° and 13° in all cases. It was determined that the required ram displacement would vary by a maximum of 3.4 mm at 85°, and 6.8 mm at 160°. Two categories of initial angle were established– low (8-10°) and high (11-13°). The welds were judged according to the tabulated angles for the appropriate range. Ram displacements required to pass the DVS standard are shown in Table 7.

Table 6- DVS ram displacement requirements.

Initial Weld Angle	Root Direction	Ram displacement, 85° (mm)	Ram displacement, 160° (mm)
Low (8-10°)	Up	22.8	45.6
	Down	21.5	43.0
High (11-13°)	Up	26.5	53.0
	Down	23.1	46.2

3.7 Optical Microscopy

This work centered around the study of weld microstructures. This study exclusively used a Nikon OPTIPHOT2-POL microscope. The microscope was equipped with a Nikon FX35-A camera. Under cross-polarized light, the characteristic microstructures of the weld sections were identified and captured photographically.

Because of the size of the specimens, it was not possible to photograph the entire weld area at once. Instead, multiple photographs were taken of each weld and digitized. Collages were then made for each weld using an image editing software package.

3.7.1 Cross-Polarization of Light

The OPTIPHOT2-POL offered the capability of using cross-polarized light. Polarization of the light allowed us to see much greater detail than white light. It was possible to distinguish between crystalline and amorphous regions. Regions of differing crystal orientations could be identified, and at higher magnifications individual spherulites could be seen.

Polarization is the process of systematically eliminating light waves which vibrate in particular planes and preserving others. In our case, we eliminated all waves which did not oscillate along either the x or y axis. As these waves passed through a given specimen, they were diffracted from their original planes. Viewing the transmitted light we observed areas of contrasting light and dark along a grayscale. Where the waves canceled each other there was darkness. To the extent that they reinforced one another, the image became brighter.

Rotating the stage caused the specimen to interact differently with the light. The degree of crystallinity of any region determined the degree of light or darkness observed. If an area could be made to oscillate between light and dark as the stage is rotated, it was determined to be a crystalline region. If a zone were constantly dark, the polymer was known to be highly amorphous in that region.

Polarization of the light dramatically increases the contrast and detail seen in the section. This is readily apparent in the two figures below. Figure 11 is a non-polarized image of a portion of a friction stir weld specimen. Figure 12 is an image of the identical specimen, this time viewed with cross-polarized light.

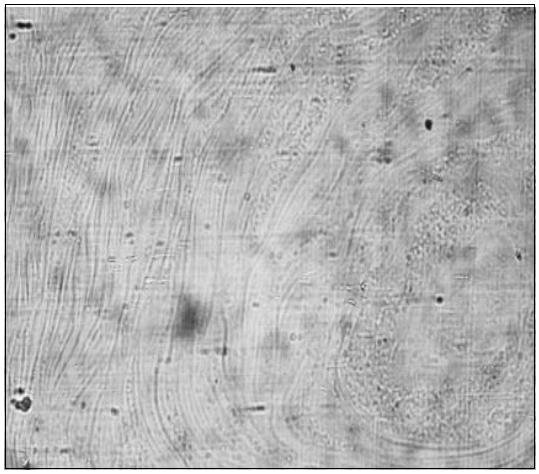

Figure 11- FSW specimen viewed under plain light

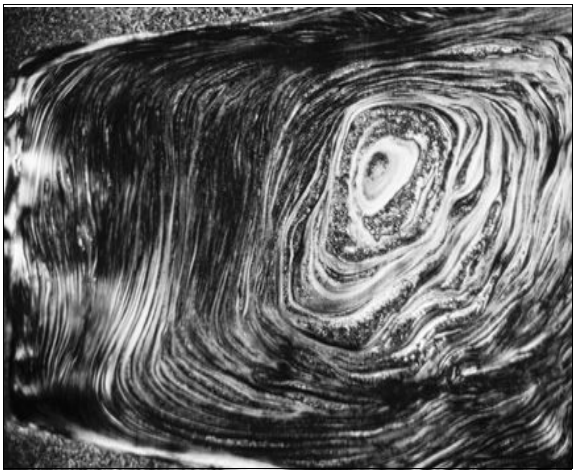

Figure 12- FSW specimen viewed under cross polarized light

3.7.2 Magnification

For the purposes of this work, high levels of magnification were unnecessary. Because this was a qualitative rather than quantitative investigation, highly resolved individual spherulites were not needed. All images were collected using a 2x objective lens. The camera lens also provided some magnification, resulting in a true magnification of 13x.

3.7.3 Linear Measurement

Limited linear measurements were performed in the course of my research. Such measurements consisted of the measurement of microstructure zones and features. A one millimeter bar was photographed under identical conditions to the welds and subsequently digitized. This digital image was overlaid on all weld collages to facilitate measurements.

CHAPTER 4

Effects of Friction Stir Welding on Polymer Microstructure

4.1 Introduction

Friction Stir Welding is a new process for joining polymeric materials. Since 1998, major research assessing the feasibility of the process has been ongoing at Brigham Young University. Several polymers have been successfully welded, retaining over 90% of base material tensile strength. However, very little has been known regarding the effect of the process on the polymer microstructure. This research sets forth the relationships between several key operational parameters, the resulting weld microstructure, and flexural properties of the welded joint.

4.1.1 Brief History of Friction Stir Welding

Friction Stir Welding (FSW) is a relatively new joining process, first performed successfully on Aluminum alloys in 1991 at The Welding Institute (TWI) in England. It has become widely accepted in the metals manufacturing realm. Extensive research has been performed on tool design, joint geometries, process parameters, and materials.

Meanwhile, the process is still in its infancy among polymer processors. Few groups have attempted and reported work with FSW of polymeric materials. Of the thousands of polymers in existence, less than a dozen have been tested for compatibility with FSW technology. Very little is known about the process, including the effects of FSW processing on the microstructure of polymers.

4.1.2 FSW of Polymers

Friction stir welding of polymers is accomplished with a few simple steps. A rotating tool is plunged into the joint between two tightly held workpieces. The friction

between the pin and workpiece causes the material to heat up and the tool is moved along the joint line. The material is stirred as it is moved around the tool within the weld zone.

FSW tooling consists of a pin and a shoe. The pin is a rotating body, and is primarily responsible to produce frictional heating of the workpiece and to stir the softened material. The shoe is primarily responsible to trap the material displaced by the pin and hold the weld under pressure as it begins to cool. Additionally, the shoe smooths any defects in the top surface of the weld.

During the process, the primary generator of heat is the friction between the workpiece and the tool. However, because many polymers tend to be self-lubricating at elevated temperatures, it is often necessary to provide additional external heat. For this work, a simple resistive heater is embedded in the shoe.

It is very important to promote a uniform cooling rate throughout the weld volume as the welded joint cools. If the outer material cools much quicker than the inner, a hard shell is formed. As the inner layers subsequently cool, the material contracts and pulls away from the shell. Large voids are formed which detract greatly from the mechanical performance of the welded joint. Increasing the shoe length allows pressure to be maintained as the weld cools through a greater temperature change. Because more cooling and solidification of the weld occurs under pressure, material shrinkage is more uniform, and void formation is reduced.

4.2 Literature Review

Little formal research has been reported regarding friction stir welding of polymeric materials. The few published reports on the subject focus on the successful joining of polymers with the process. Essentially no work has been reported regarding the mechanics of the process or the effects of the process on the microstructure of the polymer itself.

Because friction stir welding of polymers is so new, it is not surprising that very little has been published about it. Very few groups are perfoming research into the process, and even fewer have reported results. The leading research groups are working

at TWI and BYU. An extensive search revealed published results in only three areas- tool design, process parameters, and weldable materials.

4.2.1.1 Tool Design

Only preliminary work has been reported with regard to tooling issues. Johns reports several iterative attempts to create a functional FSW tool for polymers (Johns 1999). A standard aluminum style tool could form a weld, but with very poor mechanical and visual properties. Rather than holding the material within the weld volume it dragged it out, resulting in large voids throughout the weld.

Johns' final tool iteration proved much more successful, and is the model for the current tooling used at BYU. As shown in Figure 13, it consists of a rotating pin, a thrust bearing, and a stationary "shoe". The shoe allows pressure to be applied over a large area of the weld as it cools, limiting the formation of voids. It can be heated if additional energy is needed for proper fusion of the joint.

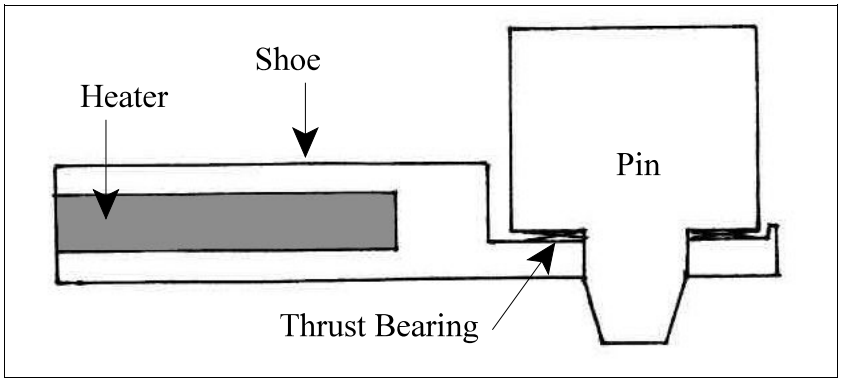

Figure 13- Final iteration of Johns' tool (Sorensen 2001).

Johns concluded that in order to increase tool life, the pin needs to be kept as short as possible. This minimizes the moment acting on the tool, thus helping to overcome the effects of cyclic loading.

TWI has only reported the shape of their tool. They have reported the successful welding of polypropylene with "an airfoil shaped reciprocating tool"(ASM International, 2000).

4.2.1.2 Process Parameters

Researchers at BYU are the only group to have reported successful operating parameters. Various parameters including shoe temperature, spindle speed, weld feedrate, tool offset depth (distance from the bottom of the pin to the top of the anvil), and pin geometry were studied. The rotational speed of the tool was found to be very critical, as was the feedrate of the weld. In general, higher spindle speeds (1500-1800 rpm) resulted in higher tensile strengths. Lower feedrates (10-25 cpm) were found to yield superior properties (Nelson 2000).

4.2.1.3 Materials

To date, very few of the thousands of available polymers have been investigated for compatibility with FSW. Polymers for which data has been reported include various grades of polyethylene (PE), polypropylene (PP), polyamide (PA), polycarbonate (PC), polymethylmethacrylate (PMMA), and polytetrafluoroethylene (PTFE). While some niche markets can be entered with these materials, widespread acceptance and use of FSW will only occur when a greater selection of materials can be joined.

TWI reported success in joining PP, with above 90% of the base material tensile strength (ASM International 2000). Johns reported that acrylonitrile butadiene styrene (ABS) could be readily joined by FSW, achieving 75% of the base material tensile strength. He also found however, that PTFE was not weldable with FSW given the present state of technology (Johns 1999).

BYU research has shown promising results in welding various materials. Most materials have undergone some optimization of operating parameters. Others have received only cursory attention thus far. Welded specimens have been tested under tensile loading, with the results shown in Table 7.

Table 7- Tensile test results for various polymers. (Sorensen 2001)

Material	Base Material	Friction Stir Welding Results	
	Ultimate Tensile Strength (MPa)	Ultimate Tensile Strength (MPa)	% base material Tensile Strength
ABS	34.1	32.7	96
HDPE	22.5	21.5	95
PA	72.4	28.4	39
PC	68.3	57.1	83
PMMA	42.0	21.5	51
PP	31.3	30.6	98
UHMWPE	28.8	20.0	69

4.2.2 Microstructure in Welded Polymer Joints

While no research has been reported regarding the microstructure of FSW joints in thermoplastic materials, several published reports were found regarding the microstructure of hot-plate butt welds. These reports identified not specific structure types but zones of common structure within a weld.

In 1967 microscopic studies identified four zones of common microstructure within hot plate butt welds in HDPE (Menges 1967). Menges and Zohren offered no details on the microstructural features seen or their causes, stating only that they were caused by thermal affects of the welding process.

Barber concluded that five zones exist in the butt welds, rather than four (Figure 14). Observing differing rates of attack by chromic acid for each of the zones, he proposed that different crystal structures existed in each region (Barber 1972).

Work by Atkinson and DeCourcy gives perhaps the most detailed explanation of the formation of zones. They concluded that the zones represent areas of molecular orientation (Atkinson 1981). The degree of orientation varies for each region, and the rate of etchant attack depends on the degree of orientation. DeCourcy theorized that shear forces during the welding process formed these zones (DeCourcy 1976). As the weld is brought together under pressure, the molten material within the weld zone is forced to flow. The extent of flow determines the extent of orientation, most markedly

when there is substantial flow of material having a low melt index. Thus, near the center of the weld where the least amount of flow occurs, there is the least molecular alignment. Near the outer surface of the weld the material flows furthest, and hence is aligned to a higher degree at a singular orientation.

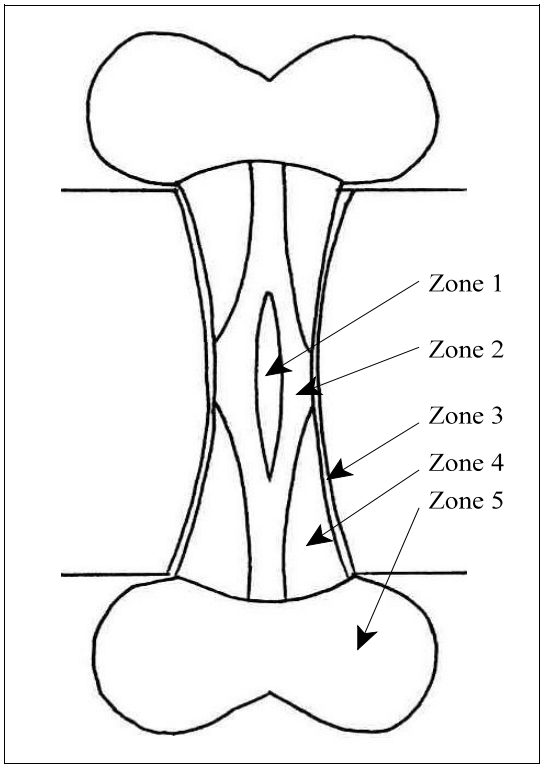

Figure 14- Microstructure zones in hot plate butt weld of HDPE (Barber 1972).

4.3 Experimental Procedures

This work was performed in several stages. First, the parameters and levels were selected. Second, the tools needed were created. Third, the welds were made. Fourth, the three-point bend tests were performed, and the final step was to study the microstructure.

4.3.1 Experimental Design

During this research each parameter was studied in a one-at-a-time fashion. The one-at-a-time design was selected in place of a full factorial design for two major reasons. First, because no previous work had been performed there was little knowledge of how each parameter would affect the material microstructure. Weld parameter levels were selected to represent a wide range of possibilities. Second, the factorial design was rejected due to the large number of welds needed to fully populate the design. With repetition, the one-at-a-time design allowed us to explore the influences of 4 parameters with 32 welds. A full factorial design populated with the same number of parameters, levels, and repetitions, would require 480 welds. In decreasing the number of welds, there were drawbacks. No interaction effects could be studied; only the individual effects of the parameters were determinable.

Table 8- Weld parameter combinations and run order.

Weld Number	Run Order	Spindle Speed	Pin Diameter	Feedrate	Pressure Time	Shoe Temp.
		rpm	mm	mm/min	seconds	°C
PD6 a & b	19,23	1080	9.5	102	90	160
PD9 a & b	9,26	1080	12.7	102	90	160
PD12 a & b	16,12	1080	6.4	102	90	160
FR51 a & b	7,1	1080	9.5	51	90	160
FR102 a & b	22,2	1080	9.5	102	90	160
FR203 a & b	11,28	1080	9.5	203	90	160
FR305 a & b	21,32	1080	9.5	305	90	160
PT30 a & b	8,13	1080	9.5	102	30	160
PT60 a & b	10,6	1080	9.5	102	60	160
PT90 a & b	30,4	1080	9.5	102	90	160
PT120 a & b	25,27	1080	9.5	102	120	160
ST110 a & b	17,20	1080	9.5	102	90	110
ST127 a & b	18,29	1080	9.5	102	90	127
ST143 a & b	5,14	1080	9.5	102	90	143
ST160 a & b	3,15	1080	9.5	102	90	160
ST177 a & b	24,31	1080	9.5	102	90	177

A total of sixteen weld parameter combinations were explored in this research. Two welds were made for each combination. A listing of the parameter combinations, their corresponding weld numbers, and the actual weld run order are found in Table 8. Pressure time is herein defined as the length of time (in seconds) the weld is held under the shoe after the weld has been formed.

4.3.2 Equipment

As mentioned earlier, one of the great advantages of FSW is the simple machinery and tooling required. At BYU, all polymer FSW is performed using a standard Lagun Model mill, shown in Figure 15. Only three modifications were made to the mill in preparation for FSW use. First, a collar was clamped around the quill. This collar held the shoe stationary and applied forging pressure through the shoe. Second, a small temperature controller was bolted to the side of the mill head. The final modification was to replace the mill's vise with the anvil which secured the part during welding.

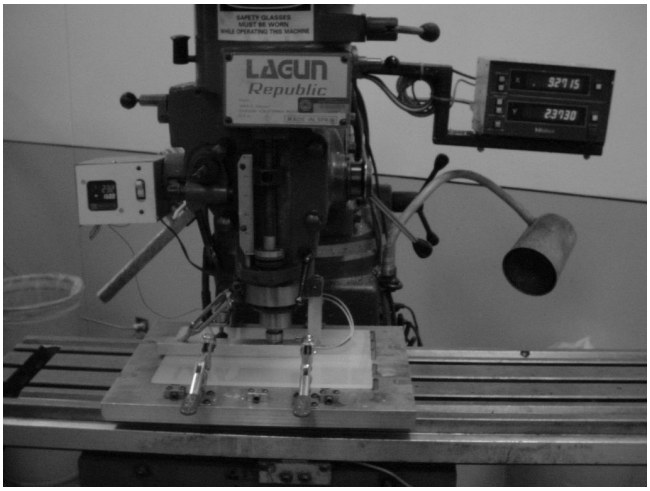

Figure 15- Milling machine used for FSW of polymers.

The tooling used for this research was very simple. As shown in Figure 16, the tool consisted of a shoe, pin, heater, and thermocouple. The shoe was solid aluminum, with a hole for the heater drilled in front of the pin. A bearing was pressed into the shoe. The pins used for this work were turned from H13 tool steel. They were tapered at the

tip, with a decrease in diameter of 3 mm over the last 6 mm of the pin. The pins were also threaded to a very coarse 4.2 mm pitch.

Figure 16- Typical FSW tool for polymers.

4.3.3 Welding

Friction stir welding was quite easily accomplished. A simple fixture held the workpieces tightly together during the process. This fixture, called the anvil, also provided a stiff backing against which the tool could apply forging pressure. Several simple steps were followed to make each weld.

First, the machine parameters were set. The parameters controlled as part of this work were the weld feedrate, shoe temperature, pressure time, and pin diameter. With the spindle stopped, the tool depth was set such that the pin would run .08 mm above the anvil. Second, the plates to be joined were secured onto the anvil. The third step was to plunge the pin into the joint and initiate the FSW process. With the spindle spinning at the desired speed, the pin was slowly plunged into the butt joint. Once full depth was achieved, the tool was allowed to heat the material and create a pool of semi-molten material. This usually required 10-15 seconds. When the pin was plunged into the material, solid chunks of material were trapped under the shoe. As the tool and workpiece heated up, those solid chunks began to soften and melt. When sufficiently

heated this material was extruded from under the shoe. Once this occurs, the tool could be advanced to form the weld.

The fourth step was to engage the bed feed and move the pin along the joint. The weld was formed and allowed to cool somewhat under pressure. After the rear of the shoe passed the end of the welded plates, the feed was disengaged and the spindle stopped. The shoe was cooled with compressed air until it reached 38 °C. For the sake of uniformity, all welds were allowed to cool for 10 minutes while still clamped in the fixture.

4.3.4 Specimen Preparation

Once the weld was made and allowed to cool for 24 hours, testing could begin. For this research two distinct types of testing (three-point bending and microscopy) were carried out. All specimens were taken from prescribed locations along the weld. To eliminate the effects of initiating and ending the FSW process, no specimens were taken from the first or last 30 mm of the weld. Microscopy specimens were staggered between the bend test specimens, so that microscopic data was directly related to the bend test data. The layout and relative positions of the specimens is shown in Figure 17. Six bend test specimens and 3 microscopy blocks were taken from each weld.

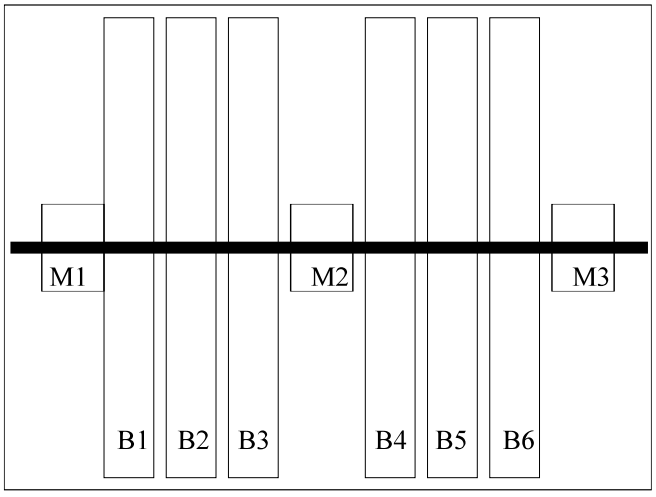

Figure 17- Test specimen layout.

4.3.3.1 Bend Test Specimens

The preparation of three-point bend test specimens was governed by DVS 2203-5. Each specimen was marked for identification according to weld number and location. By recording the location of the specimen along the weld, important information regarding process trends could be gathered.

The width and thickness of the specimens were measured to the nearest 0.01 mm at the center of the weld, directly over the root. Before testing the specimens were conditioned for a minimum of 8 hours by exposure to an ambient temperature of 18-21°C with not more than 50% relative humidity. The three-point bend testing was then carried out under identical ambient conditions.

4.3.3.2 Microscopy Sections

A Sorvall JB-4 microtome equipped with a tungsten carbide knife was used to section the welds. Nine 8 µm thick sections were cut from each microscopy block and placed on microscope slides. A drop of water on the slide held each section in place.

Each weld had a separate slide. The slides were placed in a 60°C oven for 24 hours. During this time the water evaporated from the slide, and the sections relaxed. Sectioning the weld left many residual stresses that occasionally caused the sections to curl. The warm oven allowed the sections to release the residual stresses.

A cover slip was applied to seal dust and other environmental contaminants out of the slide. Permount® (Toluene solution) was used to affix the coverslip because it filled those needs while not interfering with the optical observation of the sections under polarized light.

The sections were placed on the slide so that the advancing side of the weld was always to the right. The “advancing” side is where the pin is rotating against the direction of the weld feed. This was done so as to enable the comparison of processing effects across the weld.

4.3.4 Three-Point Bending

For this research, all three-point bend testing was performed on an Instron model 4204 mechanical testing machine. Data acquisition was performed using National Instruments software and firmware at a frequency of 5 Hz. A three-point bend fixture was constructed (Figure 18) according to the dimensions given in DVS 2203-5. The travel rate of the ram was set at the specified rate of 20 mm/min. The point of 0 deflection was defined as the point of contact between ram and specimen resulting in not more than .5 kg load.

During the test the specimen acted as a simply supported beam with a single point load at its midpoint. The fixture was designed to apply the load directly to the welded joint. Six specimens were tested from each weld. Three were placed in the fixture so the ram touched the root or bottom of the weld. The other three were placed so that the ram touched the top of the weld.

Bend tests were run to either specimen rupture or crack initiation. If a crack were estimated to be 1.25 mm deep, the test was stopped. "No failure" was entered in the case that the specimen bent without crack initiation to a bend angle of 160°. In the case of rupture without previous yielding of the specimen, yield and break were labeled as the same point.

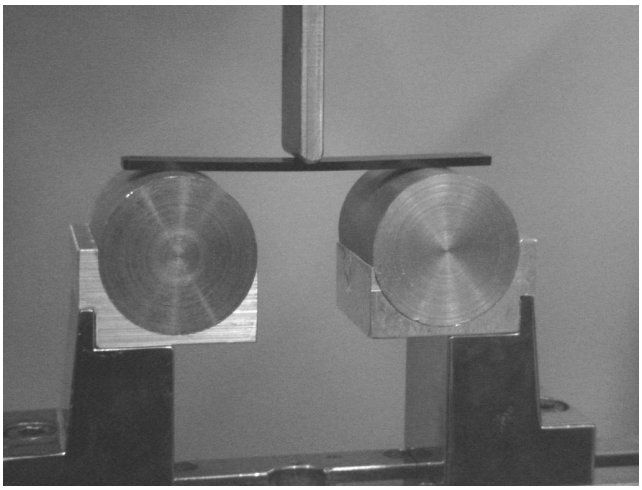

Figure 18- Three-point bend test fixture.

4.3.5 Optical Microscopy

This work centered around the study of weld microstructure. This study exclusively used a Nikon OPTIPHOT2- POL microscope, equipped with a Nikon FX-35A camera. Under polarized light, the characteristic structures of the weld sections could be identified, measured, and captured photographically.

Polarization of the light allowed us to distinguish between crystalline and amorphous regions. The orientation of various regions could also be investigated. Polarization of the light dramatically increased the detail seen in the section. This is readily apparent in the two figures below. Figure 19 is a non-polarized image of a FSW specimen. Figure 20 is an image of the same specimen viewed under polarized light.

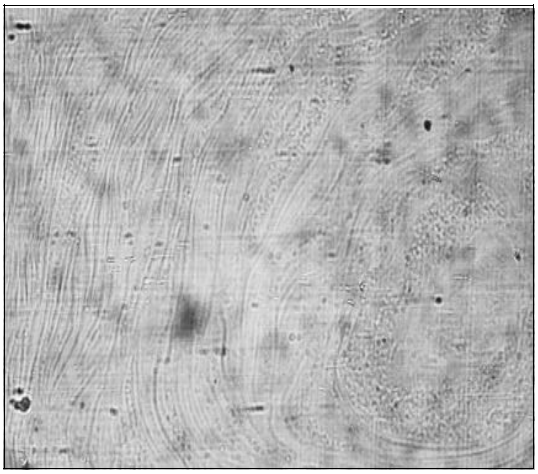

Figure 19- FSW specimen viewed under plain light.

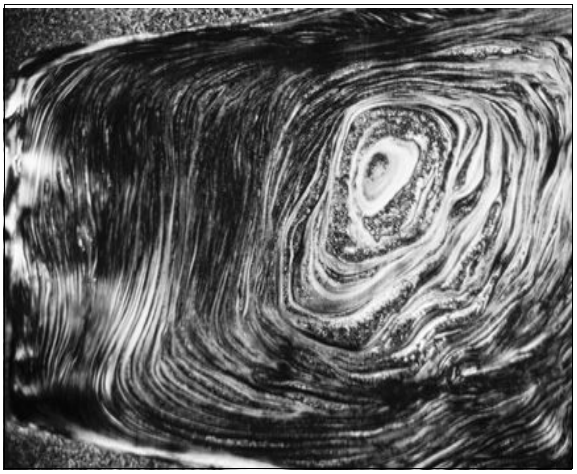

Figure 20- FSW specimen viewed under cross polarized light.

4.3.6 Measurements

Several measurements were taken during the course of the three-point bend tests and microscopic studies. These included the bend angle, ram displacement, loads on the specimen, and microstructure zones and features.

4.4 Results

Three distinct sets of results were collected and analyzed as part of this research. First, the welds were evaluated according to their DVS bend angles. Second, the flexural properties were compared using maximum fiber stresses and strains. Third, the microstructures of the welds were examined.

4.4.1 DVS Bend Angles

In testing the welds made for this work, tests only ended by rupture or by non-failure. No crack initiation was observed. In all cases of weld rupture, the failure occurred along the weld/ base material interface on the advancing side of the tool. Failures in root-up tests initiated under the flash on the top surface of the weld. In those tested root-down, the failure initiated at or very near the root. In all cases observed under the microscope, the failure occurred outside of the weld region, within 0.5 mm of the interface.

Welding the PP plates caused them to deflect somewhat. The angle of deflection was measured for all welds before testing, and was found to be between 8° and 13° in all cases. It was determined that for this range of initial angles, the required ram displacement would vary by a maximum of 3.4 mm at 85°, and 6.8 mm at 160°. Two categories of initial angle were established– low (8-10°) and high (11-13°).

To evaluate the DVS bend angle, the maximum ram displacement before failure was recorded. Ram displacements were converted to a bend angle empirically. The average ram displacements and bend angles achieved by root-up and root-down specimens for each weld are given in Table 9. Due to the geometry of the test fixture, the maximum bend angle possible was 160°.

Table 9. DVS bend angle results

Weld ID	Initial deflection (degrees)	Ram displacement before failure (mm)			Bend angle before failure (degrees)		
		Root up	Root down	Average	Root up	Root down	Average
PD6a	10	15.7	10.9	13.2	58.5	43	50.7
PD6b	8	9.1	9.9	9.7	34	39.8	36.9
PD9a	9	57.9	16.3	37.1	160	64.4	112.2
PD9b	9	53.8	16.3	35.1	160	64.7	112.4
PD12a	10	56.3	15	34.3	160	59.9	110
PD12b	9	49.8	12.7	31.2	160	50.9	105.4
PT30a	10	24.4	14	19.1	90.1	55.7	72.9
PT30b	9	35.6	15.2	25.4	131.9	60.8	96.4
PT60a	9	50	13.7	31.8	160	54.1	107.1
PT60b	8	41.1	15.2	28.2	153	60.5	106.7
PT90a	9	57.9	16.3	37.1	160	64.4	112.2
PT90b	9	53.8	16.3	35.1	160	64.7	112.4
PT120a	9	16.8	11.9	14.5	62.5	47.4	55
PT120b	10	13.5	13.2	13.5	50.3	52.2	51.3
FR51a	9	41.1	17	29.2	153.2	67.8	110.5
FR51b	11	49.8	20.3	35.1	160	72.8	116.4
FR102a	9	57.9	16.3	37.1	160	64.4	112.2
FR102b	10	53.8	16.3	35.1	160	64.7	112.4
FR203a	10	15.2	7.6	11.4	56.7	30.2	43.5
FR203b	10	18	9.4	13.7	67	37.2	52.1
FR305a	8	14.5	10.7	12.7	53.6	42.9	48.2
FR305b	10	18	8.6	13.5	67.3	34.8	51
ST110a	8	14.2	12.2	13.2	53	48.1	50.5
ST110b	9	15.2	15.7	15.5	56.8	63	59.9
ST127a	8	19.6	13.5	16.5	72.6	53.2	62.9
ST127b	10	16.3	15.2	15.7	60.4	60.2	60.3
ST143a	10	44.7	16.3	30.5	160	64.2	112.1
ST143b	10	33.8	17.5	25.7	125.5	69.5	97.5
ST160a	11	57.9	16.3	37.1	160	58	109
ST160b	10	53.8	16.3	35.1	160	64.7	112.4
ST177a	11	47.2	16.5	32	160	59.2	109.6
ST177b	13	44.5	16.5	30.5	160	58.8	109.4

4.4.2 Three-Point Bend Tests

Maximum fiber stresses and strains were used to evaluate the flexural performance of the welds. All values in Table 6 were calculated at the point of maximum load.

Table 10- Three-point bend test results.

	Max Fiber Stress (Mpa)			Max Fiber Strain (mm/mm)		
Weld ID	Root Up	Root Down	overall	Root Up	Root Down	overall
PD6a	73.6	46.6	60.1	0.085	0.037	0.061
PD6b	50.5	47.8	49.1	0.042	0.046	0.044
PD9a	74.4	66.3	70.4	0.110	0.070	0.090
PD9b	72.6	65.0	68.8	0.105	0.071	0.088
PD12a	74.0	70.1	72.0	0.091	0.061	0.076
PD12b	74.0	64.3	69.2	0.087	0.064	0.076
FR51a	79.0	72.4	75.7	0.104	0.076	0.090
FR51b	73.4	72.3	72.9	0.104	0.085	0.095
FR102a	74.4	66.3	70.4	0.110	0.070	0.090
FR102b	72.6	65.0	68.8	0.105	0.071	0.088
FR203a	65.7	35.4	50.5	0.035	0.068	0.052
FR203b	67.0	42.5	54.7	0.042	0.075	0.059
FR305a	61.0	45.5	53.3	0.050	0.065	0.057
FR305b	65.0	40.4	52.7	0.039	0.077	0.058
PT30a	66.1	58.5	62.3	0.093	0.070	0.081
PT30b	69.3	59.0	64.1	0.122	0.067	0.094
PT60a	75.0	67.2	71.1	0.092	0.057	0.074
PT60b	75.2	67.8	71.5	0.099	0.063	0.081
PT90a	74.4	66.3	70.4	0.110	0.070	0.090
PT90b	72.6	65.0	68.8	0.105	0.071	0.088
PT120a	66.4	51.7	59.1	0.070	0.054	0.062
PT120b	61.4	54.6	58.0	0.058	0.059	0.059
ST110a	64.6	60.3	62.4	0.074	0.043	0.058
ST110b	68.9	61.1	65.0	0.068	0.068	0.068
ST127a	68.8	57.8	63.3	0.059	0.081	0.070
ST127b	67.2	60.6	63.9	0.067	0.070	0.069
ST143a	72.1	64.9	68.5	0.093	0.064	0.079
ST143b	72.6	67.9	70.2	0.088	0.074	0.081
ST160a	74.4	66.3	70.4	0.110	0.070	0.090
ST160b	72.6	65.0	68.8	0.105	0.071	0.088
ST177a	72.1	66.4	69.2	0.091	0.065	0.078
ST177b	71.6	68.0	69.8	0.093	0.063	0.078

4.4.3 Microstructure

Sections of each weld were photographed and examined microscopically. The structure of the welds were compared against that of the unwelded PP. In this study, several structure types were found to exist. An example and description of each follows.

4.4.3.1 Spherulites

Spherulites are the basic building block of PP microstructure. As the polymer chains form, they are folded and twisted about themselves and each other. Where they fold neatly, a crystalline region forms. Where they twist, an amorphous structure is created. The chains are further organized into small spheroids, or spherulites. Figure 21 is a micrograph of as-extruded PP. The spherulites are visible as black or white areas, differentiated by their level of crystallinity and the crystal orientation.

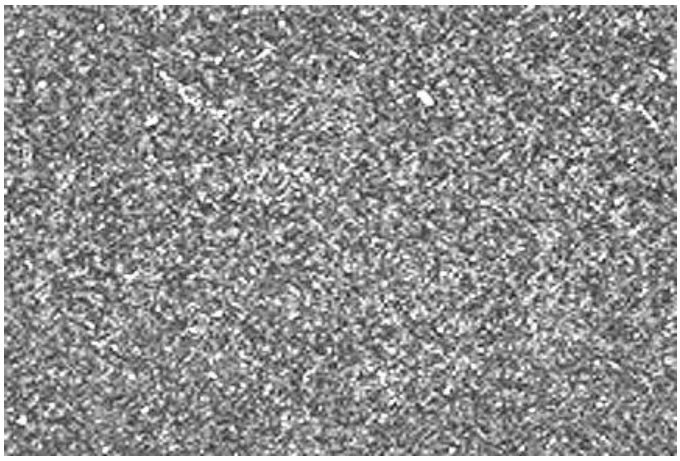

Figure 21- Microstructure of as-extruded PP.

4.4.3.2 Voids

Voids are empty volumes within the weld. They are thought to be created when the outer material cools quickly, and the inner material shrinks away from the resulting shell during cooling. They were common in preliminary welds, but none were found to exist in the welds used for the current work.

4.4.3.3 Flow Line

Flow lines are areas of organized material apparently showing flow patterns. Flow lines are defined as layers of material with similar molecular structure and orientation. Apparently showing the pattern of material flow during FSW, they look like parallel layers, as seen on the right side of the weld in Figure 22.

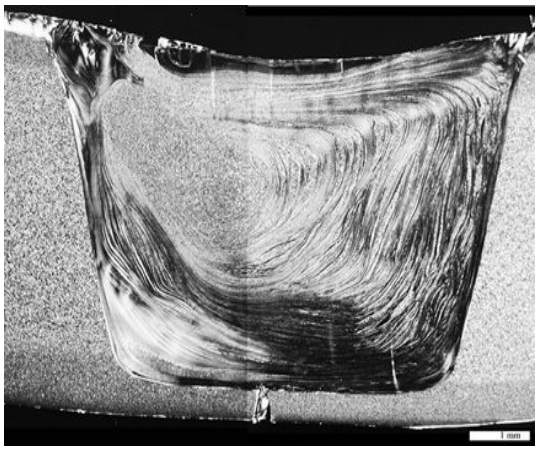

Figure 22- Weld showing flow lines.

4.4.3.4 Onion Ring

Onion ring is a special case of flow line that arises when the flow lines form complete, concentric circles. A typical example of onion ring is shown as figure 23. Through the central section of the weld, the flow lines have created closed loops.

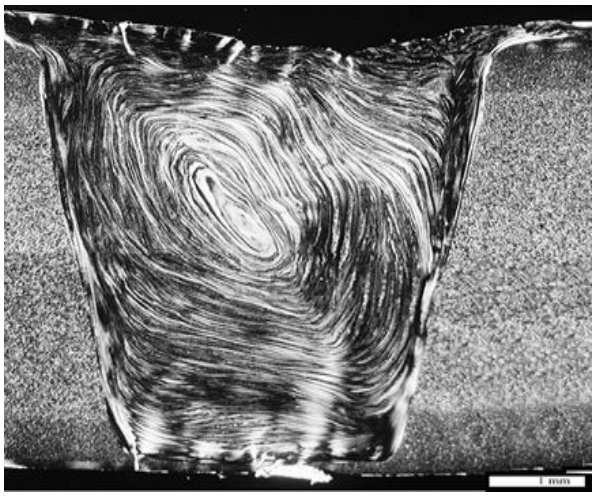

Figure 23- Typical onion ring structure.

4.4.3.5 Root Defect

Root defects were common to every weld created in this research. A root defect is defined as an area at the bottom of the joint that is not welded (Figure 24). Because the welds were made with the pin raised .08 mm from the anvil, the bottom of each joint

was not stirred, and thus left unwelded. In most cases, a small portion of the molten material was extruded into this gap, helping to bond the workpieces, but this extrusion weld was far weaker than the FSW region.

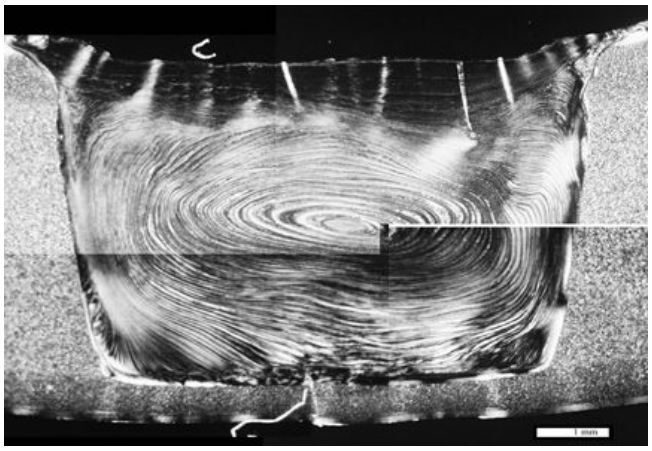

Figure 24- Root defect in FSW weld.

4.4.3.6 Weld Zones

Four zones were found to exist in FSW joints. Figure 25 shows a typical FSW joint in PP. The four weld zones are labeled, being the bottom disturbance, advancing interface, retreating interface, and central zones.

The bottom disturbance is an area of apparently turbulent flow. In this zone, the flow lines are pronounced, and show random swirls. The extreme bottom edge of this zone shows the bottom of the material displaced by the pin.

An interface zone exists on both the advancing and retreating sides of the weld. These interfaces show the area of transition from base material to displaced, stirred polymer. It is common to see very fine flow lines in these zones.

The final zone is the central zone, covering the vast majority of the weld. This region is made up entirely of material that has been displaced and stirred by the pin. Measurements of flow line severity, onion ring severity were only made in these areas.

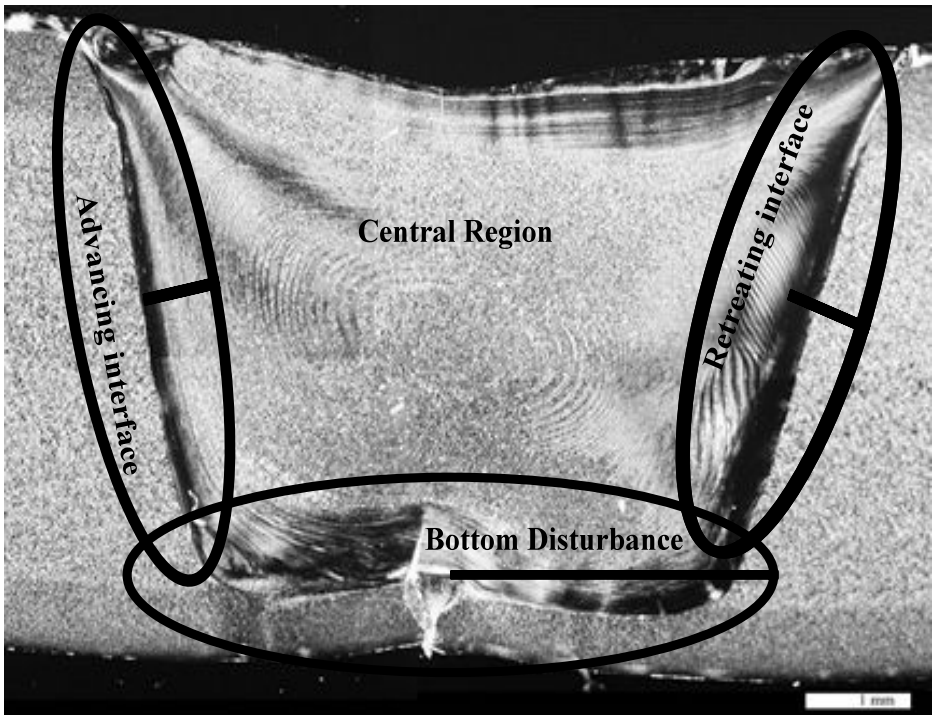

Figure 25- Weld Zones in FSW butt weld.

4.4.3.7 Microstructure Measurements

For each weld section several microstructural measurements were made. Subjectively, the flow lines and onion ring were assessed as to their severity. Severity was based on the density of flow lines (number of flow lines crossing a 1 mm line), the degree of contrast between adjacent flow lines, and the visibility of the lines. A scale of none (0), mild (1), moderate (2), and severe (3) was employed. Physical measurements were made of the area covered by the flow lines, onion ring, and three key disturbance areas.

The average width of the interface disturbances were reported for both the advancing and retreating sides of the weld. In addition, the average depth of the bottom disturbance was reported. Table D gives the measurements recorded for the microstructure specimens.

Table 11- Microstructural observations.

Weld	Bottom	Onion ring		Flow lines		Interface	
	depth	area	severity	area	severity	Retreat	Advance
	mm	mm^2		mm^2		mm	mm
FR51a	8	0	0	11	1	0	4
FR51b	9	0	0	7.4	1	0	4
FR102a	11	8.8	2	27.5	1	2	2
FR102b	4	14.7	3	32.9	3	1	2
FR203a	6	0	0	32.9	3	1	1
FR203b	5	7.9	1	4.5	1	2	3
FR305a	5	4	1	11.3	1	1	2
FR305b	7	7.8	1	20	2	1	2
PD6a	7	3.4	3	14.5	3	3	3
PD6b	6	3.7	3	13.2	3	3	3
PD9a	11	8.8	2	27.5	1	2	2
PD9b	4	14.7	3	32.9	3	1	2
PD12a	8	0	0	0	0	0	2
PD12b	8	0	0	0	0	0	2
PT30a	9	1.2	1	10.9	2	2	2
PT30b	8	4.7	2	10.6	2	2	3
PT60a	10	5	3	20	2	2	3
PT60b	4	0	0	0	0	1	2
PT90a	10	8.8	2	23.5	1	3	2
PT90b	5	15.2	3	21.9	3	1	1
PT120a	11	4.2	2	20.4	2	1	1
PT120b	11	8.8	3	18	2	1	3
ST110a	12	0	0	3	1	1	2
ST110b	11	0	0	1.7	1	1	3
ST127a	8	1.8	1	1.8	1	1	3
ST127b	5	2.2	1	0	0	1	3
ST143a	5	0	0	0	0	1	3
ST143b	5	0	0	0	0	1	3
ST160a	11	9	3	24	1	2	2
ST160b	4	14.4	3	20.8	3	1	2
ST177a	4	0	0	0	0	1	2
ST177b	5	0	0	0	0	1	2

4.5 Analysis and Discussion

Statistical analyses of variance were performed using the data from the DVS bend angle, three-point bend, and microstructural investigations. A one-way analysis of variance (ANOVA) was used to determine the effect of each parameter and its significance. No interactions could be studied because of the one-at-a-time design of the experiment. Unless otherwise specified, all statistical means and standard deviations are overall values– the analyses were performed using all six specimens, not only root-up or root-down.

4.5.1 DVS Bend Angle

A strong relationship was discovered between the root orientation of the specimen and the DVS bend angle achieved. With few exceptions, those specimens tested root-up outperformed those tested root-down. This difference is attributed to the open root condition of the welded specimens. When the root is not welded, a stress concentration develops immediately as a stress is applied to the joint. In the root-down configuration, the discontinuity in the material does not allow stress to be distributed over the thickness of the part and a crack forms at the root. Once some critical stress is reached, rupture occurs.

There was an average difference of 61.8° between root-up and root-down specimens. Because of this dramatic difference, analyses of DVS bend angles were made only for the root-up specimens for each parameter. The root-down tests do not shed additional light on the effects of the parameters because they are overwhelmingly influenced by the root defect.

4.5.1.1 Pin Diameter

Pin diameter has a very significant relationship with the DVS bend angle. The average bend angle for 6.4 mm pin welds was 46.2°, with a standard deviation of 21.84°. For pin diameters of 9.5 and 12.7 mm, all welds achieved a bend angle of 160°.

4.5.1.2 Feedrate

Feedrate had a stepped effect on the DVS bend angle of the weld. The lower feedrates (51 and 102 mm/min) showed high bend angles, while the higher feedrates investigated (203 and 305 mm/min) resulted in much lower angles.

The means were very similar for feedrates of 51 and 102 mm/min, with one significant difference. Welds made at 51 mm/min bent to an average of 156° then ruptured. For those made at 102 mm/min, no failures were recorded in any of the six specimens tested root-up. All 102 mm/min welds bent to 160° without crack initiation. Welds created at 203 and 305 mm/min were very nearly equivalent in terms of DVS test

performance. At 203 mm/min, a mean of 61.9° was calculated, with a standard deviation of 7.9°. At 305 mm/min, the mean fell only 1.5°.

4.5.1.3 Shoe Temperature

Shoe temperature also had a stepped effect on the DVS bend angle of the welds. Lower shoe temperatures (110 and 127 °C) produced welds of low bend angle capability. Welds produced in this range had means of 54.9° and 66.5°, respectively. Welds made at higher shoe temperatures (143 to 177 °C) showed dramatic improvements in mean DVS bend angle. Welds at 160 °C all surpassed the required 160° bend angle. No statistical difference existed between welds made at 143 and 177 °C.

It is important to note that 143 °C seemed to be a transitional temperature. Among the shoe temperature welds these were those of highest standard deviation, and hence greatest variation among themselves.

4.5.1.4 Pressure Time

Looking at the boxplot for the pressure time experiment (Figure 26) shows the impact that cooling under pressure can have on weld performance. At 30 seconds, the mean is low and the variation among specimens is high. The characteristics improve as the time is increased to 60 seconds. At 90 seconds, the distribution shows a the mean is 160° with no deviation.

The drop in weld performance observed in the 120 second welds is attributed to the lack of any pressure monitoring system. As the shoe length increased, the absolute force and pressure applied through the shoe were unknown.

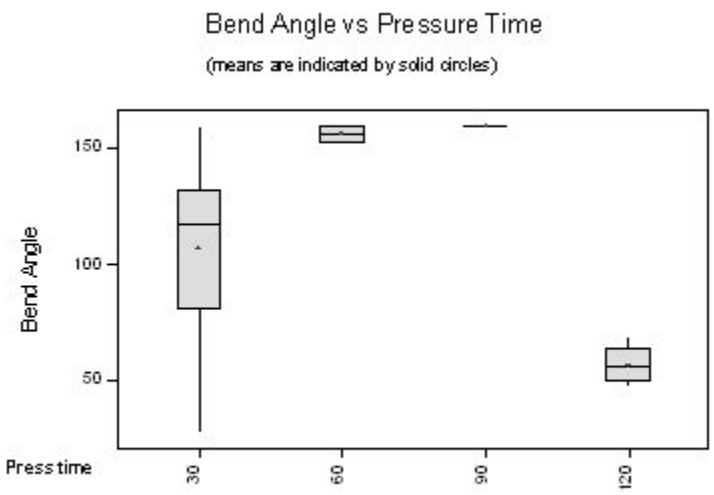

Figure 26- Boxplot of bend angles for pressure time experiment.

4.5.2 Three-Point Bending

4.5.2.1 Root Orientation

It was quickly seen that the root orientation of the specimen also had a marked impact on the performance of the weld in three-point bend tests. Specimens tested root-up outperformed those tested root-down in every case. To examine this effect, the six specimens for each weld were set up as three pairs having one root-up specimen and one root-down. The differences in maximum fiber stress at the point of maximum load were taken, and averaged for the three pairs. The resulting average differences in maximum fiber stress are plotted in Figure 27. There was an average difference in maximum fiber stress of 9.8 MPa. The average differences in the pin diameter, pressure time, and shoe temperature welds were fairly constant, being 7.3, 8.8, and 8.9 MPa respectively. For the feedrate welds, the average difference was 30.3 MPa. The maximum difference was seen in weld F.R.5, being 14.8 MPa.

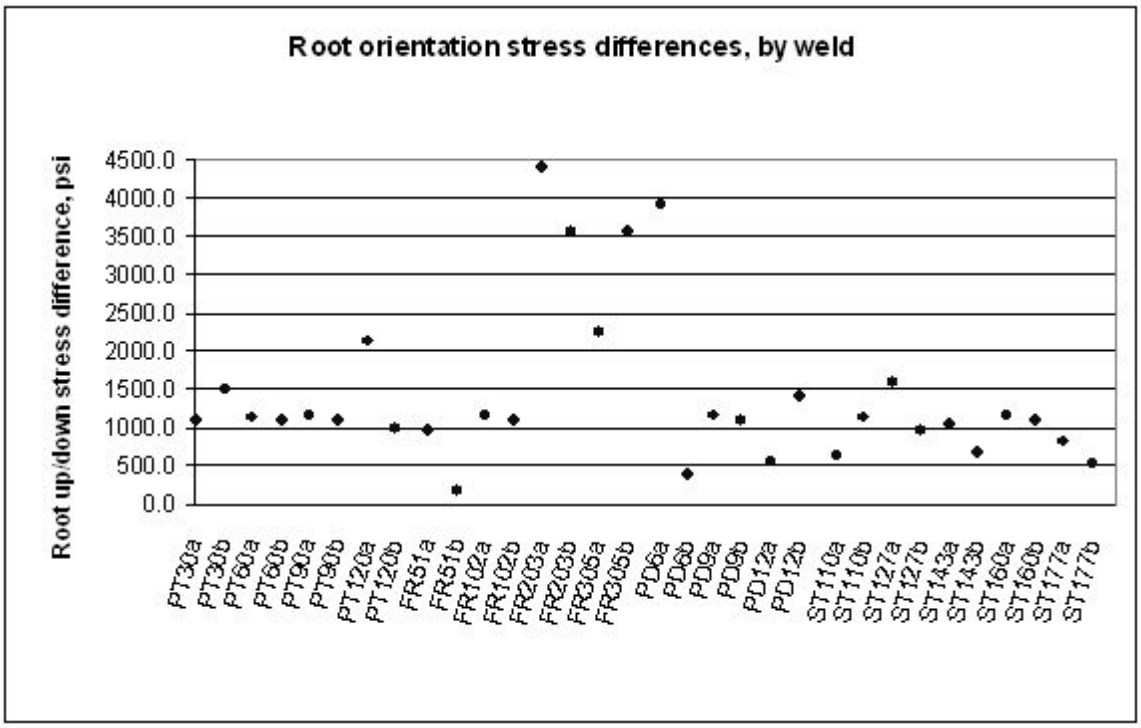

Figure 27- Average root-up/down difference in maximum fiber stress.

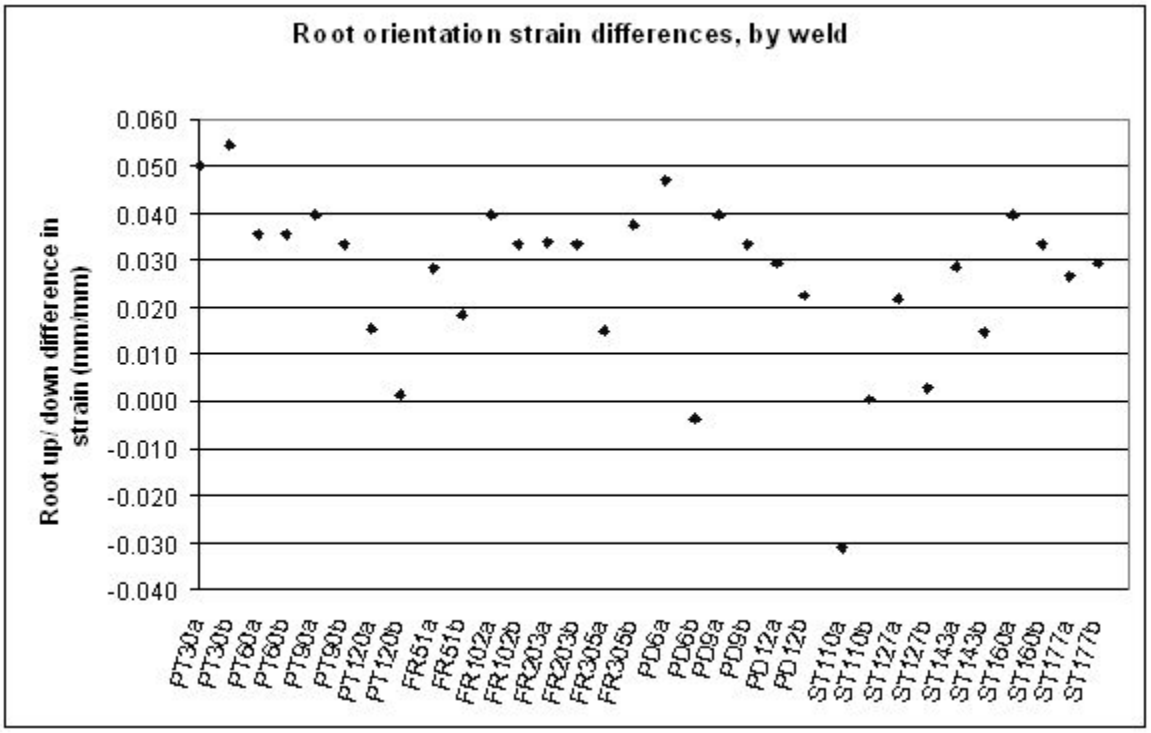

Figure 28- Average root-up/down difference in maximum fiber strain.

A similar analysis was performed with the strain-at-failure results for the three-point bend tests. There was again a distinct difference between the specimens tested root-up and root-down. In this case, two welds showed negative average differences, meaning that the root-down specimens out performed the root-up. The average differences in strain (plotted by weld) are shown in Figure 28. The overall average maximum fiber strain was .026 mm/mm. The parameter averages were as follows: pin diameter .028, feedrate .030, pressure time .033, and shoe temperature .0170 mm/mm.

4.5.2.2 Pin Diameter

The normal probability plot for the maximum fiber strain in the pin diameter experiment is shown as Figure 29. It is typical of the normal probability plots of this research. There are deviations from a straight line, but the general trend is linear. The existence of outliers near the top of the graph was common throughout the research, and is not in itself an indicator of abnormality.

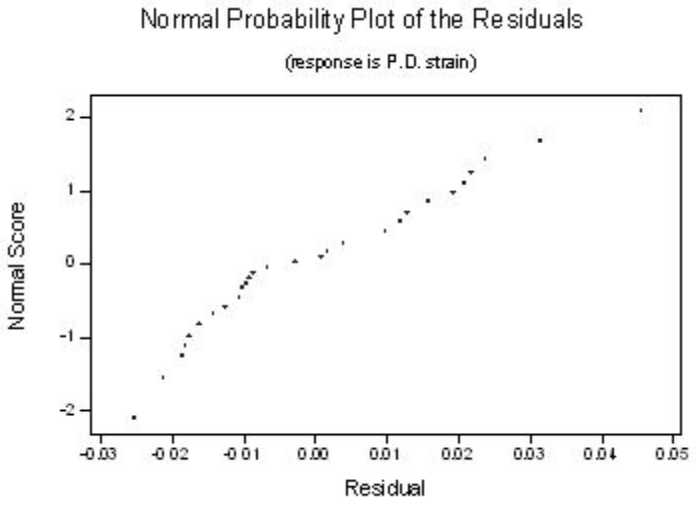

Figure 29- Normal probability plot for maximum fiber strain, pin diameter.

A strong trend exists in the mean maximum fiber stress. As the pin diameter increases, so does the flexural strength of the weld. From 6.4 to 9.5 mm diameter there is a 27% increase in maximum fiber stress. From 6.4 to 12.7 mm diameter, the increase is 35%. Simultaneously, there is a marked decrease in the standard deviation of the specimens. Over the same range of pin diameters, there was a 87% drop in standard deviation. Not only is the weld becoming stronger under bending loads, it is becoming more consistent. This is very easily seen in a boxplot of the pin diameter data, Figure 30.

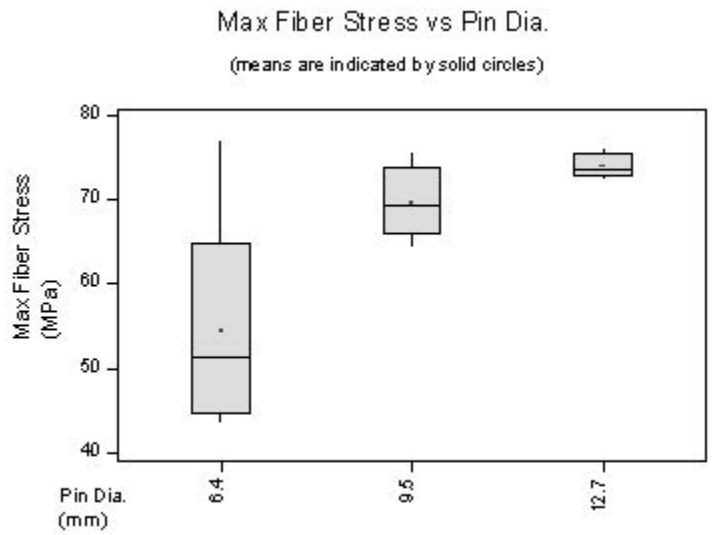

Figure 30- Pin diameter effect on maximum fiber stress.

Statistically, the change in maximum fiber stress is very significant. A P score of 0, and an F score of 19.97 indicate that there is very little chance that random variation in the material or process as responsible for such a change in the maximum fiber stress.

Examining the maximum fiber strain shows a stepwise difference in performance. From 6.4 to 9.5 mm diameter, there was a 69.7% increase in maximum fiber strain at the point of maximum load. From 9.5 to 12.7 there was a 7.9% decrease. This stepped effect indicates that over the range of tools investigated, there is a dramatic improvement from diameters of 6.4 and below to 9.5 and above.

4.5.2.3 Pressure Time

Analyzing the effect of pressure time on the weld flexural properties only left the author with many more questions than at the start. There is a trend in the maximum fiber stress data that is completely counter-intuitive. It was expected that there would be a rapid increase in the properties from low to medium times, which would then turn toward some asymptotic maximum value. Instead, we observed that the maximum fiber stress of the material peaked at 60 seconds, then decreased until at 120 seconds it was lower than at 30 seconds.

Some of the counter-intuitiveness in the data may be explained by examining the research tooling. In this work, no force measurement or control was conducted on the shoe. Without such measurement, there was no guarantee that the pressure being applied to the weld was consistent from weld to weld. This is particularly true as the shoe length increased by 4x when the pressure time changed from 30 to 120 seconds.

4.5.2.4 Feedrate

The results of the feedrate experiment were very much what would be expected– as feedrate increased, weld strength declined. There was a very linear decrease in maximum fiber stress for feedrates of 51- 203 mm/min. Over that range, the mean maximum fiber stress declined by 14 Mpa for each 10 mm/min increase in feedrate. Then the decline ended, and at 305 mm/min the maximum fiber stress had not decreased further. In terms of feedrate's effect on maximum fiber strain, once again we see a stepped affect. There were two distinct levels of performance. For feedrates of 102 mm/min and less, the mean strain was 0.090 mm/mm. For feedrates of 203 mm/min and more, the mean strain was 0.019 mm/mm.

4.5.2.5 Shoe Temperature

Of all welds made during this work, those made for the shoe temperature experiment were the most consistent. They were divided into two groups, one (110-127 °C) with a mean fiber stress of 63.6 MPa and strain of 0.066 mm/mm, the other (143-177 °C) with a mean stress of 69.5 MPa and strain of 0.017 mm/mm. The stepwise

```
Analysis of Variance for Max Fiber Stress
Source     DF        SS        MS         F         P
C           4     490.7     122.7      7.09     0.000
Error      55     951.1      17.3
Total      59    1441.9

                                    Individual 95% CIs For Mean
                                    Based on Pooled StDev
Shoe Temp N     Mean     StDev  ------+---------+---------+---------+
110       12    63.722   4.720  (-------*-------)
127       12    63.610   5.140  (-------*-------)
143       12    69.367   3.531                    (-------*-------)
160       12    69.600   4.260                     (-------*-------)
177       12    69.536   2.674                     (-------*-------)
                                ------+---------+---------+---------+
Pooled StDev =    4.158             63.0      66.0      69.0
```

Figure 31- ANOVA table for shoe temperature maximum fiber stress.

improvement in flexural strength was an increase of 5.9 MPa. Figure 31 shows the confidence intervals created during the ANOVA. It is clear that the two low temperature welds have the same strength, and the three higher temperature welds have equal and higher flexural strengths.

The mean maximum fiber strains of the welds were divided into the same two groups, the lower temperature (110-127 °C) welds averaged 0.066 mm/mm maximum fiber strain while the higher temperature (143-177 °C) welds had more than twice the strain, 0.017 mm/mm average. However, while there is a statistical difference in the means for maximum fiber strain, it is not a significant one.

4.5.3 Weld Microstructures

"Average" microstructures corresponding to each FSW parameter combination were plotted as seen in Figures 32 and 33. The plots allow the visualization of process windows. The effect of the parameter change can be seen by visually comparing the overall microstructural changes are evident. In this section overall changes will be discussed. The effects of the parameters on specific microstructural features will be discussed later.

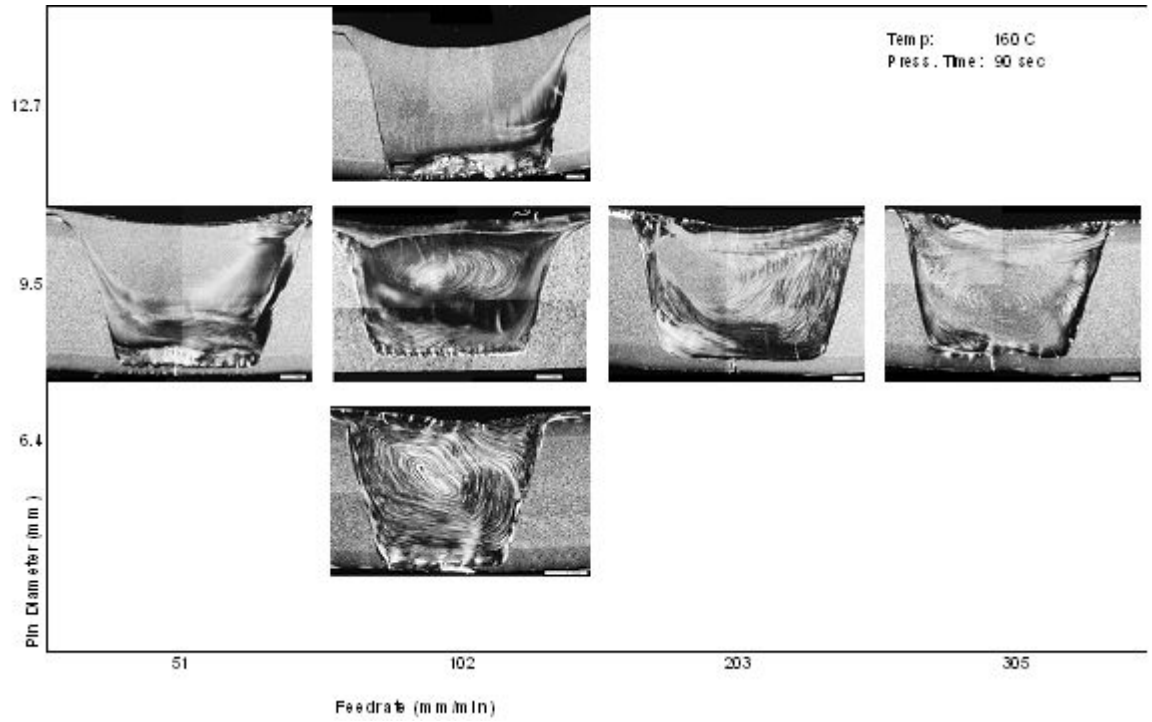

Figure 32- Process effects: feedrate and pin diameter.

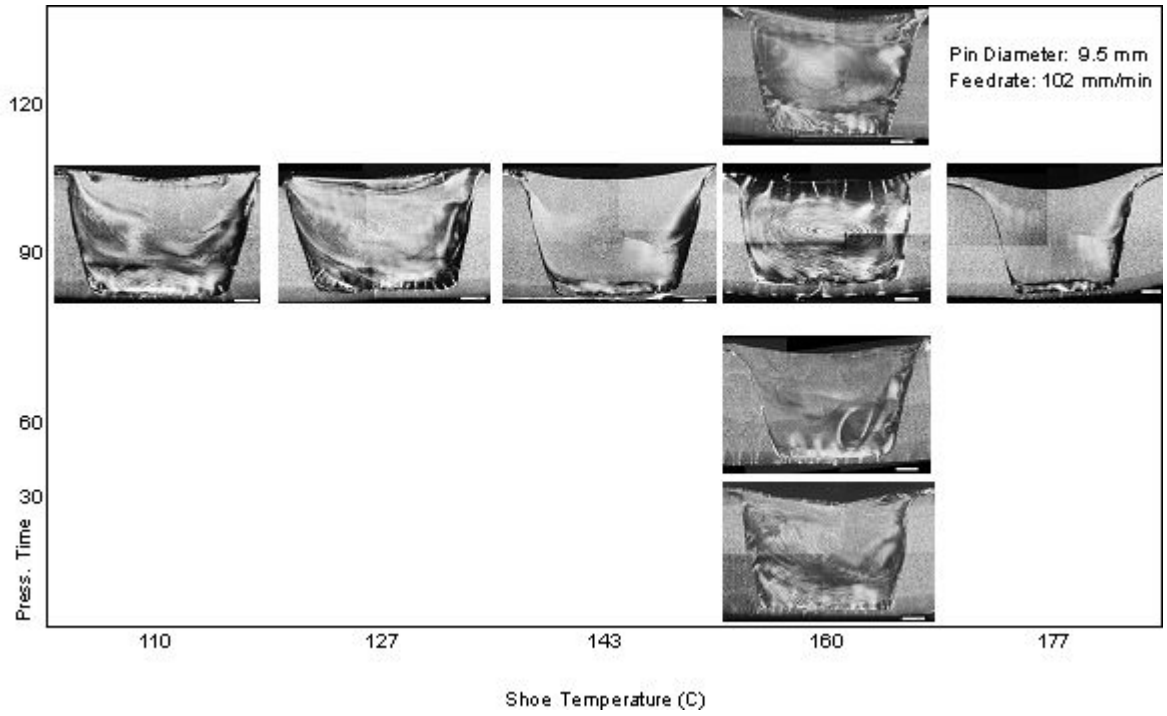

Figure 33- Process effects: shoe temperature and pressure time.

As the pin diameter increases, the structure of the weld region more closely resembles the base material. While the weld made with a 6.4 mm bears no resemblance to the base PP, the vast majority of the 12.7 mm weld maintains a spherulitic structure similar to the base material.

Only a slight difference in overall weld structure occurs as the feedrate increases from 51 to 305 mm/min. The majority of the weld has a spherulitic structure at all levels (excluding 102 mm/min). The area of non-spherulitic material decreases slightly as the feedrate increases.

There is no well-defined change in microstructure as the pressure time increases. This is attributed to the lack of proper control or monitoring of the pressure time during welding. Therefore, pressure time is not included in subsequent statistical analyses of weld microstructure.

Shoe temperature shows a stepped improvement in weld microstructure. At or above 143° C the majority of the weld region shows that the spherulitic structure of the PP has been maintained, with narrow disturbances along the sides and bottom of the weld. Below this temperature, the disturbance areas are much more pronounced, and the area of preserved spherulites shrinks.

4.5.3.1 Bottom Disturbance Depth

Strong relationships were found between the process parameters and the depth of the bottom disturbance zone. Feedrate had a positive effect on the zone depth while pin diameter had a negative effect. Shoe temperature showed no statistically significant effect on the depth of the bottom disturbance zone.

The mean depth of the bottom disturbance decreased from 0.95 mm to 0.55 mm when the feedrate increased from 51 to 305 mm/min. There were two distinct sets of means in the distribution. Feedrates of 51 and 102 mm/min resulted in “deep” bottom disturbances of 0.95 to 1.16 mm. Feedrates of 203 and 305 mm/min resulted in “shallow” bottom disturbances, of 0.55 to 0.59 mm. The ANOVA table (Figure 34) shows the stepped distribution clearly. The P value of 0.008 and F value of 18.78 give

strong indications that changing the feedrate does have a statistically significant effect on the bottom disturbance zone.

```
Analysis of Variance for Bottom Depth
Source     DF        SS        MS        F        P
Feedrate    3   0.51344   0.17115    18.78    0.008
Error       4   0.03645   0.00911
Total       7   0.54989
                                  Individual 95% CIs For Mean
                                  Based on Pooled StDev
Feedrate  N     Mean     StDev  --------+---------+---------+--------
 51       2    0.9450    0.0071                (------*-----)
 102      2    1.1600    0.0849                       (------*-----)
 203      2    0.5500    0.0707  (-----*------)
 305      2    0.5900    0.1556   (------*-----)
                                --------+---------+---------+--------
Pooled StDev =   0.0955              0.60      0.90      1.20
```

Figure 34- ANOVA table for feedrate effects on bottom disturbance depth.

Pin diameter also proved to have a statistically significant effect on the bottom disturbance zone. In this case, the 6.4 mm pin resulted in the shallowest disturbance zone. The disturbance zones created by 9.5 and 12.7 mm diameter pins were nearly 3 times as deep, measuring 1.16 and 1.19 mm respectively. The P value for the pin diameter experiment was 0.004, and the F score was nearly 58.

Shoe temperature showed a somewhat complicated effect. There is a general trend of decreasing zone depth as the temperature increases. The means for 110, 127, 143, and 177 °C are 1.13, 0.62, 0.55, and 0.52 mm. Observing these four points (Figure 35) we see that not only does the mean depth of the zone decrease, but the variation from weld to weld decreases simultaneously by a factor of 4. The calculated P value is 0.004, and the F value is 17.66, both very strong indicators of a statistically significant effect. All of this changes, however, at 160 °C. The welds made at this level had a mean bottom depth of 1.16 mm. This is double what would be expected according to the other four temperatures.

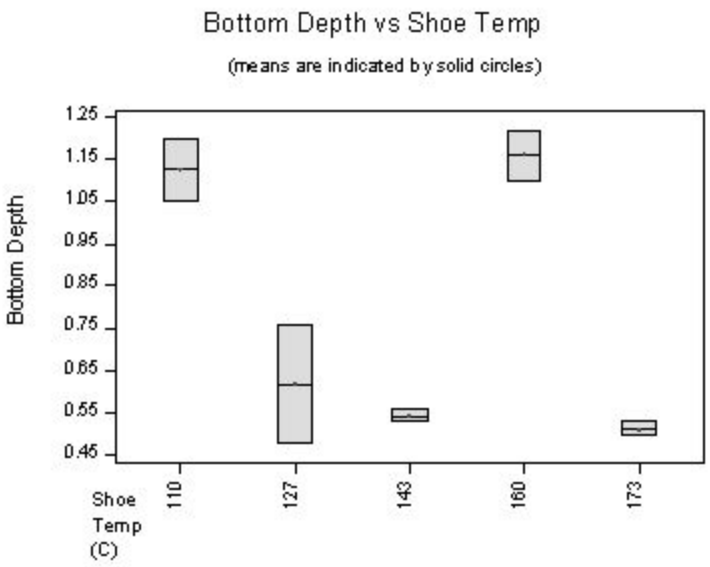

Figure 35- Shoe temperature effect on bottom disturbance.

4.5.3.2 Advancing Interface

The average width of the advancing interface was significantly affected by pin diameter, shoe temperature, and feedrate. As in the case of the bottom disturbance, no significant effect was calculated for pressure time. Increasing any of the three significant parameters decreased the average interface width.

Pin diameter was extremely significant. The 6.4 mm pin created the largest interface, while the 9.5 and 12.7 mm pins resulted in much smaller (and nearly equal) interface zones. As seen in Figure 36, the mean drops by 0.11 mm, or 33% when the pin diameter increases from 6.4 to 12.7 mm. At the same time, there is a marked decrease in the variation between welds, witnessed by the narrowing of the quartile ranges in the boxplot. For the pin diameter experiment, the P value was 0.005 and the F value was calculated to be 51.3. Both of these values indicate that changing the pin diameter was responsible for the change in observed microstructure, and that that change was indeed significant.

Feedrate only affected the advancing interface width over a small range. A feedrate of 51 mm/min resulted in an average interface width of 0.44 mm. Increasing the feedrate to 102 mm/min decreased the interface to 0.23 mm. Beyond this, there was no

further change in the mean. Feedrates of 102 to 305 mm/min all resulted in virtually identical advancing interface zones.

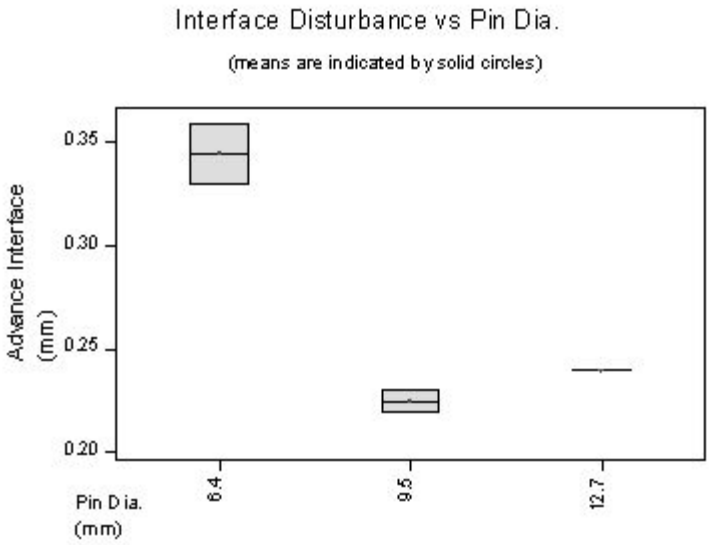

Figure 36- Pin diameter effect on advancing interface.

The final parameter to have a significant effect on the advancing interface was the shoe temperature. In this case, the width of the interface could also be decreased by raising the parameter level, i.e.- increasing the shoe temperature. Once again, a stepwise improvement was observed in the microstructure. Temperatures of 110, 127, and 143 °C resulted in wide interface zones, of at least 0.29 mm. Temperatures of 160 and 177 °C resulted in narrower interfaces, at most 0.24 mm. The P value was still low at 0.032, but was more than 6 times that calculated for the pin diameter experiment.

4.5.3.3 Retreating Interface

There was a linear relationship between the measured interface width and the pin diameter, seen in the ANOVA table for the experiment (Figure 37). As pin diameter increased, the average width of the retreating interface decreased. A pin diameter of 6.4 mm resulted in a retreating interface of 0.35 mm, a 9.5 mm pin 0.17 mm, and a 12.7 mm pin did not create a measurable interface disturbance zone. The significance of the

parameter's effect is emphasized by the low P value of 0.009 and the high F value of 32.76. There was also little variation observed between repeated welds. The standard deviations calculated for the experiment were never greater than 0.07 mm.

```
Analysis of Variance for Retreat Interface
Source     DF        SS        MS         F        P
Pin dia.    2   0.11903   0.05952    32.76    0.009
Error       3   0.00545   0.00182
Total       5   0.12448
                                  Individual 95% CIs For Mean
                                  Based on Pooled StDev
Pin dia. N      Mean     StDev  -------+---------+---------+---------
  6.4    2   0.34500   0.02121                          (-----*-----)
  9.5    5   0.17000   0.07071              (-----*------)
 12.7    2   0.00000   0.00000   (-----*-----)
                                -------+---------+---------+---------
```

Figure 37- ANOVA table for pin diameter effect on retreating interface.

Feedrate showed a marked effect on the retreating interface over a small range of levels. At 51 mm/min, no measurable interface disturbance is created. However, at 102 mm/min the interface is at its largest observed value. Above this, the width decreases once again. Thus, a small change in feedrate can have a dramatic effect on the weld microstructure. The effect of the parameter may not be as drastic, however, when we examine the ANOVA table. A P value of 0.081 is not small enough to state with certainty that the parameter studied is totally responsible fo the change in microstructure. A low F value, 4.85, also introduces uncertainty as to the cause of the change in mean.

Changing the shoe temperature had virtually no effect on the width of the retreating interface. With the exception of 160 °C, all temperatures from 110 to 177 °C resulted in 0.11- 0.12 mm wide retreating interfaces. The P value calculated for the shoe temperature welds was 0.421. This is very high, and is a strong indicator of the absence of a significant effect on weld microstructure due to changing the level of the parameter.

4.5.3.4 Flow Line Severity

Flow lines were only measured within the central region of the welds. They were sorted by the area covered by the flow lines, and the severity of the flow lines observed. Flow lines occurring in the bottom disturbance or interface zones of the weld were not included in this analysis.

A similar affect was observed for pin diameter as in the preceeding experiment. As the diameter of the pin increased, there was an approximately linear decrease in the severity of the flow lines. Welds created with a 6.4 mm pin had severe flow lines covering the entire weld region. Welds made with a 9.5 mm pin showed mild to moderate flow lines, covering most of the central weld zone. Those welds made with a 12.7 mm diameter pin showed no observable flow lines.

Shoe temperature had some effect on the creation of flow lines, but to the same extent as pin diameter. As was seen in the retreating interface observations, there was a general trend of decreasing flow line severity as the shoe temperature increased. The 160 °C welds were again an anomaly. As seen in Figure 38, the flow line severity drops from mild in welds of 110 and 127 °C to none in welds of 143 and 176 °F. At 160 °C, there is a sudden increase to moderate severity in the observed flow lines. For this sudden change, the author has no explanation.

Too much variation existed between weld repetitions to establish the effect of feedrate on the severity of flow lines in the weld regions. There is no statistical difference in the means between the various feedrates, and in all cases the difference in means is less than one standard deviation.

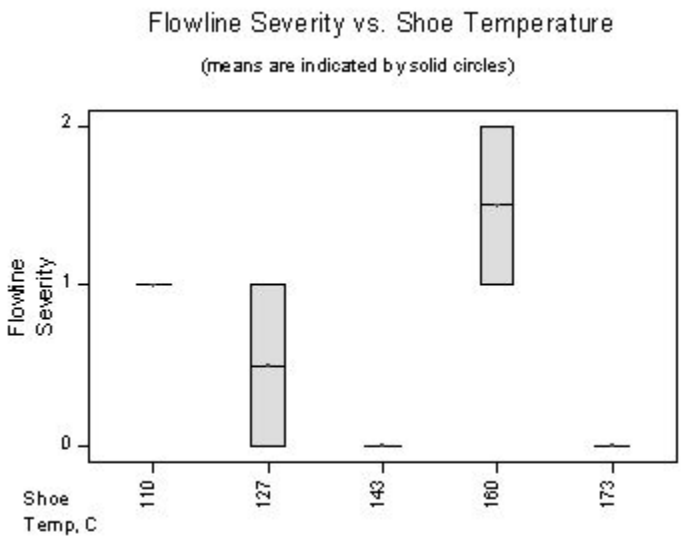

Figure 38- Shoe temperature effects on flow line severity.

4.5.3.5 Onion Ring Severity

As defined earlier, onion ring is a specific type of flow line. Therefore, it is expected that the effect of any one parameter will be much the same for both microstructure types. This was the case in the current work. The effects observed for onion ring were not as strong as those in the flow line observations, but they did follow a similar pattern. Increasing the pin diameter decreased the severity of the onion ring structure. However, shoe temperature and feedrate showed no significant effect.

The severity of the onion ring structures observed in welds made by 6.4 and 95 mm pins were roughly the same- moderate to severe. Welds made with the 12.7 mm pins showed no measurable onion ring formation.

No clear relationship could be established between feedrate and onion ring structures. As feedrate increases, there is a slight increase in the severity of observed onion ring structures. However, this general trend does not hold true for the 102 cpm feedrate. At this level, moderate and severe areas were seen.

Onion ring structures were only observed in welds made at two shoe temperatures- 127 and 160 °C. In the welds made with the 127 °C shoe, mild onion ring areas were present. Severe areas of onion ring were identified in the welds made with a

160 °C shoe. Because of the oscillating pattern seen in the data (Figure 39) no relationship could be established.

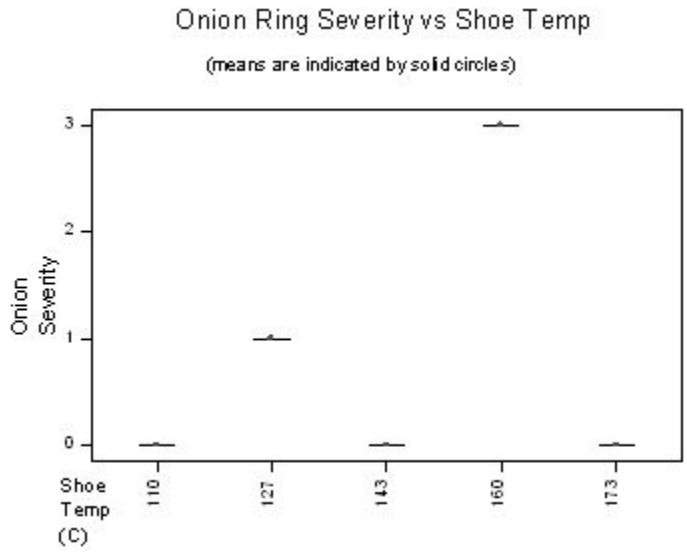

Figure 39-Shoe temperature effects on onion ring severity.

4.6 Conclusions

4.6.1 Effects of Process Parameters on Flexural Properties

Three of the four parameters studied had statistically significant effects on the DVS bend angle performance of the welded joint. A large pin diameter was favorable, resulting in a 25% improvement in bend angle before failure. A slow feedrate proved best, a setting of 51 mm/min showing an increase of 13% over the next best. A high shoe temperature was best, with a temperature of 177 °C being 20% better than 110 °C. However, it is important to note that only a slight improvement (2%) was achieved by increasing from 160 to 177 °C. Therefore, it is the conclusion of the author that welding with a 160 °C shoe will be most efficient.

All FSW joints surpassed the minimum performance for "good weld" classification. Every weld parameter combination created a "good weld" according to the 50° requirement (hot-gas, extrusion, etc.) Of the thirty two welds created, twenty surpassed the required 85° for "good weld" classification for hot-plate welds, the most

stringent DVS requirement. This is significant in that even relatively poor performing FSW joints will perform as well as welds produced by most traditional welding processes.

As to the mechanical performance of the welded joint, the results are the same. A large pin resulted in welds of superior maximum fiber stress and strain. Shoe temperature also had a positive effect; as the temperature increased, so did the weld performance. Low feedrates resulted in the best performance, both in terms of maximum fiber stress and maximum fiber strain.

4.6.2 Effect of Process Parameters on Weld Microstructure

Four common microstructural zones were found to exist in the FSW joint. These are a bottom disturbance zone, an interface zone along the tool edge on both the advancing and retreating side of the tool, and the central zone.

Three typical weld microstructure types were identified. The base material is made up of spherulites, individual entanglements of multiple polymer chains. Each spherulite has both crystalline and amorphous regions. This spherulitic structure is the principle microstructure of the material. Flow lines were identified as areas of organized microstructure, consisting of alternating bands of crystalline and amorphous material. Onion ring was defined as a special case of flow lines, where the lines formed complete concentric annular rings.

The hypothesis that the weld which most closely approximated the microstructure of the base material would demonstrate the best performance was proven correct. In terms of both DVS bend angle before failure and maximum fiber stress and strain at ultimate flexural load, the weld that looked most like the base material did in fact have the best performance.

Three of the four parameters studied had significant effects on the microstructure of the weld. A large pin diameter (12.7 mm) resulted in a superior microstructure in all cases. Using the large pin resulted in the smallest bottom and interface disturbance zones, and eliminated the formation of flow lines within the weld zone. A low feedrate was also desirable, resulting in the least severe flow lines, onion ring, and retreating

interface. In three of the five microstructural observations, shoe temperature had little effect. In flow lines and advancing interface, where strong effects were found, a high (160- 177 °C) shoe temperature was favorable.

CHAPTER 5

Recommendations for Future Work

Friction Stir Welding has only begun to be developed as a viable joining option for polymeric materials. This is the first work dedicated to the processing effects on the microstructure of the material, and to attempt to establish the relationships between operational parameters, weld microstructure, and mechanical properties.

Many opportunities exist for the improvement of the process, and the enlargement of its capabilities. Here the author lists only four areas of research. They are the vital areas of work if FSW of polymers is to become a widely accepted, widely used polymer welding technique.

5.1 Molecular Weight

One of the fundamental properties of any polymer is molecular weight. Questions regarding how FSW affects the average molecular weight and the molecular weight distribution of the polymer must be answered. Many physical, chemical, and mechanical properties are directly related to the molecular weight of the polymer, and if those are to be preserved, the effects of the process on this issue must be known.

5.2 Spherulite Size

In the course of the microstructure study reported herein the author often wondered what the true average spherulite size was– both of the base material and the weld zone. If the theory is correct that the maximum joint efficiency is achieved when the weld material and base material are the same, then knowing the spherulite size is crucial to the success of a FSW joint.

Simply knowing how the current technology (tooling, speeds, feedrates, etc.) changes the spherulite size would be a great step forward. However, even more powerful

would be an understanding of why the process changes the spherulitic structure, and how to control those changes. Preserving the spherulitic structure may well involve a fundamental evolution in FSW technology. New tooling may be required, as well as new techniques.

5.3 Tooling Issues

As stated earlier, the only tool parameter considered in this work was the major diameter of the pin. Much work lies ahead in developing a robust, industrial tooling scheme. So many parameters of the tooling need to be addressed– pin size, shape, material, thread style and geometry; all these and many more must be studied and understood.

Methods of tool construction also need to be revisited. The current technology is functional, but has a very short useable lifetime.

The author believes that one of the most critical tooling issues to address is that of applying pressure to the weld as it cools. Whether manufacturing discrete parts or continuous, this technology will be vital to the success of the process.

5.4 Microscopy Technique

At the outset of this research, no methodology for the microscopy of polymer welds could be found. Thus, all the techniques employed herein were developed principally by the author, with very valuable assistance from a few associates. It is highly recommended that this foundation be built upon, and that a better method for microscopic evaluation be developed.

Of particular benefit would be the development of an optical system capable of imaging the entire weld region in a single photograph. The creation of collages is not only time consuming, but results in non-uniformly lit images.

APPENDIX 1

Tool Drawings

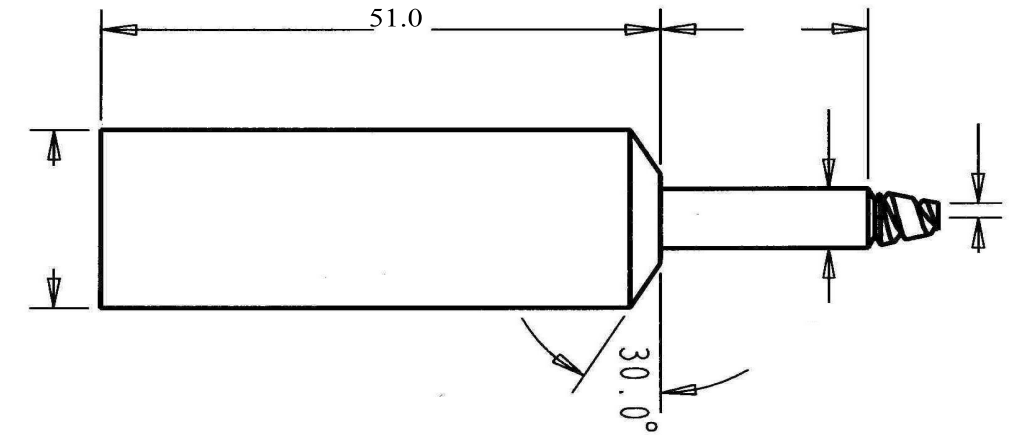
51.0
30.0°

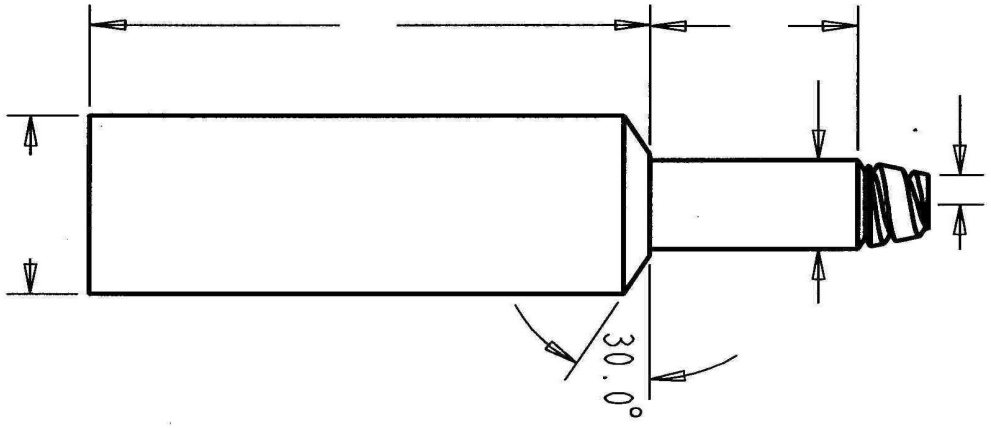
30.0°

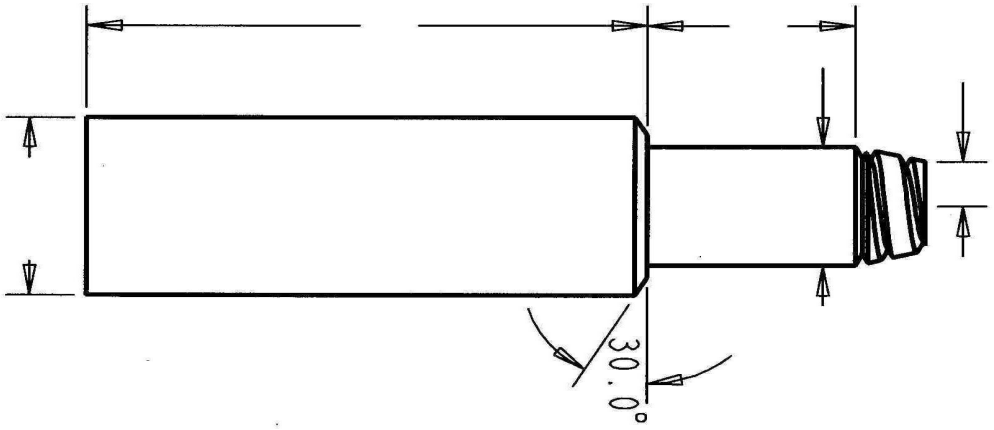
30.0°

REVISIONS				
ZONE	REV.	DESCRIPTION	DATE	APPROVED

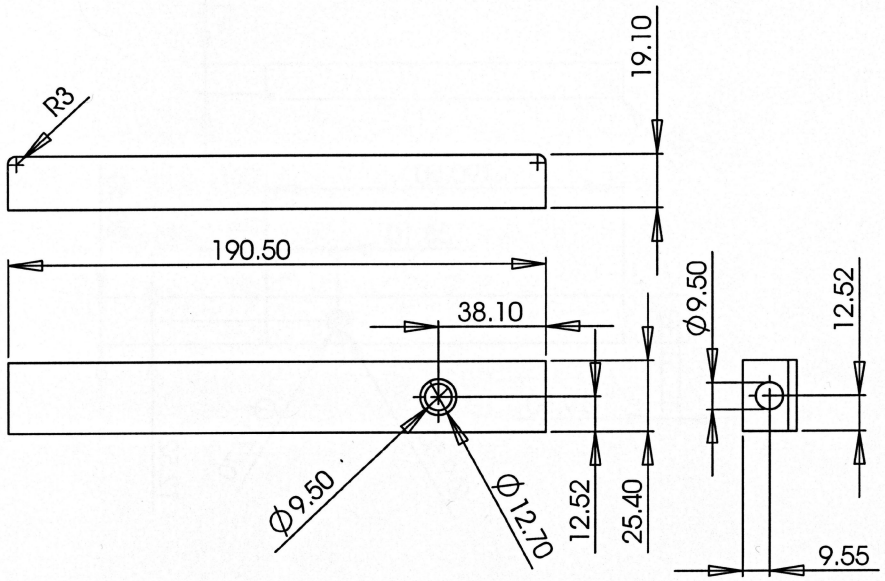

		DIMENSIONS ARE IN INCHES TOLERANCES: FRACTIONAL ± ANGULAR: MACH ± BEND ± TWO PLACE DECIMAL ± THREE PLACE DECIMAL ±		NAME	DATE
			DRAWN		
			CHECKED		
			ENG APPR.		
			MFG APPR.		
		MATERIAL	Q.A.		
			COMMENTS:		
NEXT ASSY	USED ON	FINISH			
APPLICATION		DO NOT SCALE DRAWING			

SIZE	DWG. NO.	REV.
A	6.4 mm Shoe	
SCALE: 1:2	WEIGHT:	SHEET 1 OF 1

REVISIONS				
ZONE	REV.	DESCRIPTION	DATE	APPROVED

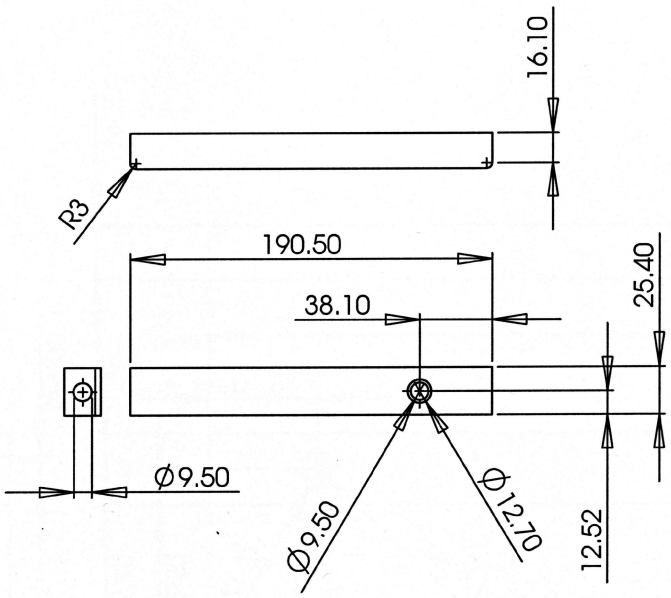

NEXT ASSY	USED ON	
APPLICATION		

DIMENSIONS ARE IN INCHES
TOLERANCES:
FRACTIONAL ±
ANGULAR: MACH ± BEND ±
TWO PLACE DECIMAL ±
THREE PLACE DECIMAL ±

MATERIAL

FINISH

DO NOT SCALE DRAWING

	NAME	DATE
DRAWN		
CHECKED		
ENG APPR.		
MFG APPR.		
Q.A.		

COMMENTS:

SIZE	DWG. NO.	REV.
A	9.5 mm Shoe	
SCALE:1:3	WEIGHT:	SHEET 1 OF 1

REVISIONS				
ZONE	REV.	DESCRIPTION	DATE	APPROVED

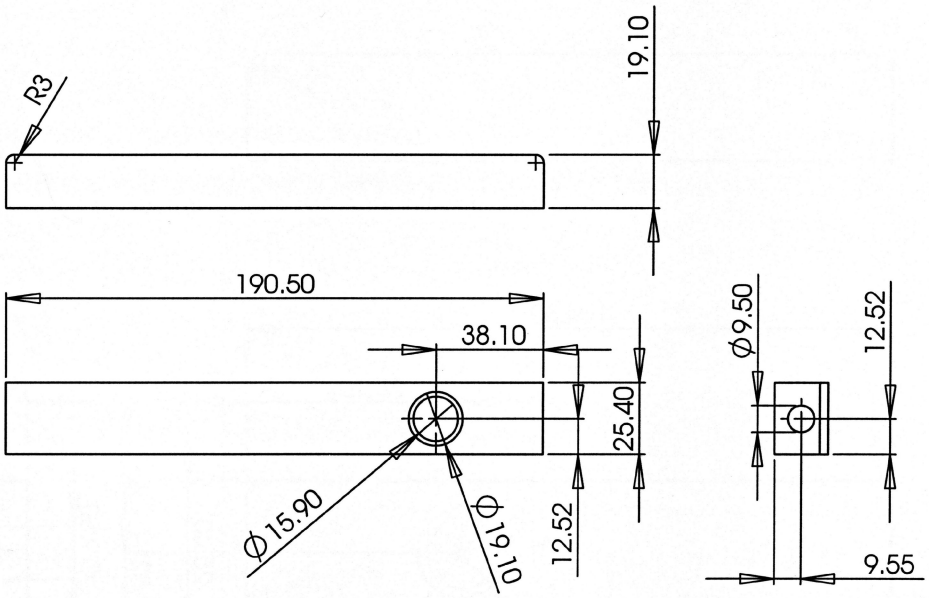

PROPRIETARY AND CONFIDENTIAL

THE INFORMATION CONTAINED IN THIS DRAWING IS THE SOLE PROPERTY OF <INSERT COMPANY NAME HERE>. ANY REPRODUCTION IN PART OR AS A WHOLE WITHOUT THE WRITTEN PERMISSION OF <INSERT COMPANY NAME HERE> IS PROHIBITED.

NEXT ASSY	USED ON
APPLICATION	

DIMENSIONS ARE IN INCHES
TOLERANCES:
FRACTIONAL ±
ANGULAR: MACH ± BEND ±
TWO PLACE DECIMAL ±
THREE PLACE DECIMAL ±

MATERIAL

FINISH

DO NOT SCALE DRAWING

	NAME	DATE
DRAWN		
CHECKED		
ENG APPR.		
MFG APPR.		
Q.A.		

COMMENTS:

SIZE	DWG. NO.	REV.
A	12.7 mm Shoe	
SCALE:1:2	WEIGHT:	SHEET 1 OF 1

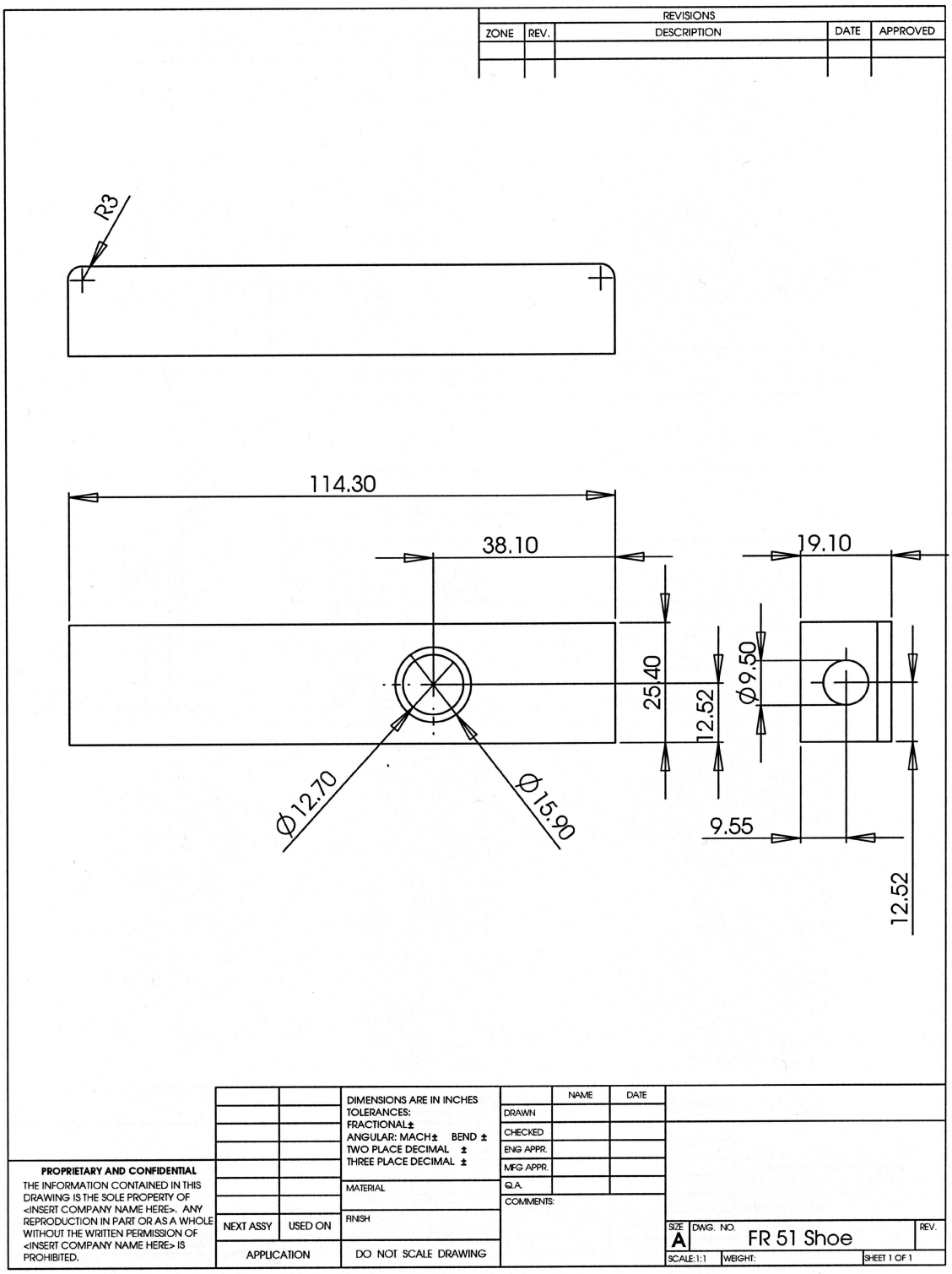
REVISIONS
ZONE
REV.
DESCRIPTION
DATE
APPROVED
R3
114.30
38.10
19.10
25.40
12.52
Ø9.50
Ø12.70
Ø15.90
9.55
12.52
PROPRIETARY AND CONFIDENTIAL
THE INFORMATION CONTAINED IN THIS DRAWING IS THE SOLE PROPERTY OF <INSERT COMPANY NAME HERE>. ANY REPRODUCTION IN PART OR AS A WHOLE WITHOUT THE WRITTEN PERMISSION OF <INSERT COMPANY NAME HERE> IS PROHIBITED.
NEXT ASSY
USED ON
APPLICATION
DIMENSIONS ARE IN INCHES
TOLERANCES:
FRACTIONAL ±
ANGULAR: MACH ± BEND ±
TWO PLACE DECIMAL ±
THREE PLACE DECIMAL ±
MATERIAL
FINISH
DO NOT SCALE DRAWING
NAME
DATE
DRAWN
CHECKED
ENG APPR.
MFG APPR.
Q.A.
COMMENTS:
SIZE
A
DWG. NO.
FR 51 Shoe
REV.
SCALE:1:1
WEIGHT:
SHEET 1 OF 1

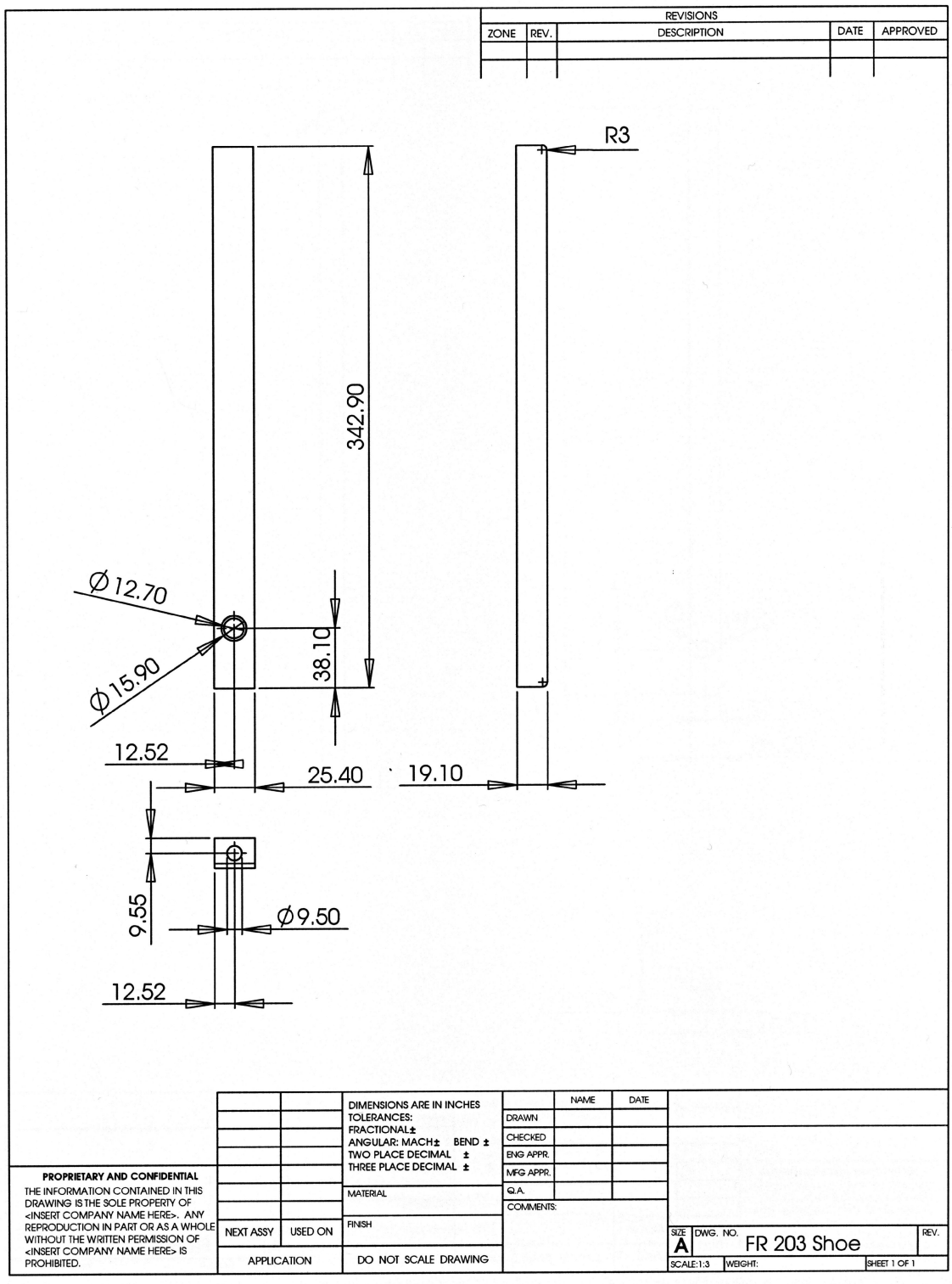
REVISIONS
ZONE
REV.
DESCRIPTION
DATE
APPROVED
R3
342.90
Ø12.70
Ø15.90
38.10
12.52
25.40
19.10
9.55
Ø9.50
12.52
PROPRIETARY AND CONFIDENTIAL
THE INFORMATION CONTAINED IN THIS DRAWING IS THE SOLE PROPERTY OF <INSERT COMPANY NAME HERE>. ANY REPRODUCTION IN PART OR AS A WHOLE WITHOUT THE WRITTEN PERMISSION OF <INSERT COMPANY NAME HERE> IS PROHIBITED.
NEXT ASSY
USED ON
APPLICATION
DIMENSIONS ARE IN INCHES
TOLERANCES:
FRACTIONAL±
ANGULAR: MACH± BEND ±
TWO PLACE DECIMAL ±
THREE PLACE DECIMAL ±
MATERIAL
FINISH
DO NOT SCALE DRAWING
NAME
DATE
DRAWN
CHECKED
ENG APPR.
MFG APPR.
Q.A.
COMMENTS:
SIZE
A
DWG. NO.
FR 203 Shoe
REV.
SCALE:1:3
WEIGHT:
SHEET 1 OF 1

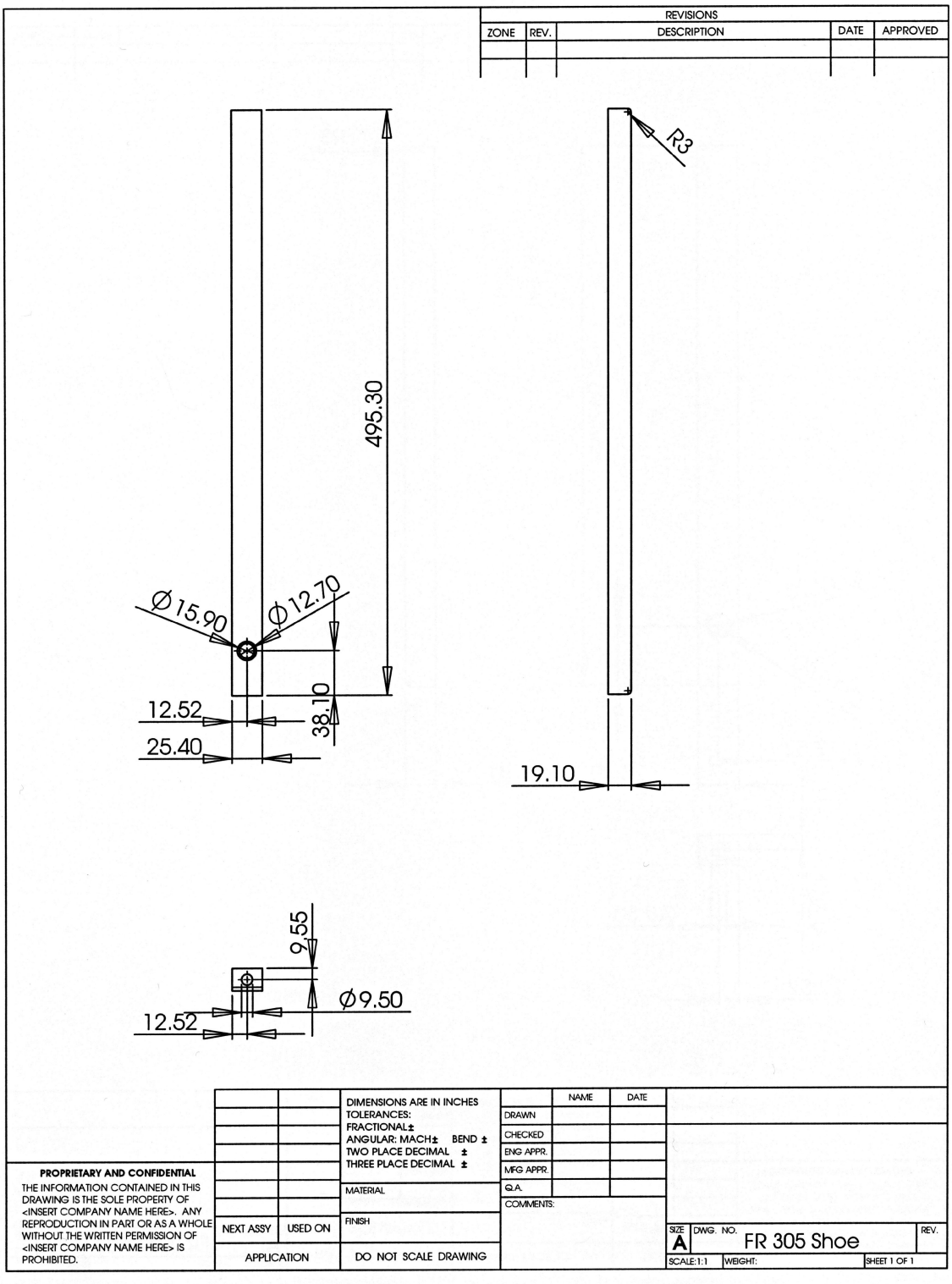
REVISIONS
ZONE
REV.
DESCRIPTION
DATE
APPROVED
R3
495.30
Ø15.90
Ø12.70
12.52
25.40
38.10
19.10
9.55
Ø9.50
12.52
PROPRIETARY AND CONFIDENTIAL
THE INFORMATION CONTAINED IN THIS DRAWING IS THE SOLE PROPERTY OF <INSERT COMPANY NAME HERE>. ANY REPRODUCTION IN PART OR AS A WHOLE WITHOUT THE WRITTEN PERMISSION OF <INSERT COMPANY NAME HERE> IS PROHIBITED.
NEXT ASSY
USED ON
APPLICATION
DIMENSIONS ARE IN INCHES
TOLERANCES:
FRACTIONAL±
ANGULAR: MACH± BEND ±
TWO PLACE DECIMAL ±
THREE PLACE DECIMAL ±
MATERIAL
FINISH
DO NOT SCALE DRAWING
NAME
DATE
DRAWN
CHECKED
ENG APPR.
MFG APPR.
Q.A.
COMMENTS:
SIZE
A
DWG. NO.
FR 305 Shoe
REV.
SCALE:1:1
WEIGHT:
SHEET 1 OF 1

REVISIONS				
ZONE	REV.	DESCRIPTION	DATE	APPROVED

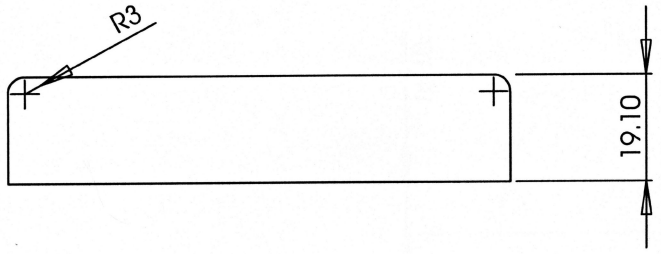

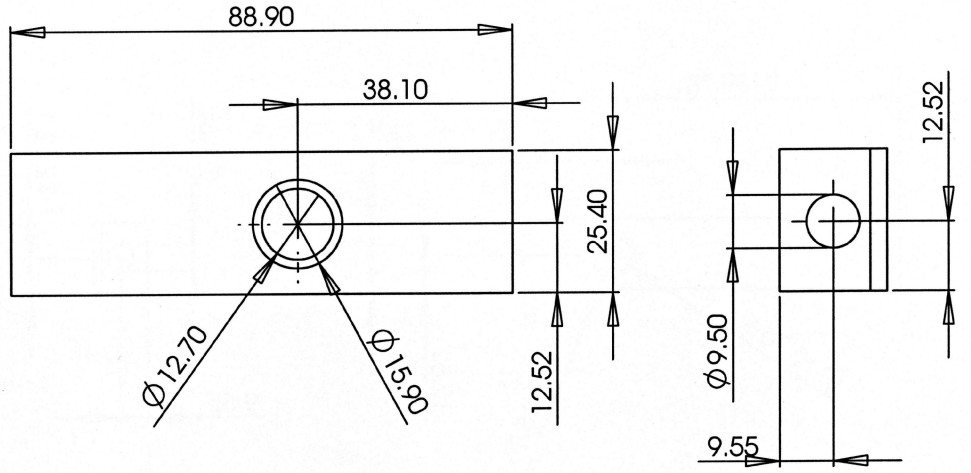

		DIMENSIONS ARE IN INCHES TOLERANCES: FRACTIONAL ± ANGULAR: MACH ± BEND ± TWO PLACE DECIMAL ± THREE PLACE DECIMAL ±		NAME	DATE
			DRAWN		
			CHECKED		
			ENG APPR.		
			MFG APPR.		
		MATERIAL	Q.A.		
NEXT ASSY	USED ON	FINISH	COMMENTS:		
APPLICATION		DO NOT SCALE DRAWING			

SIZE	DWG. NO.	REV.
A	pt30 shoe	
SCALE:1:1	WEIGHT:	SHEET 1 OF 1

REVISIONS				
ZONE	REV.	DESCRIPTION	DATE	APPROVED

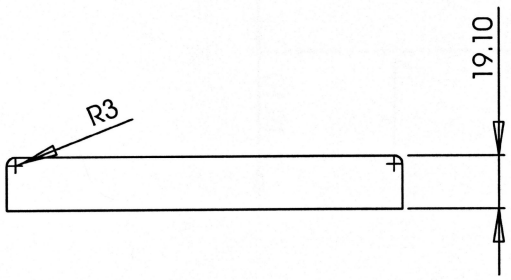

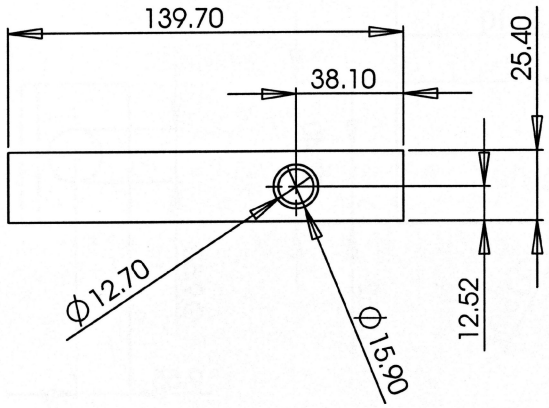

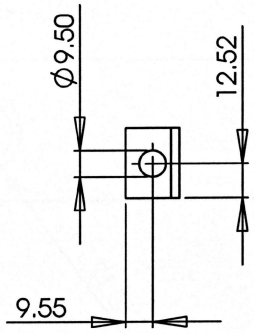

		DIMENSIONS ARE IN INCHES TOLERANCES: FRACTIONAL± ANGULAR: MACH± BEND ± TWO PLACE DECIMAL ± THREE PLACE DECIMAL ±		NAME	DATE	
			DRAWN			
			CHECKED			
			ENG APPR.			
			MFG APPR.			
		MATERIAL	Q.A.			
			COMMENTS:			
NEXT ASSY	USED ON	FINISH				
APPLICATION		DO NOT SCALE DRAWING				

PROPRIETARY AND CONFIDENTIAL

THE INFORMATION CONTAINED IN THIS DRAWING IS THE SOLE PROPERTY OF <INSERT COMPANY NAME HERE>. ANY REPRODUCTION IN PART OR AS A WHOLE WITHOUT THE WRITTEN PERMISSION OF <INSERT COMPANY NAME HERE> IS PROHIBITED.

SIZE	DWG. NO.	REV.
A	pt60shoe	
SCALE:1:1	WEIGHT:	SHEET 1 OF 1

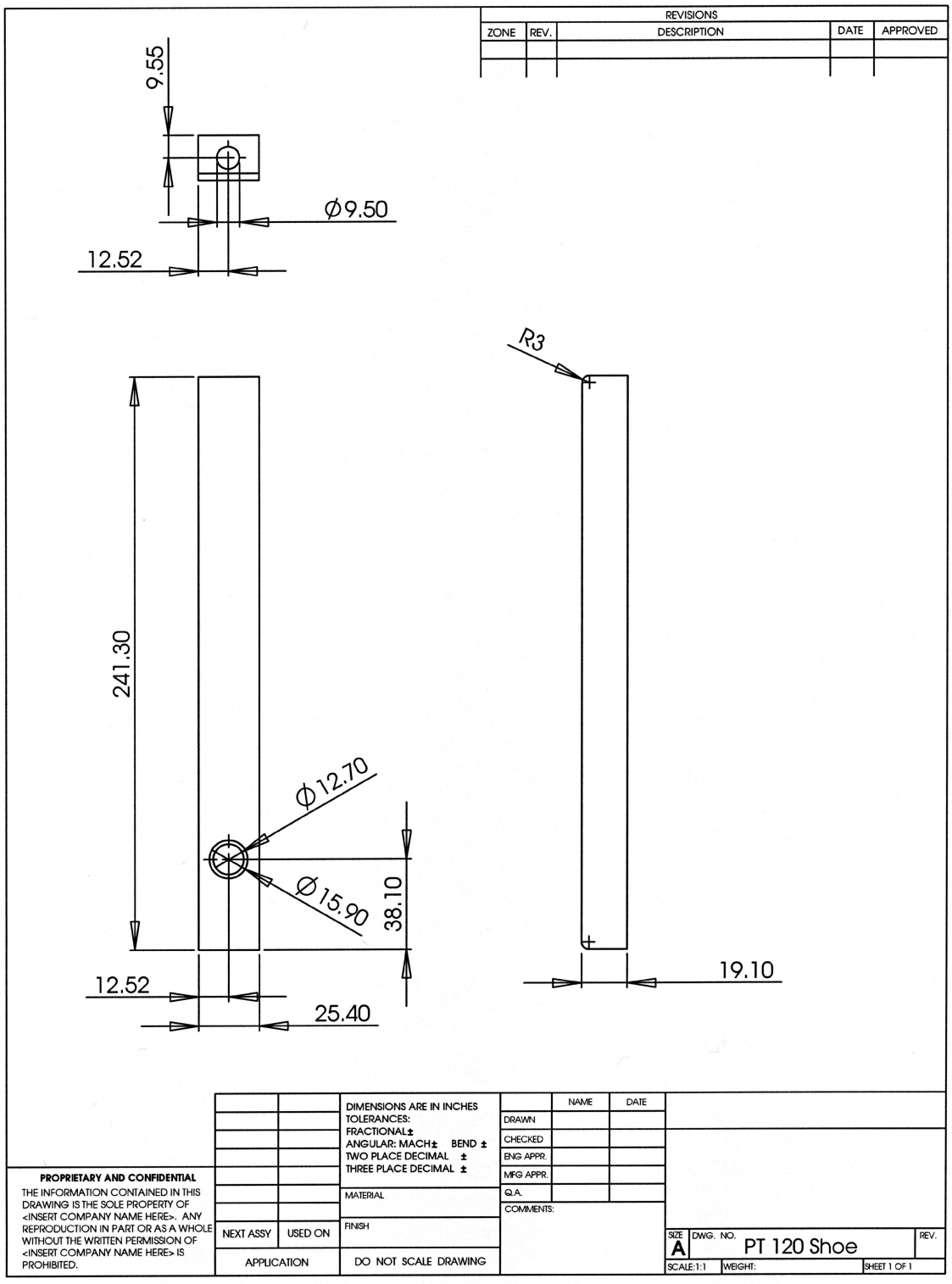
REVISIONS
ZONE
REV.
DESCRIPTION
DATE
APPROVED
9.55
Ø9.50
12.52
R3
241.30
Ø12.70
Ø15.90
38.10
12.52
25.40
19.10
DIMENSIONS ARE IN INCHES
TOLERANCES:
FRACTIONAL±
ANGULAR: MACH± BEND ±
TWO PLACE DECIMAL ±
THREE PLACE DECIMAL ±
MATERIAL
FINISH
DO NOT SCALE DRAWING
NEXT ASSY
USED ON
APPLICATION
NAME
DATE
DRAWN
CHECKED
ENG APPR.
MFG APPR.
Q.A.
COMMENTS:
SIZE
A
DWG. NO.
PT 120 Shoe
REV.
SCALE:1:1
WEIGHT:
SHEET 1 OF 1
PROPRIETARY AND CONFIDENTIAL
THE INFORMATION CONTAINED IN THIS DRAWING IS THE SOLE PROPERTY OF <INSERT COMPANY NAME HERE>. ANY REPRODUCTION IN PART OR AS A WHOLE WITHOUT THE WRITTEN PERMISSION OF <INSERT COMPANY NAME HERE> IS PROHIBITED.

APPENDIX 2

DVS Bend Angle Conversion

	Base material		Root-up, 8°		Root-up, 13°	
Bend Angle (°)	Angle (°)	Ram Disp. (mm)	Angle (°)	Ram Disp. (mm)	Angle (°)	Ram Disp. (mm)
0	180	0.00	188	0.00	193	0.00
5	175	1.09	183	1.17	188	1.63
10	170	2.41	178	2.54	183	3.12
15	165	3.68	173	3.89	178	4.62
20	160	4.95	168	5.28	173	6.22
25	155	6.22	163	6.71	168	7.57
30	150	7.49	158	7.98	163	8.99
35	145	8.73	153	9.35	158	10.64
40	140	9.99	148	10.67	153	12.11
45	135	11.25	143	12.03	148	13.62
50	130	13.61	138	13.38	143	15.12
55	125	14.63	133	14.72	138	18.01
60	120	15.65	128	16.07	133	19.28
65	115	17.27	123	17.42	128	20.80
70	110	18.64	118	18.77	123	22.10
75	105	19.91	113	20.12	118	23.39
80	100	21.18	108	21.47	113	24.79
85	95	23.22	103	22.81	108	26.52
90	90	24.40	98	24.17	103	28.25
95	85	25.85	93	25.51	98	29.82
100	80	27.30	88	26.86	93	31.39
105	75	28.76	83	28.21	88	32.96
110	70	30.21	78	29.56	83	34.53
115	65	31.66	73	30.91	78	36.10
120	60	33.12	68	32.26	73	37.67
125	55	34.57	63	33.61	68	39.24
130	50	36.02	58	34.96	63	40.81
135	45	37.47	53	36.31	58	42.38
140	40	38.93	48	37.65	53	43.95
145	35	40.38	43	39.00	48	45.52
150	30	41.83	38	40.35	43	47.09
155	25	43.29	33	41.70	38	48.66
160	20	44.74	28	43.05	33	50.23

	Root-down, 8°		Root-down, 13°	
Bend Angle (°)	Angle (°)	Ram Disp. (mm)	Angle (°)	Ram Disp. (mm)
0	172	0.00	167	0.00
5	167	1.37	162	1.27
10	162	2.39	157	2.64
15	157	3.66	152	4.17
20	152	4.98	147	5.46
25	147	6.27	142	6.76
30	142	7.60	137	8.05
35	137	8.89	132	9.65
40	132	10.09	127	10.62
45	127	11.36	122	12.01
50	122	12.62	117	13.59
55	117	13.89	112	15.09
60	112	15.15	107	16.36
65	107	16.42	102	17.66
70	102	17.69	97	19.02
75	97	18.95	92	20.38
80	92	20.22	87	21.74
85	87	21.48	82	23.10
90	82	22.74	77	24.45
95	77	24.00	72	25.80
100	72	25.26	67	27.15
105	67	26.52	62	28.50
110	62	27.79	57	29.86
115	57	29.05	52	31.21
120	52	30.31	47	32.56
125	47	31.58	42	33.91
130	42	32.84	37	35.27
135	37	34.10	32	36.62
140	32	35.36	27	37.97
145	27	36.63	22	39.32
150	22	37.89	17	40.68
155	17	39.15	12	42.03
160	12	40.42	7	43.38

APPENDIX 3

Weld Micrographs

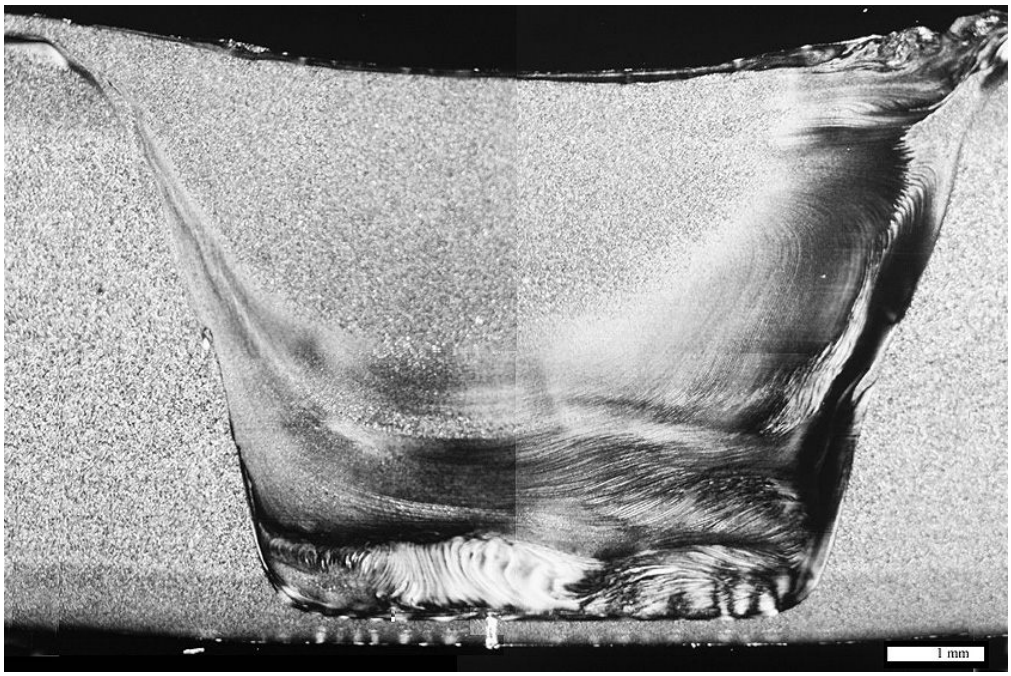

FR51a

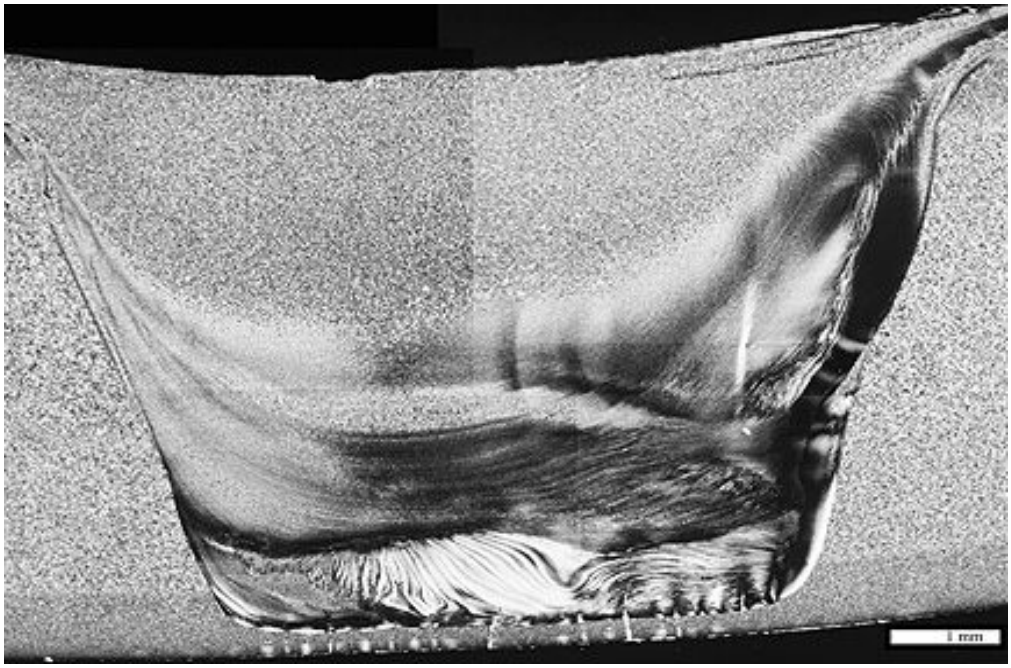

FR51b

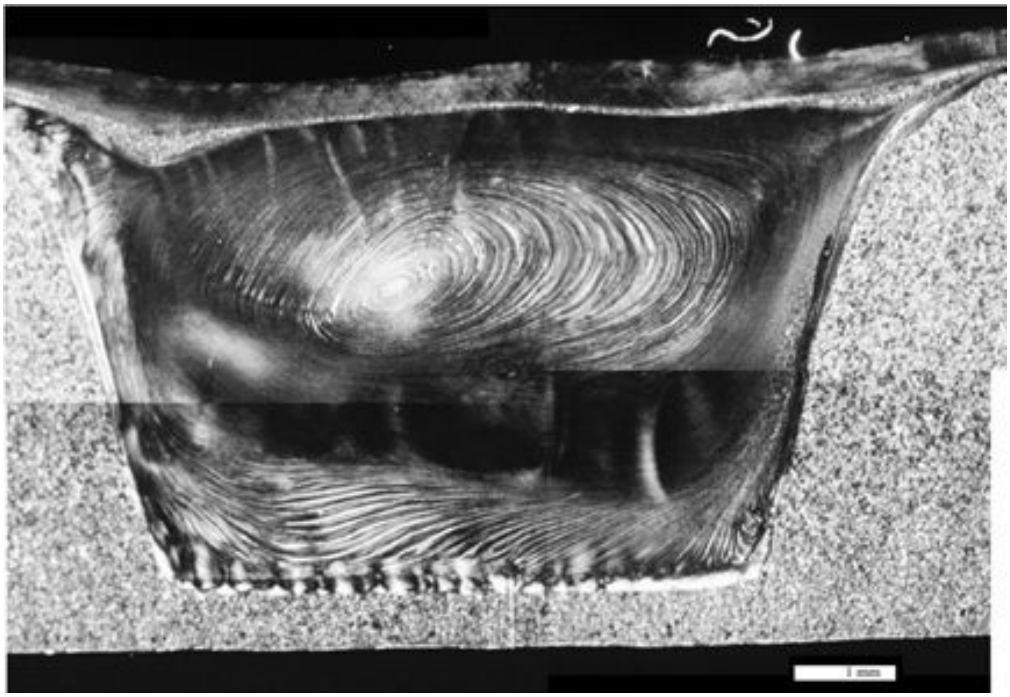

FR102a

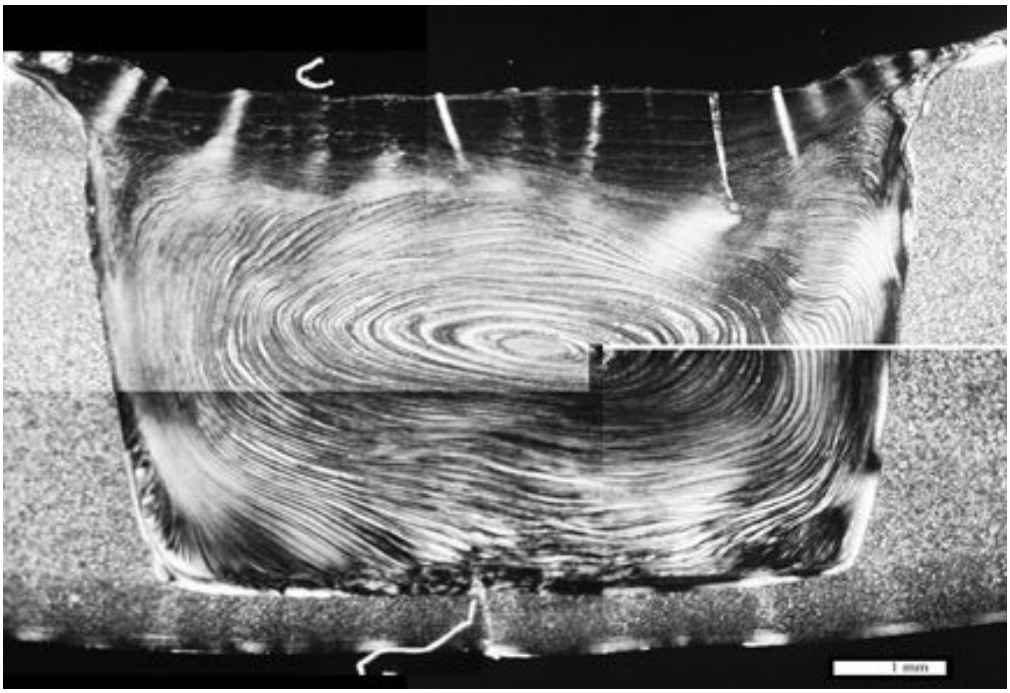

FR102b

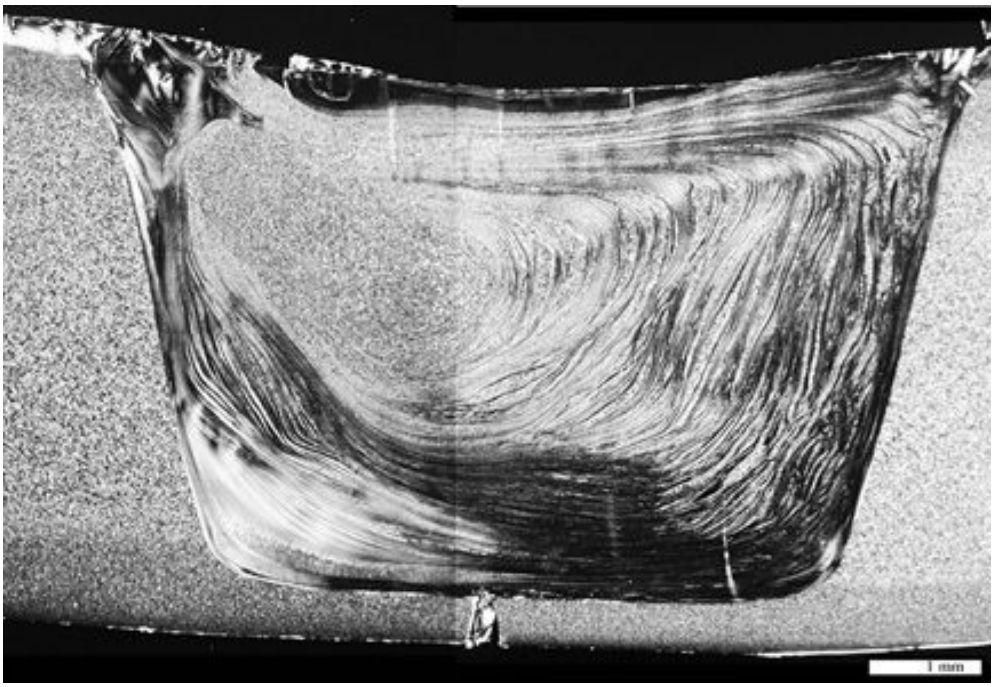

FR203a

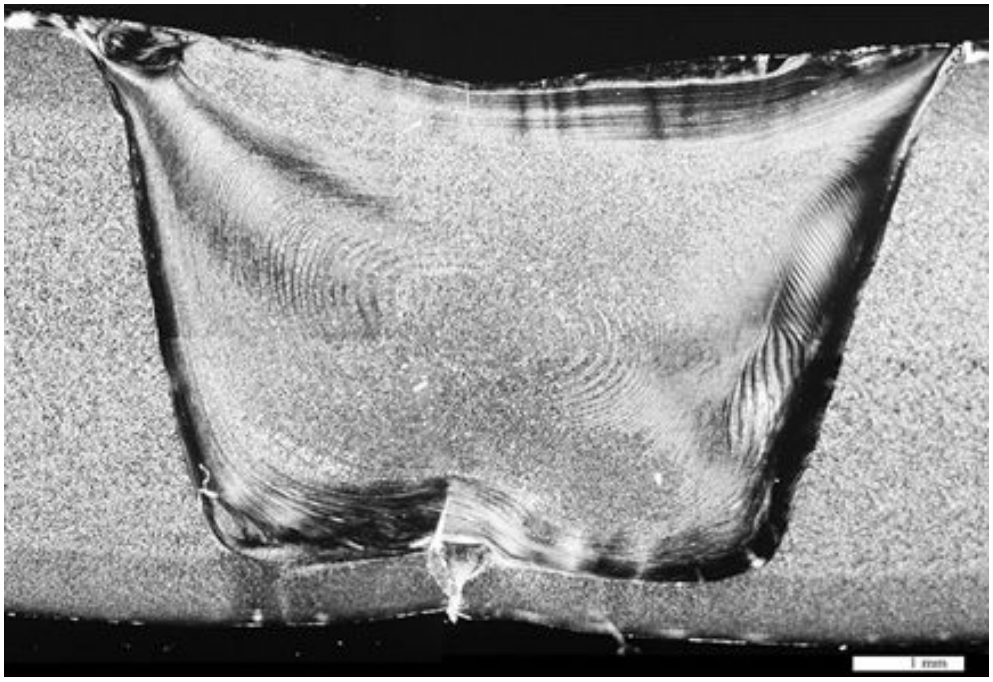

FR203b

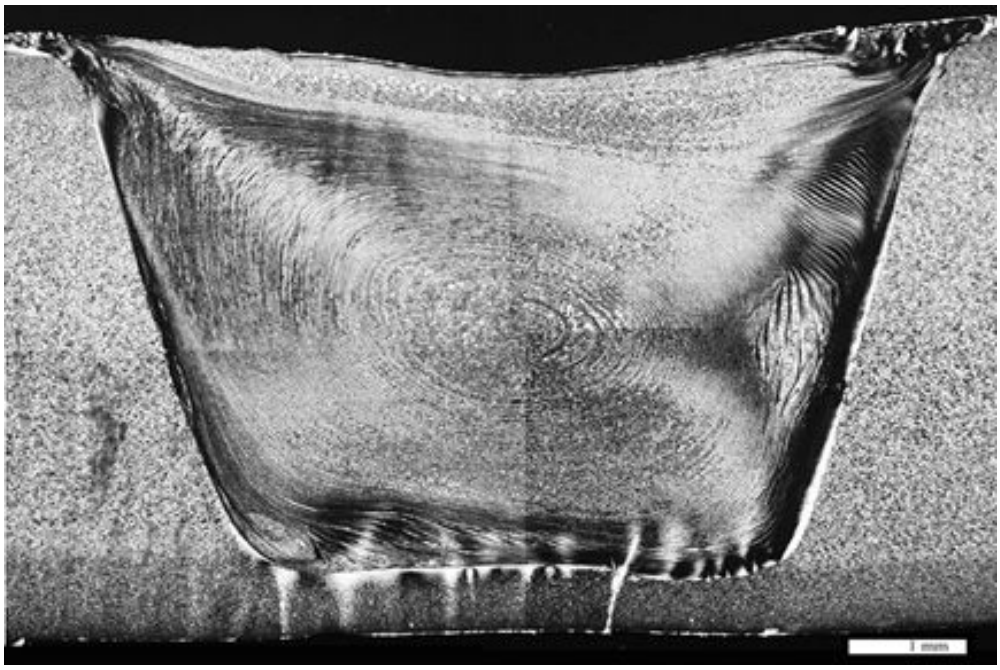

FR305a

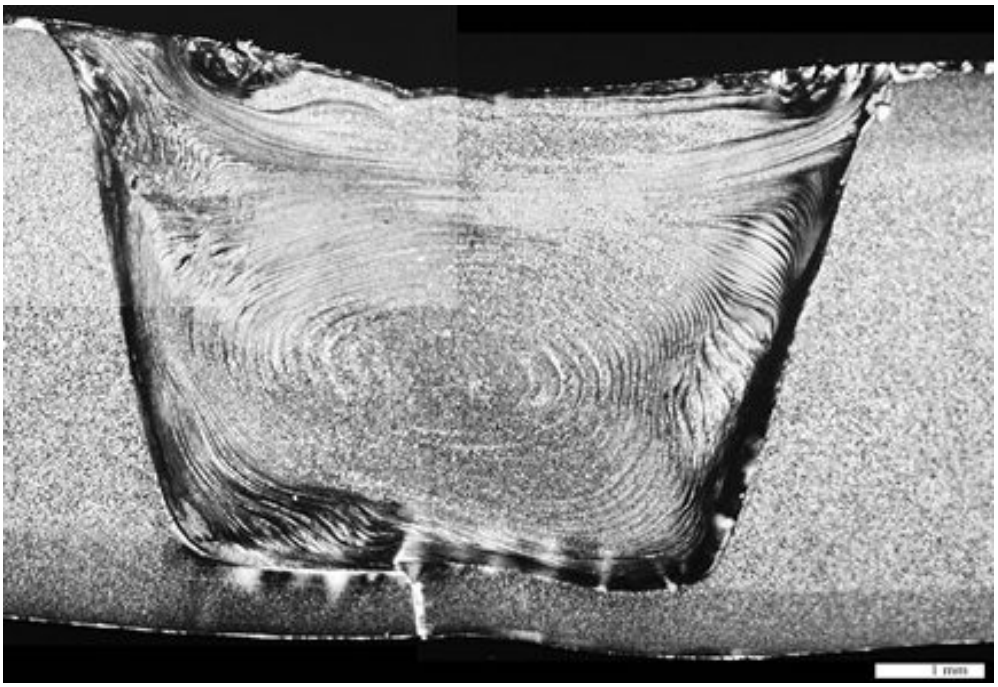

FR305b

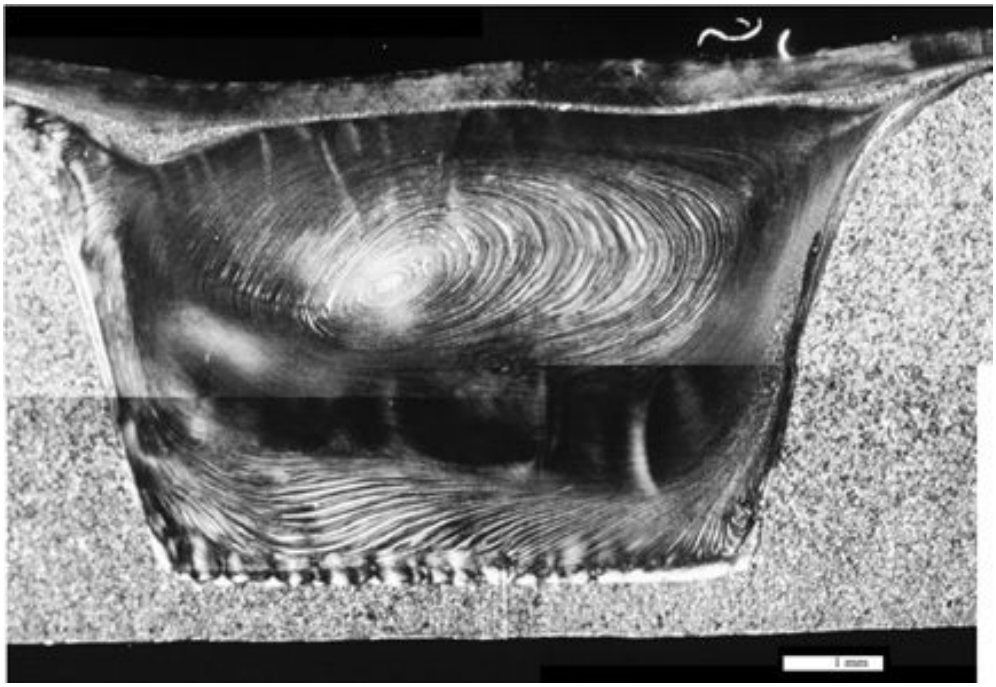

PD9a

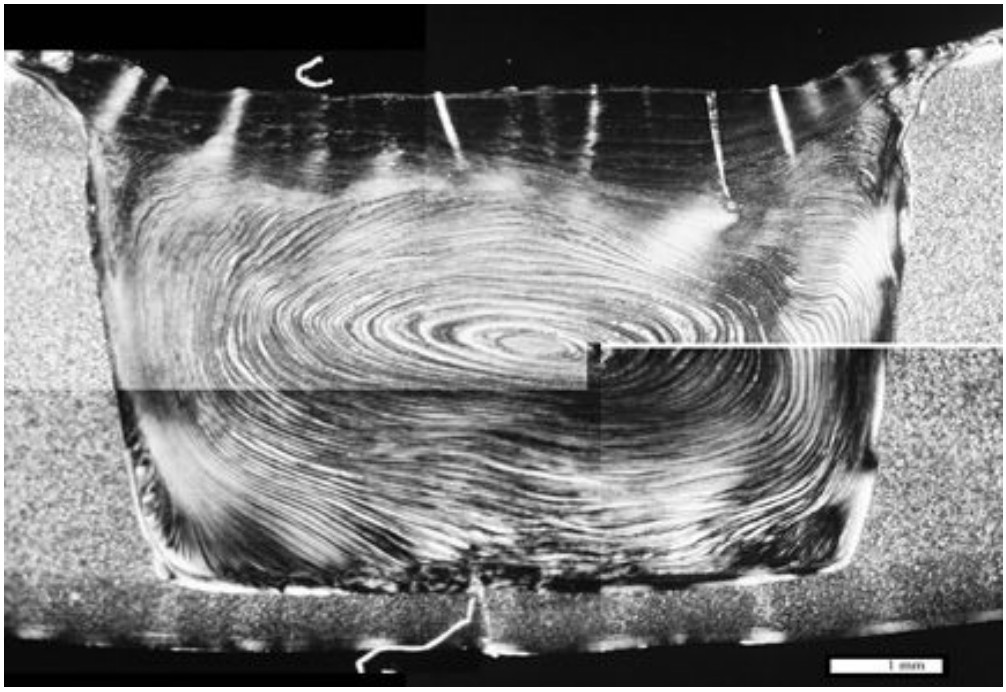

PD9b

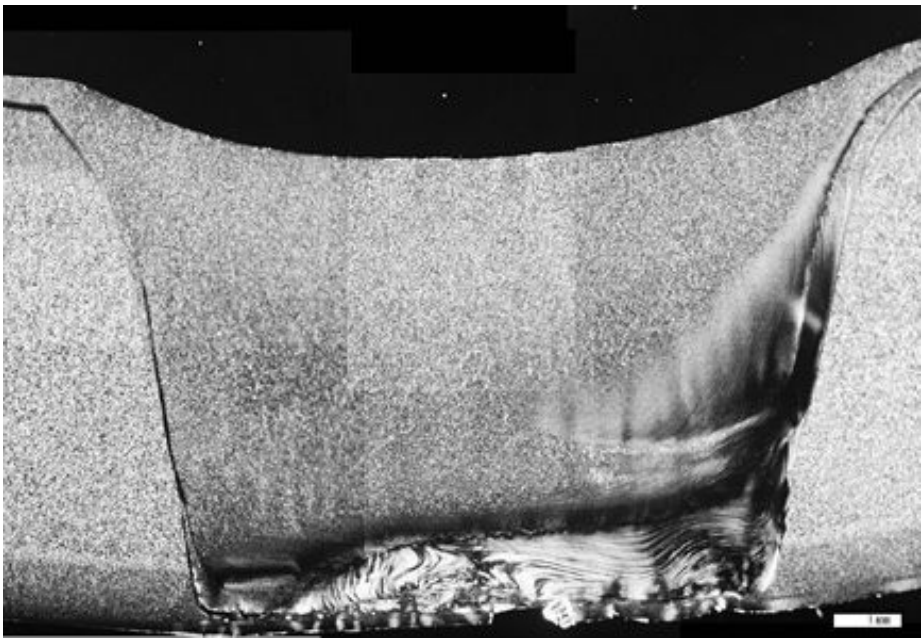

PD12a

PD12b

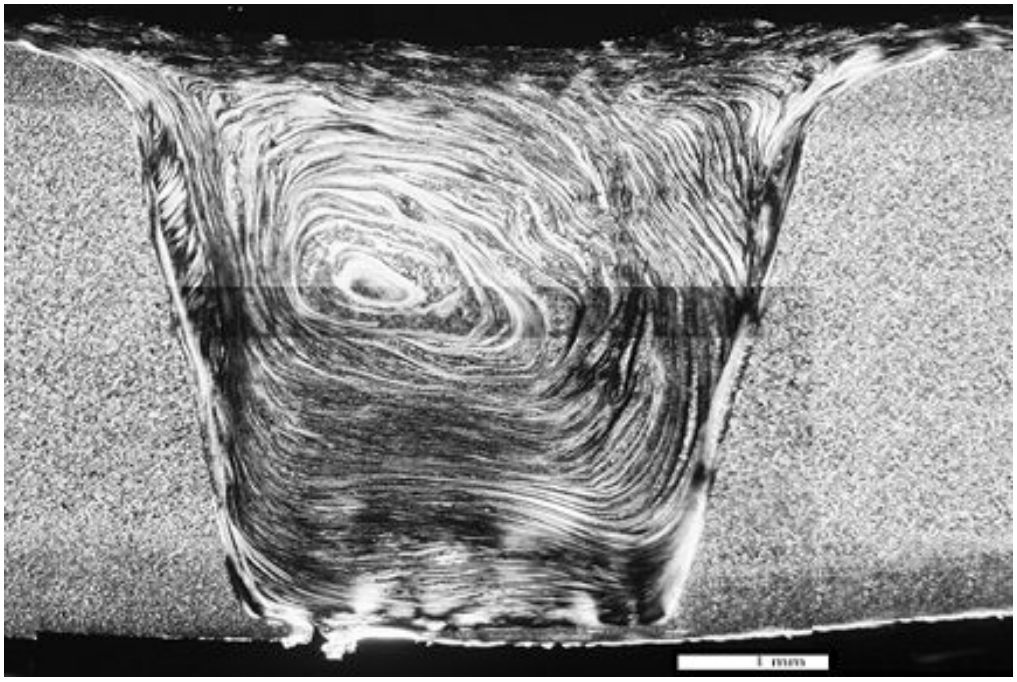

PD6a

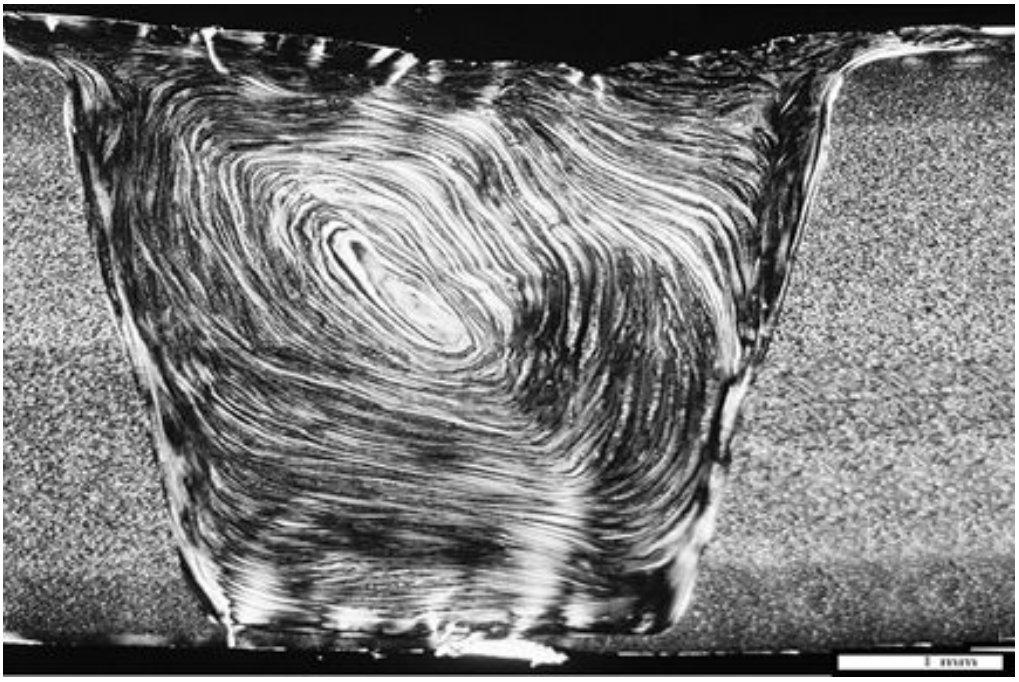

PD6b

PT30a

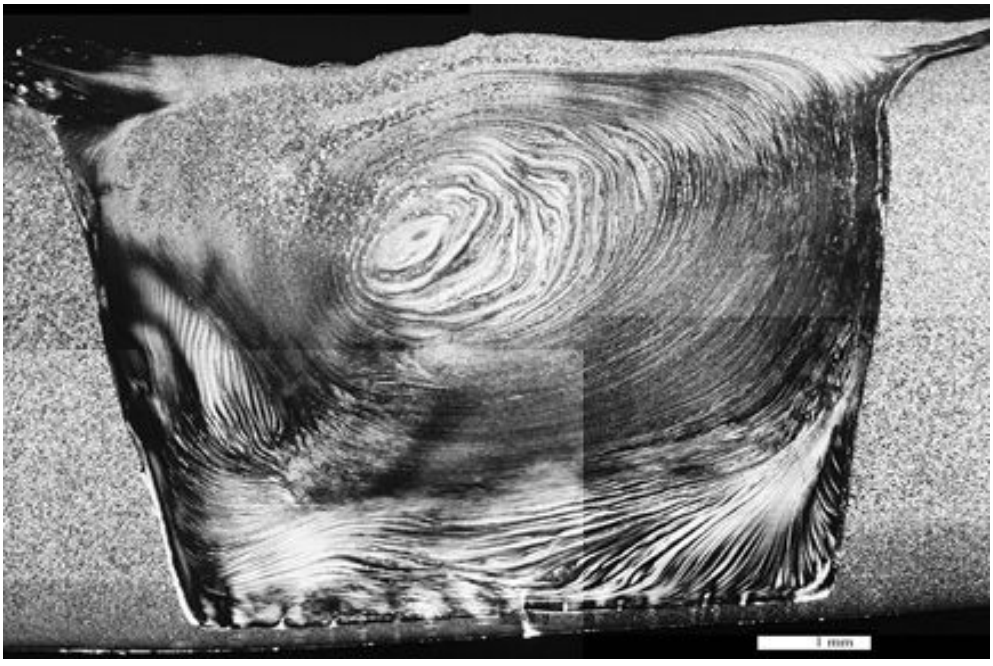

PT30b

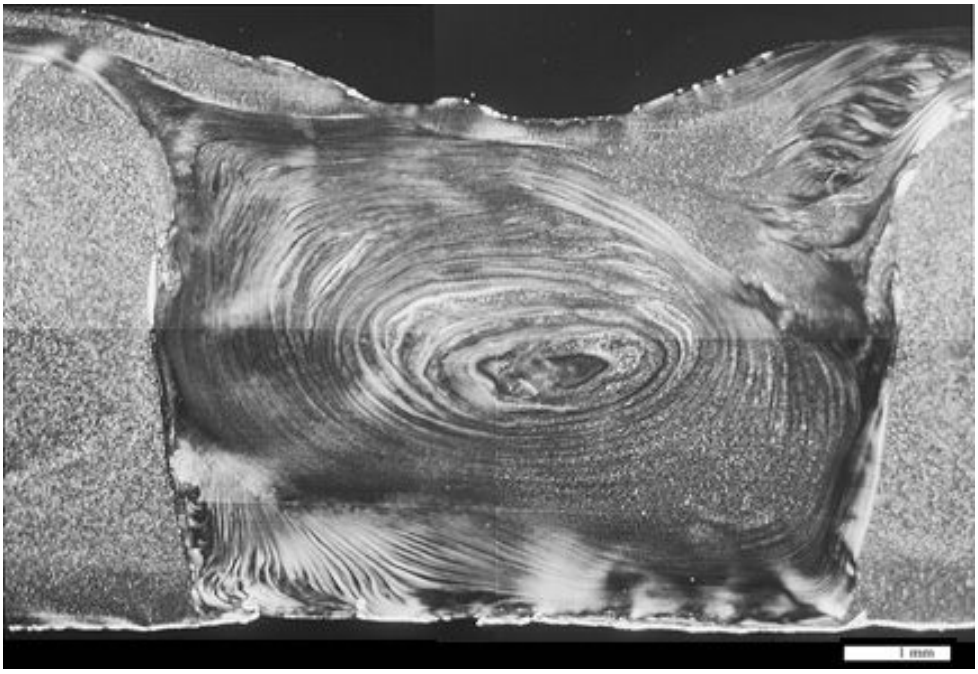

PT60a

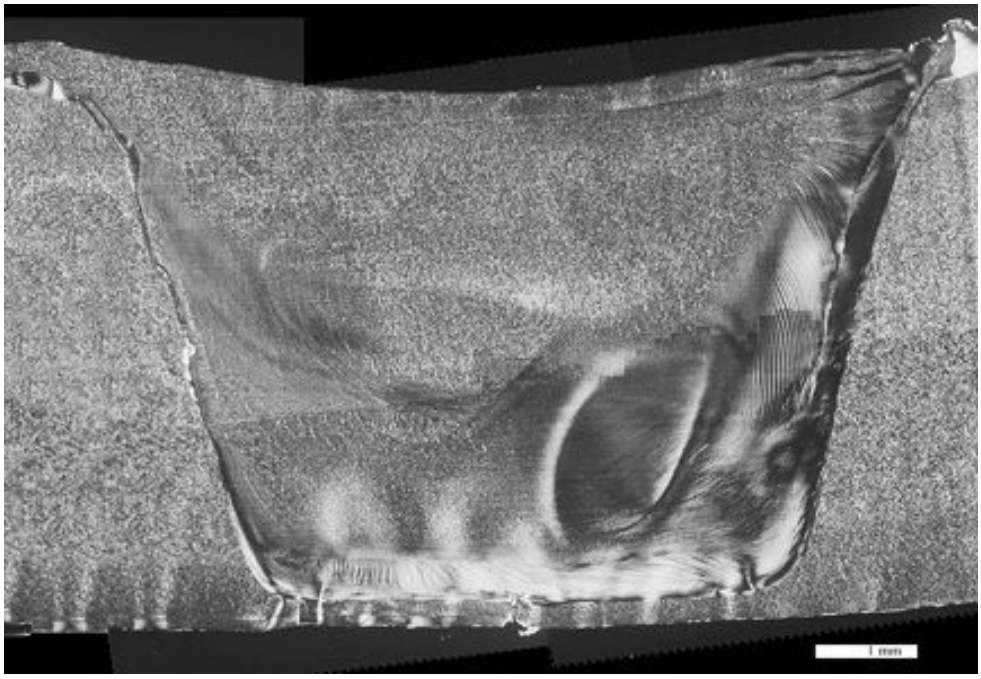

PT60b

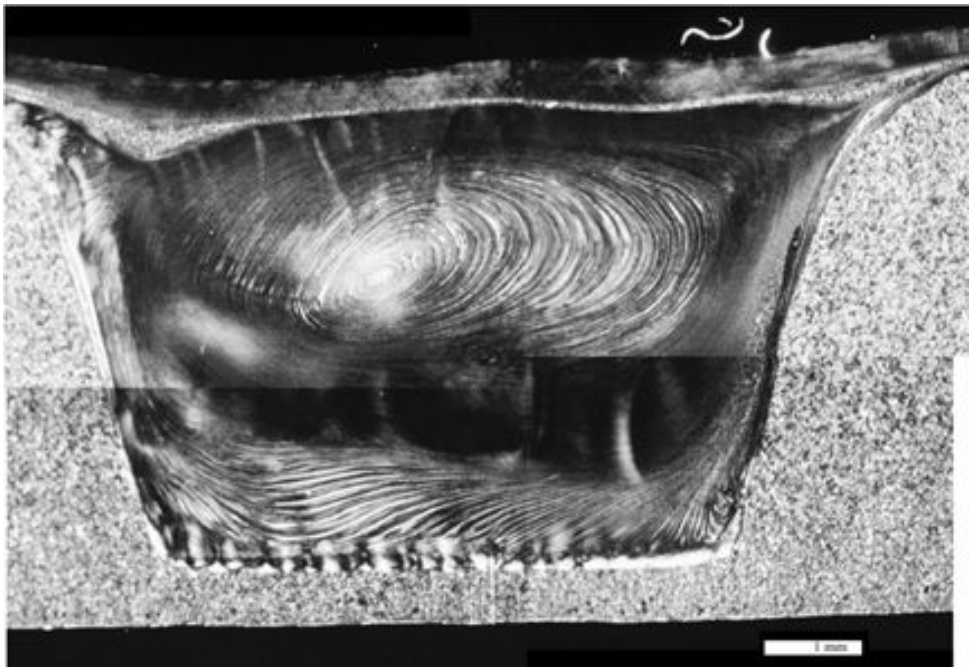

PT90a

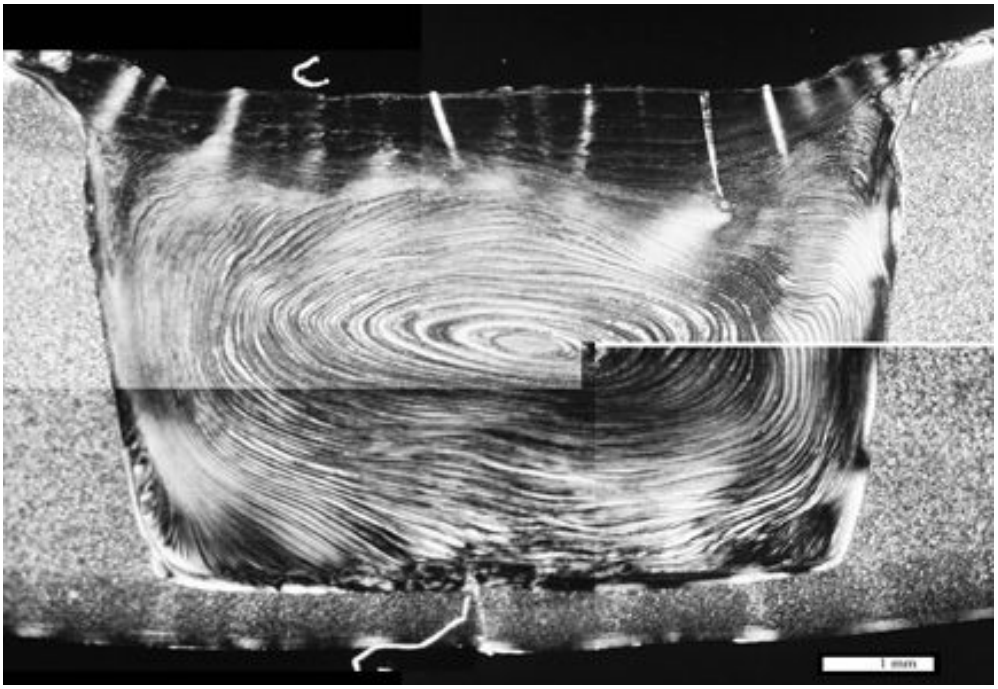

PT90b

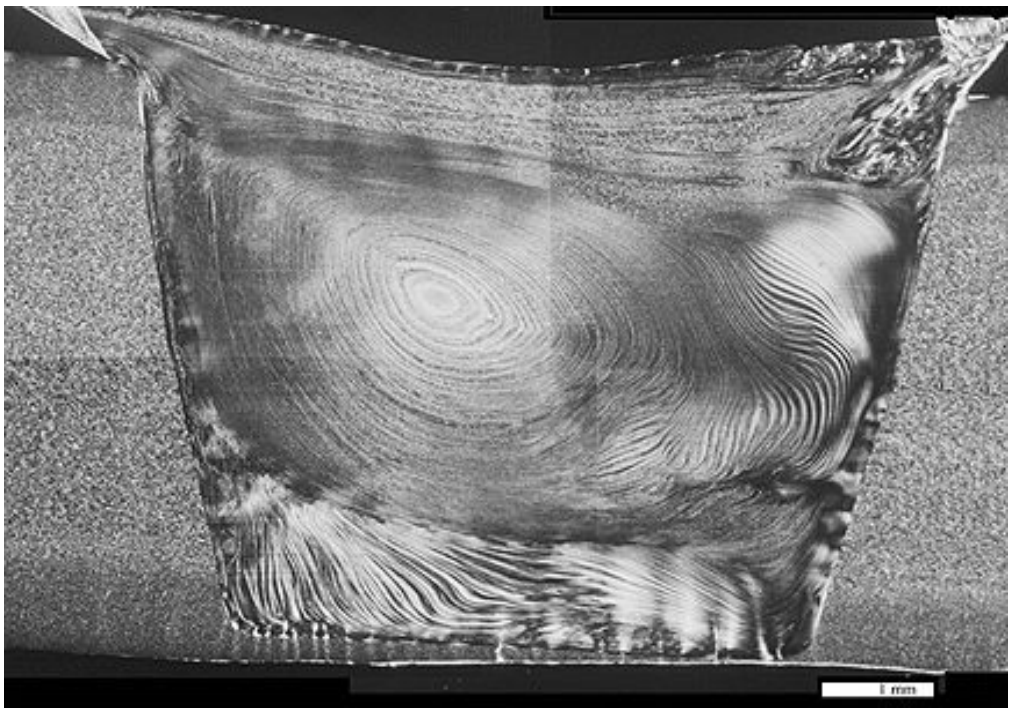

PT120a

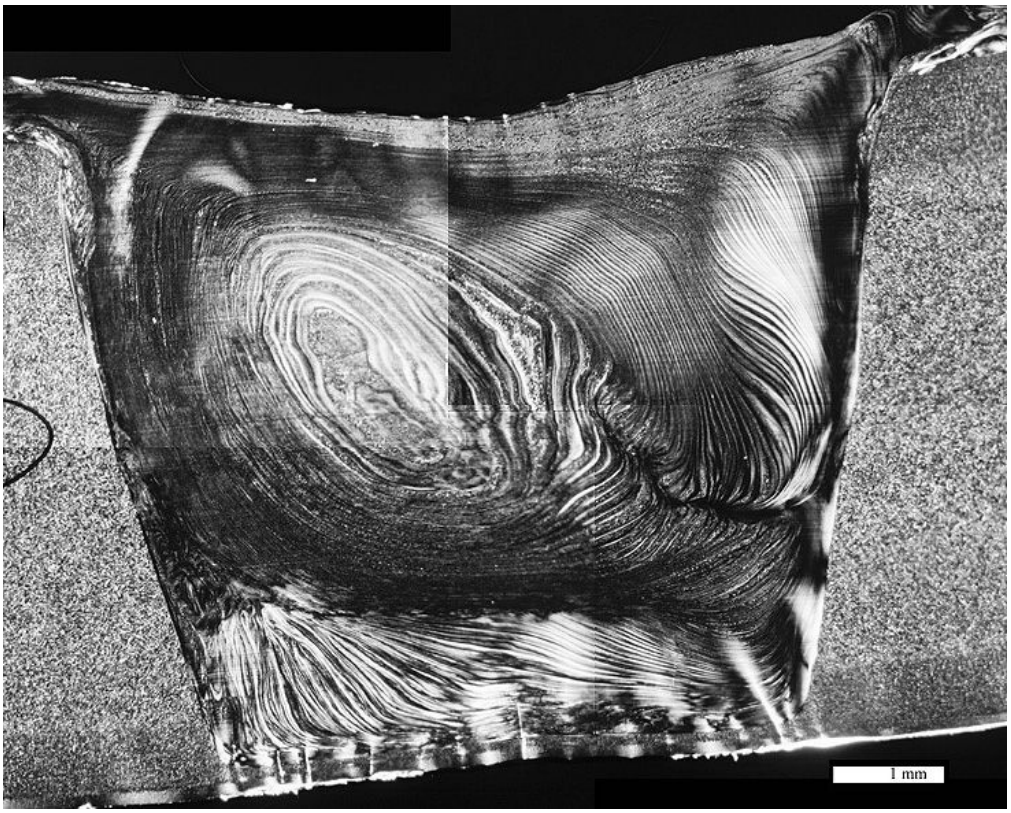

PT120b

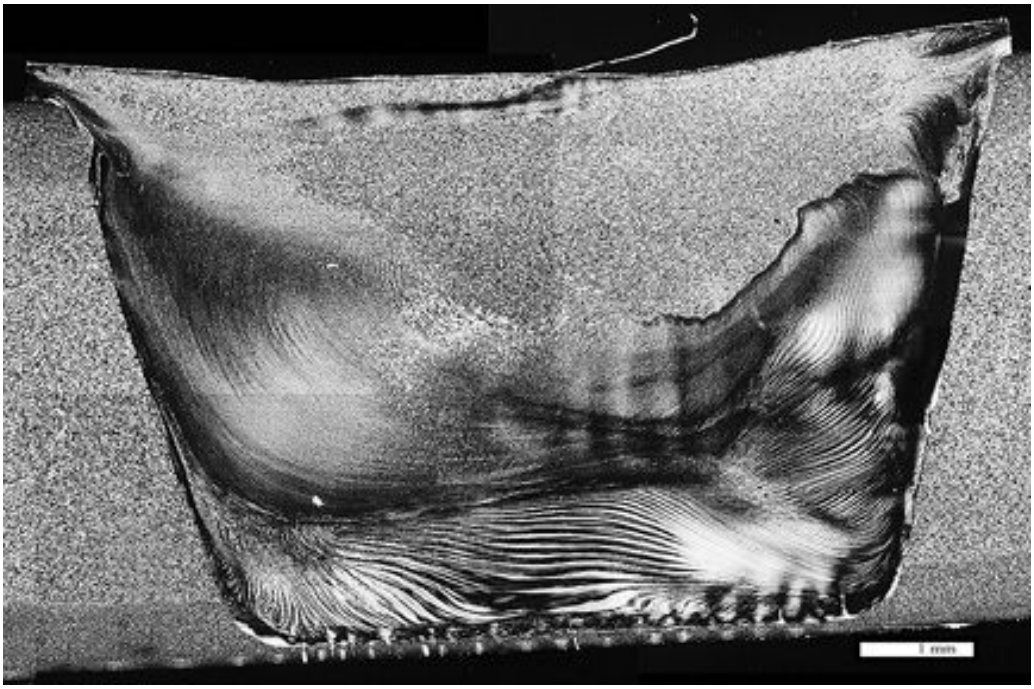

ST110a

ST110b

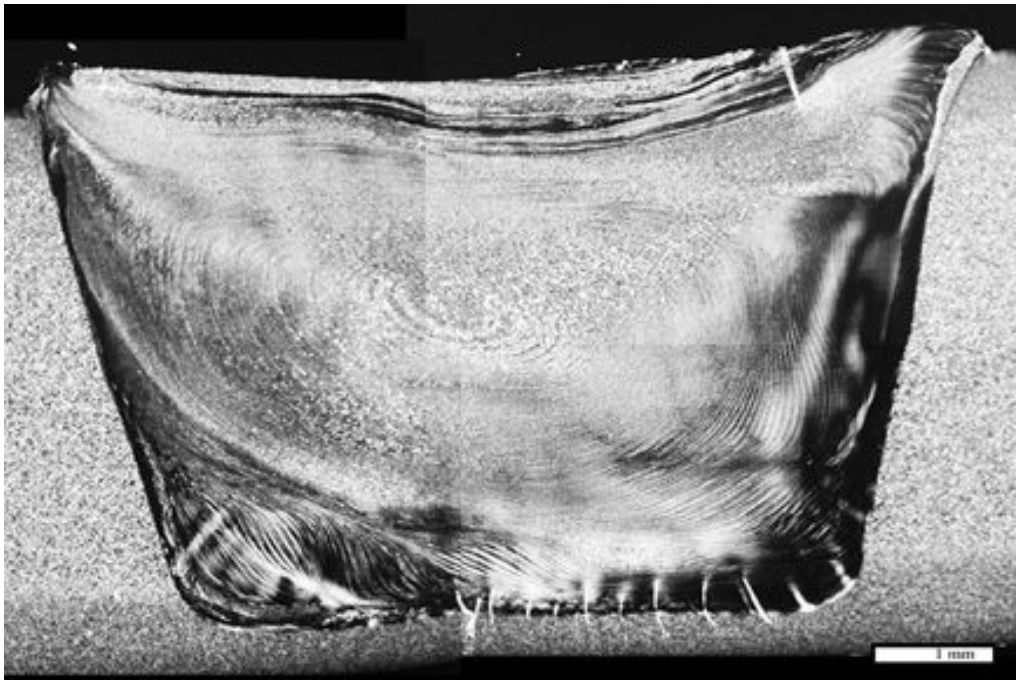

ST127a

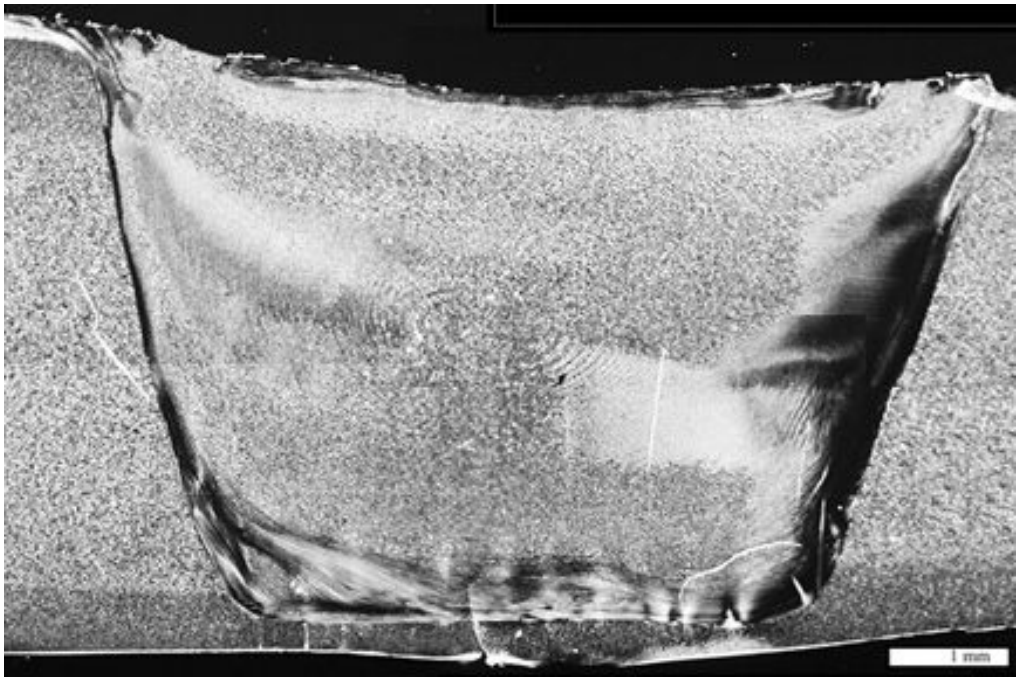

ST127b

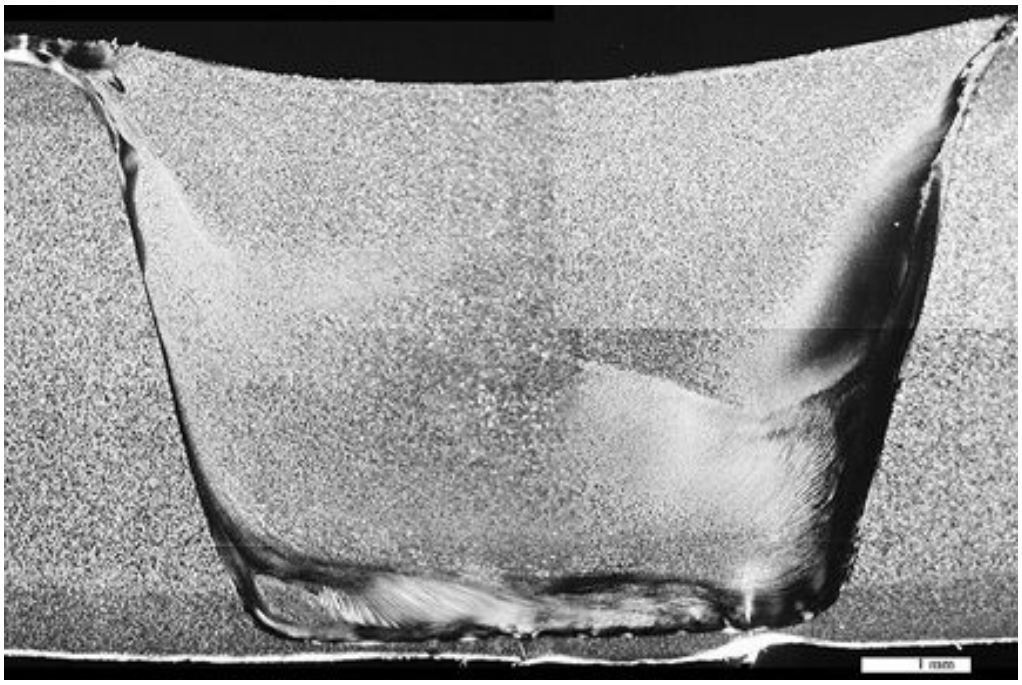

ST143a

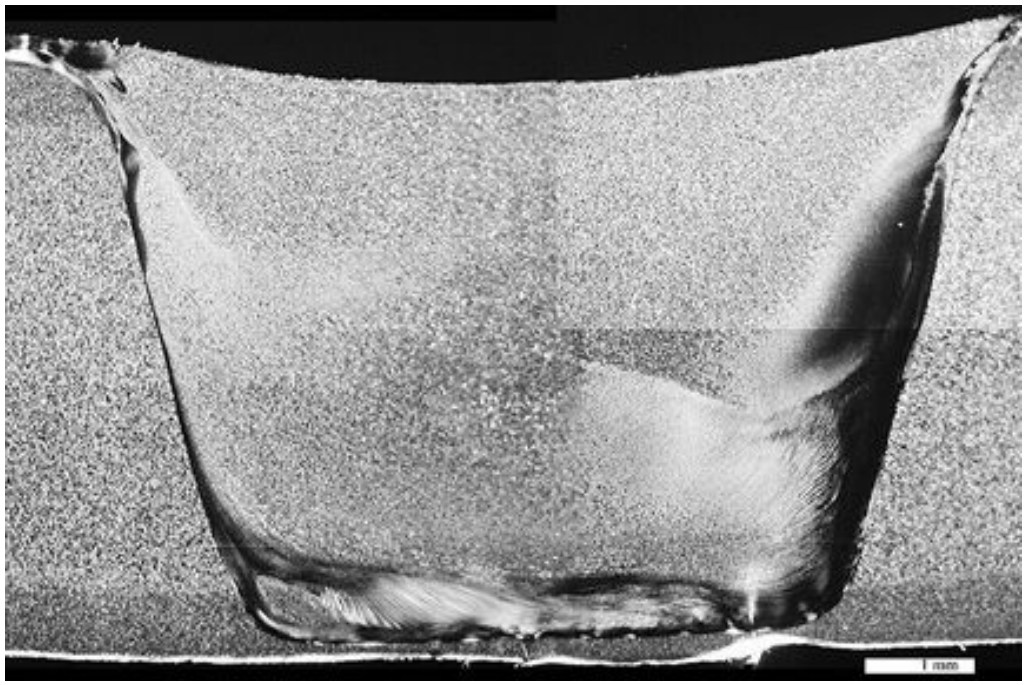

ST143b

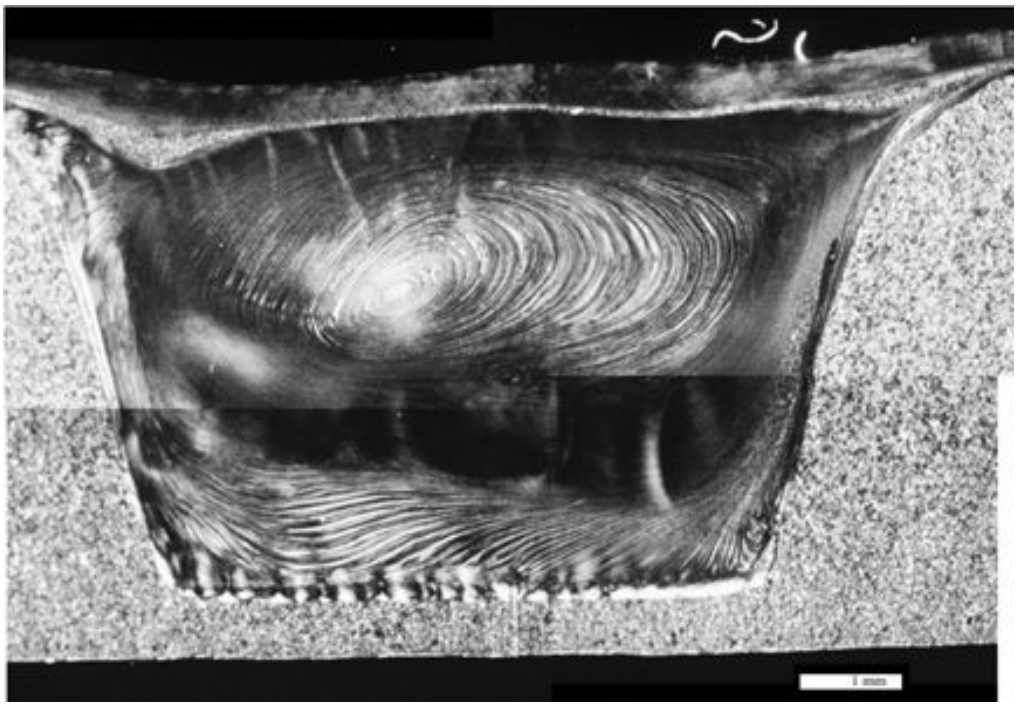

ST160a

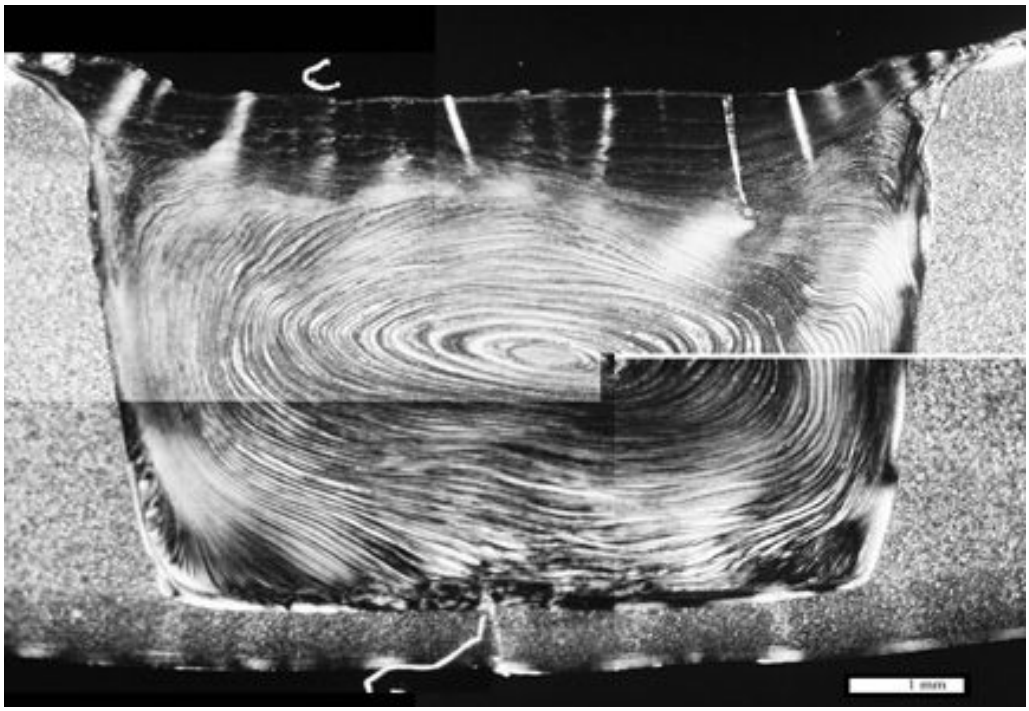

ST160b

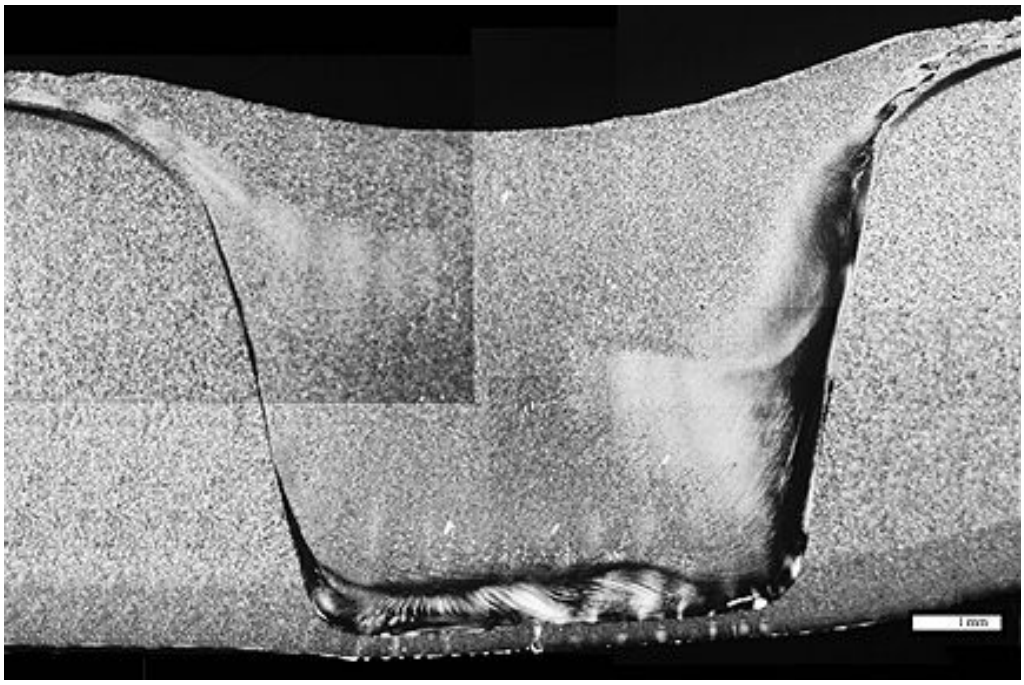

ST177a

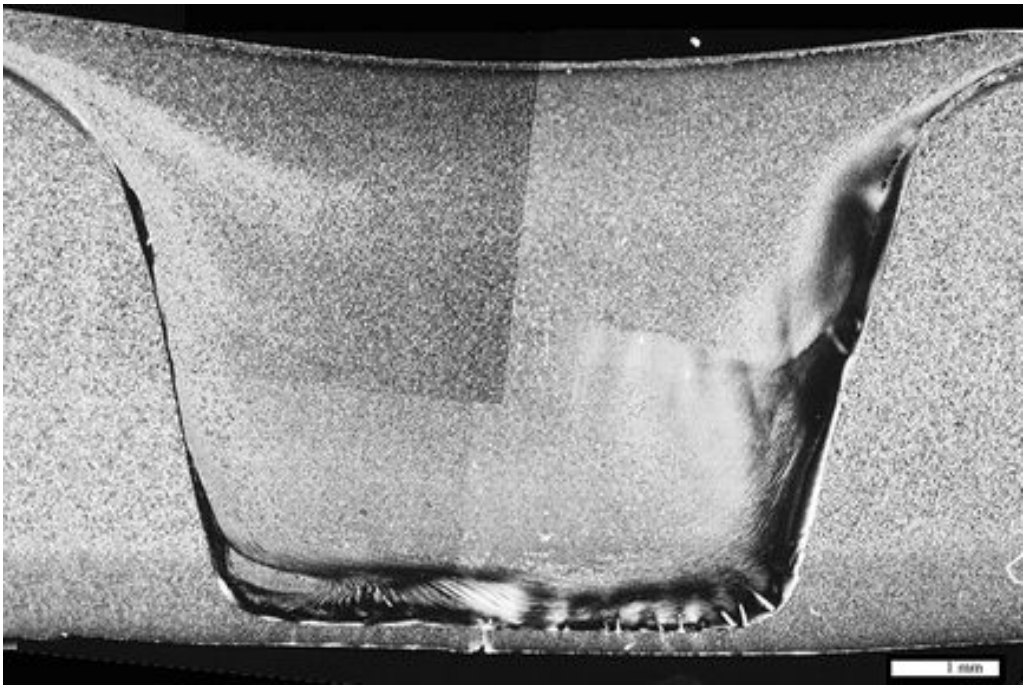

ST177b

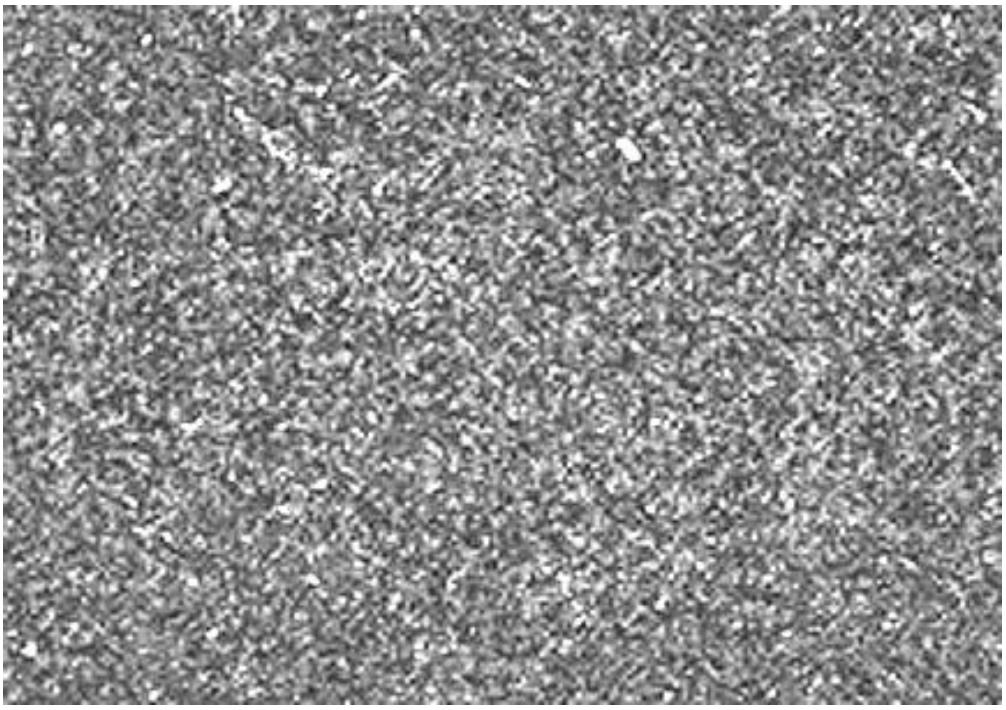

As-extruded PP.

APPENDIX 4

Statistical Analysis: DVS Bend Angle, Root Up

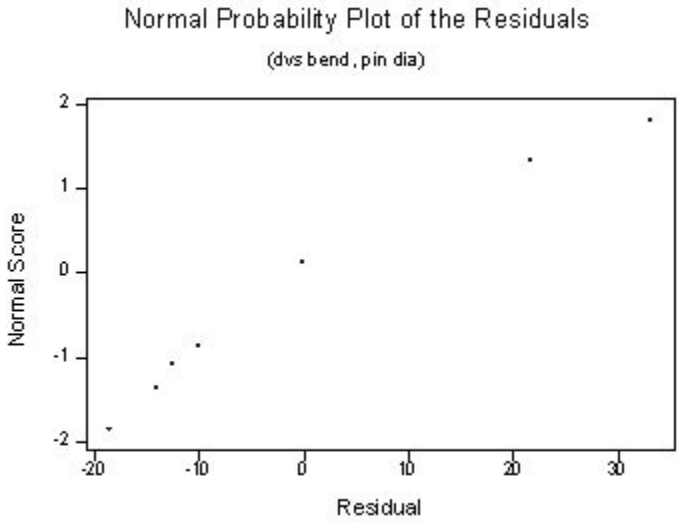

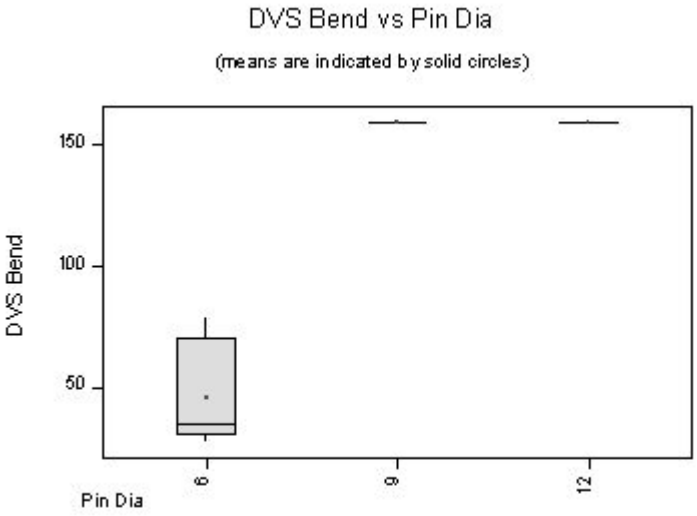


```
Analysis of Variance for DVS Bend, Pin Dia
Source     DF        SS        MS        F        P
Pin Dia.    2     51969     25984   165.05    0.000
Error      15      2361       157
Total      17     54330

                                  Individual 95% CIs For Mean
                                  Based on Pooled StDev
Pin Dia.    N      Mean     StDev  --+---------+---------+---------+----
 6          6     46.02     21.73   (--*-)
 9          6    160.00      0.00                                (--*--)
12          6    160.00      0.00                                (--*--)
                                  --+---------+---------+---------+----
```

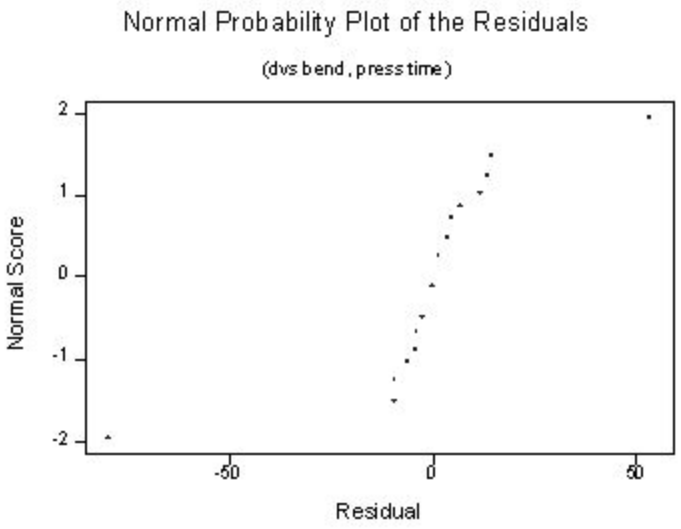

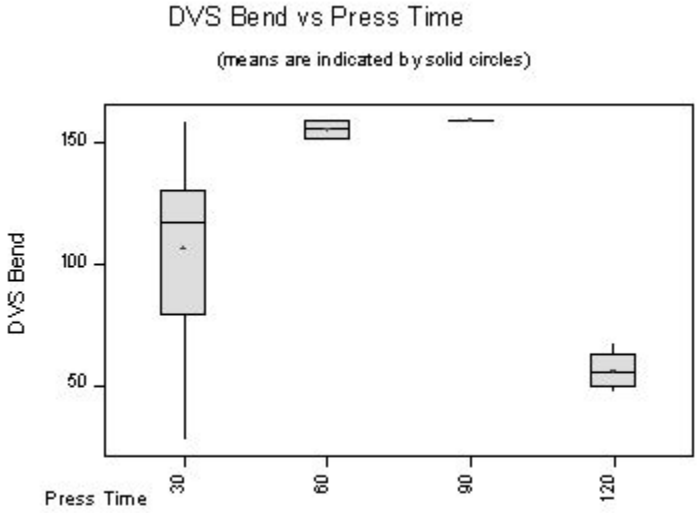


```
Analysis of Variance for DVS Bend, Press Time
Source     DF        SS        MS        F        P
Press. T    3     42968     14323    28.44    0.000
Error      20     10074       504
Total      23     53041

                                  Individual 95% CIs For Mean
                                  Based on Pooled StDev
Press time  N      Mean     StDev  -+---------+---------+---------+-----
 30         6    106.65     44.01              (----*---)
 60         6    156.12      4.25                        (----*----)
 90         6    160.00      0.00                         (----*----)
120         6     56.13      7.76  (----*----)
                                  -+---------+---------+---------+-----
Pooled StDev =    22.44           40        80       120       160
```

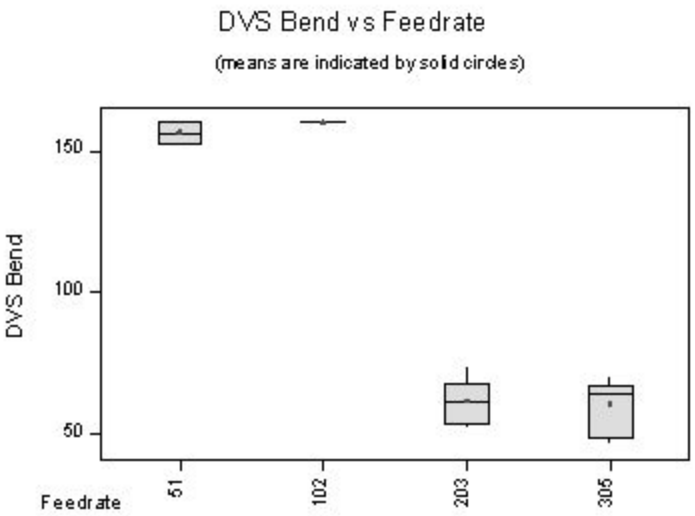

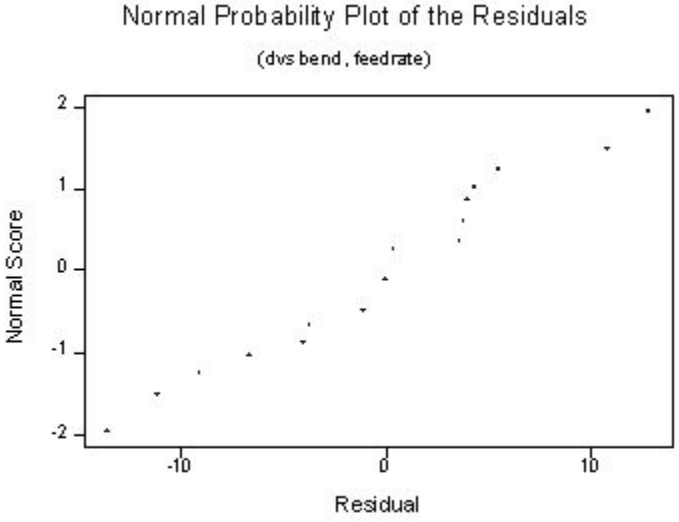


```
Analysis of Variance for DVS Bend, Feedrate
Source     DF        SS        MS        F        P
Feedrate    3   56784.7   18928.2   427.23    0.000
Error      20     886.1      44.3
Total      23   57670.8

                                  Individual 95% CIs For Mean
                                  Based on Pooled StDev
feedrate    N      Mean     StDev  -----+---------+---------+---------+-
 51         6    156.20      4.16                                (-*)
102         6    160.00      0.00                                 (-*)
203         6     61.55      7.84   (-*)
305         6     60.17      9.92   (*-)
                                  -----+---------+---------+---------+-
Pooled StDev =     6.66              70       105       140       175
```

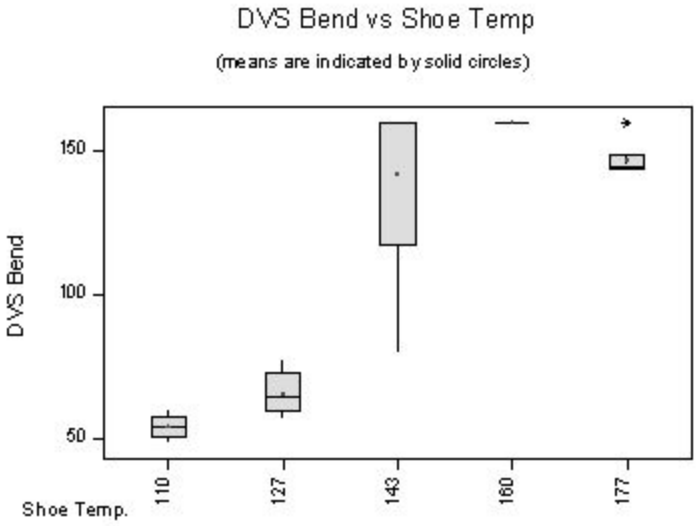

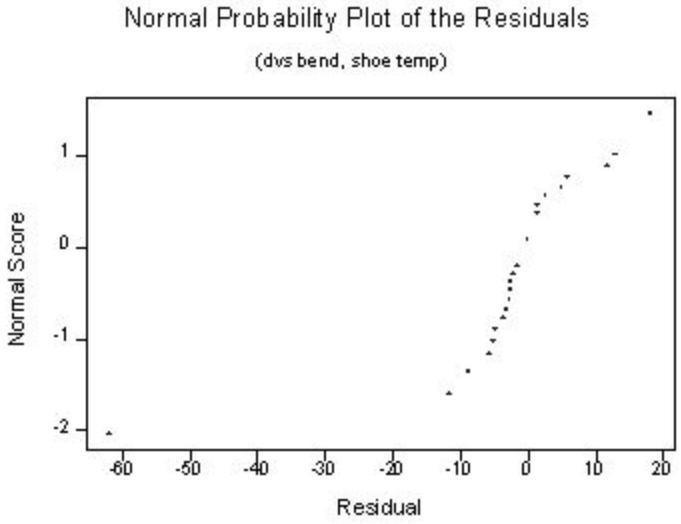

Analysis of Variance for DVS Bend, Shoe Temp

Source	DF	SS	MS	F	P
Shoe Tem	4	58653	14663	62.54	0.000
Error	25	5861	234		
Total	29	64514			

Shoe temp.	N	Mean	StDev
110	6	54.63	4.19
127	6	66.17	7.62
143	6	141.73	32.48
160	6	160.00	0.00
177	6	146.83	6.46

Pooled StDev = 15.31

Individual 95% CIs For Mean
Based on Pooled StDev

```
----------+---------+---------+------
(---*--)
   (---*--)
                        (--*---)
                             (--*--)
                         (---*--)
----------+---------+---------+------
          80       120       160
```

APPENDIX 5

Statistical Analysis: Three-Point Bending

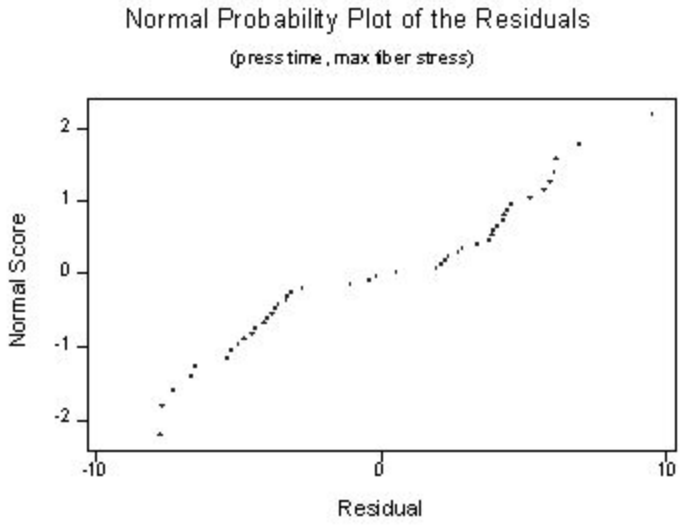

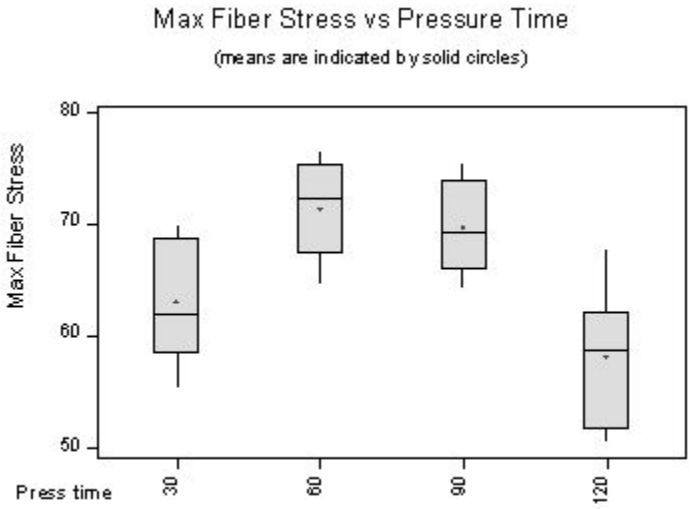

Analysis of Variance for Press Time Max Fiber Stress,

Source	DF	SS	MS	F	P
Press time	3	1270.0	423.3	17.64	0.000
Error	42	1008.2	24.0		
Total	45	2278.1			

P.T.	N	Mean	StDev	Individual 95% CIs For Mean Based on Pooled StDev
30	11	62.961	5.205	(----*----)
60	12	71.308	4.249	(----*----)
90	12	69.600	4.260	(----*----)
120	11	58.146	5.823	(----*----)

Pooled StDev = 4.899

60.0 66.0 72.0

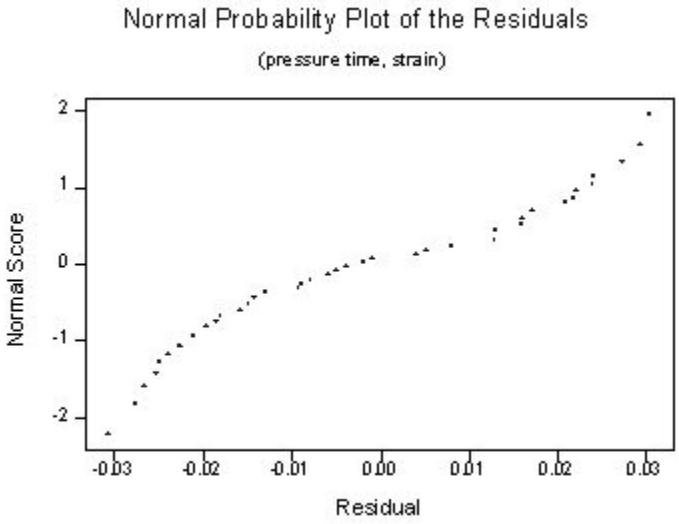

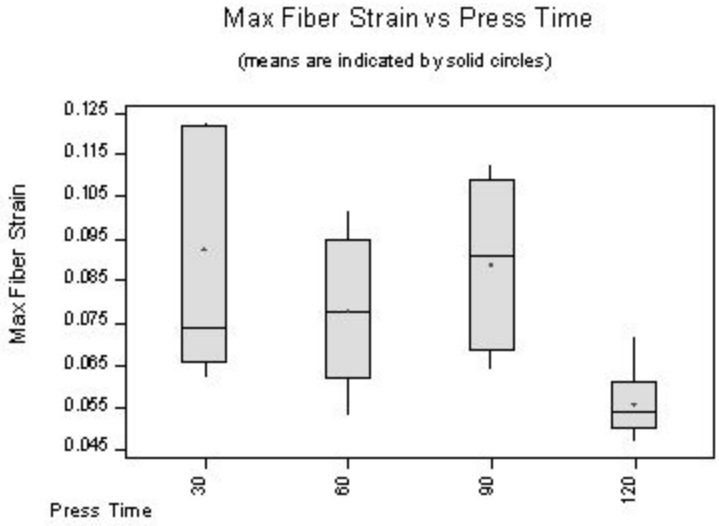

Analysis of Variance for Press Time Max Fiber Strain

Source	DF	SS	MS	F	P
Press time	3	0.009166	0.003055	7.68	0.000
Error	42	0.016703	0.000398		
Total	45	0.025869			

P.T.	N	Mean	StDev	Individual 95% CIs For Mean Based on Pooled StDev
30	11	0.09255	0.02804	(-----*-----)
60	12	0.07783	0.01919	(-----*-----)
90	12	0.08908	0.01955	(-----*----)
120	11	0.05582	0.00767	(-----*-----)

Pooled StDev = 0.01994

0.060 0.080 0.100

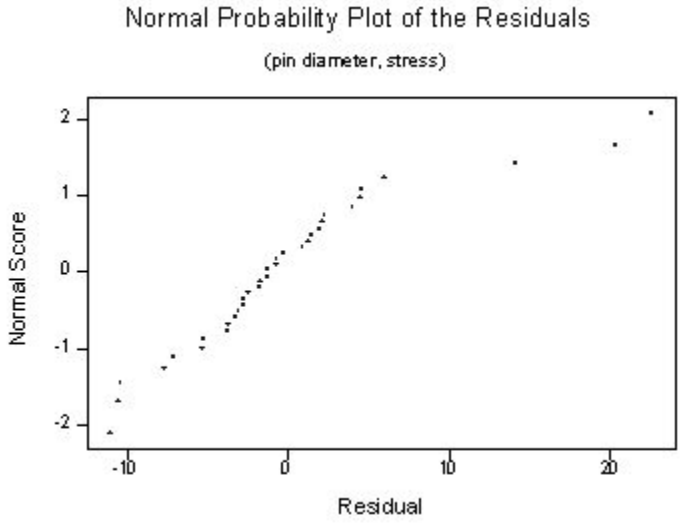

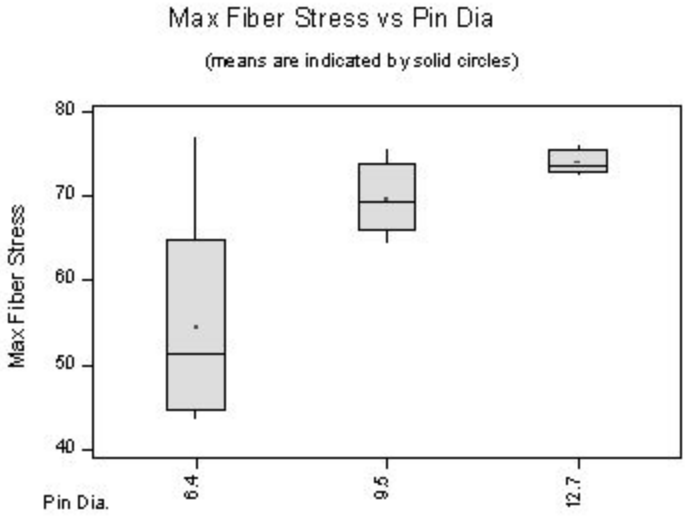


```
Analysis of Variance for Pin Dia Max Fiber Stress
Source     DF      SS        MS        F        P
Pin Dia.    2    2340.1    1170.0    19.97    0.000
Error      31    1816.0      58.6
Total      33    4156.1
                                  Individual 95% CIs For Mean
                                  Based on Pooled StDev
Pin Dia.    N      Mean     StDev  --------+---------+---------+--------
 6.4       12    54.629    12.061   (----*-----)
 9.5       12    69.600     4.260                    (-----*-----)
12.7       10    73.989     1.346                        (-----*------)
                                  --------+---------+---------+--------
Pooled StDev =    7.654            56.0      64.0      72.0
```

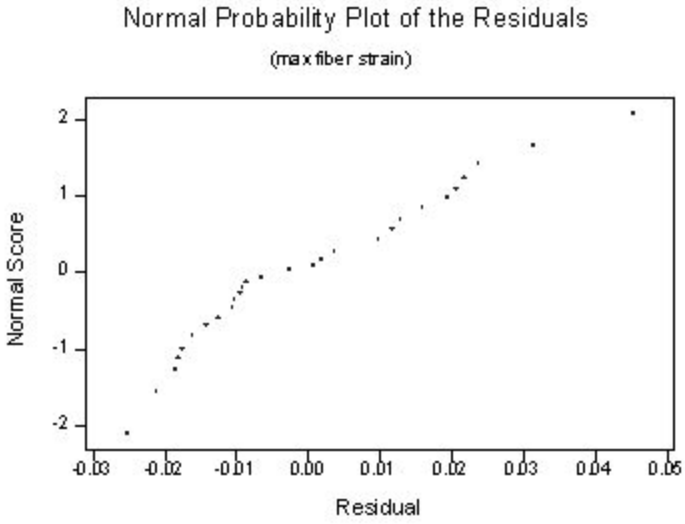

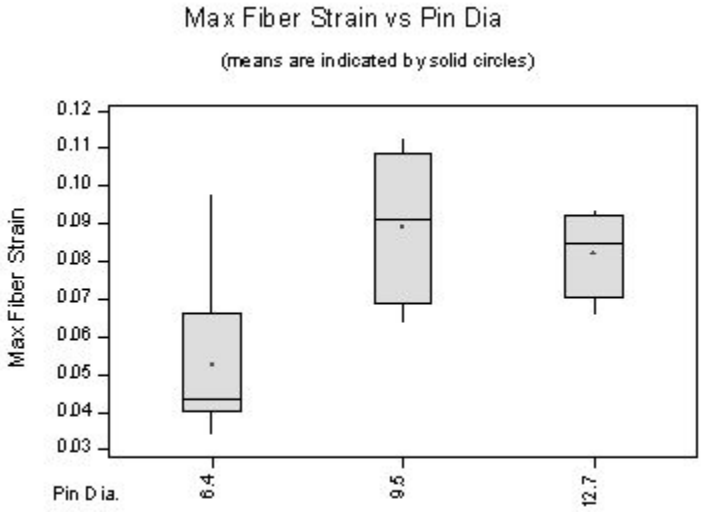

Analysis of Variance for Pin Dia Max Fiber Strain

Source	DF	SS	MS	F	P
Pin Dia.	2	0.008933	0.004466	14.02	0.000
Error	31	0.009875	0.000319		
Total	33	0.018808			

Pin Dia.	N	Mean	StDev
6.4	12	0.05250	0.02062
9.5	12	0.08908	0.01955
12.7	10	0.08210	0.01050

Pooled StDev = 0.01785

Individual 95% CIs For Mean
Based on Pooled StDev

```
----+---------+---------+---------+--
(------*-----)
                      (------*-----)
                   (------*-------)
----+---------+---------+---------+--
  0.048     0.064     0.080     0.096
```

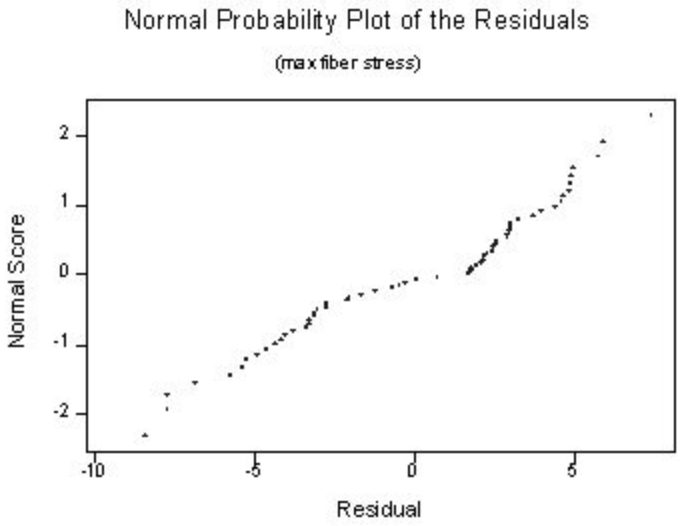

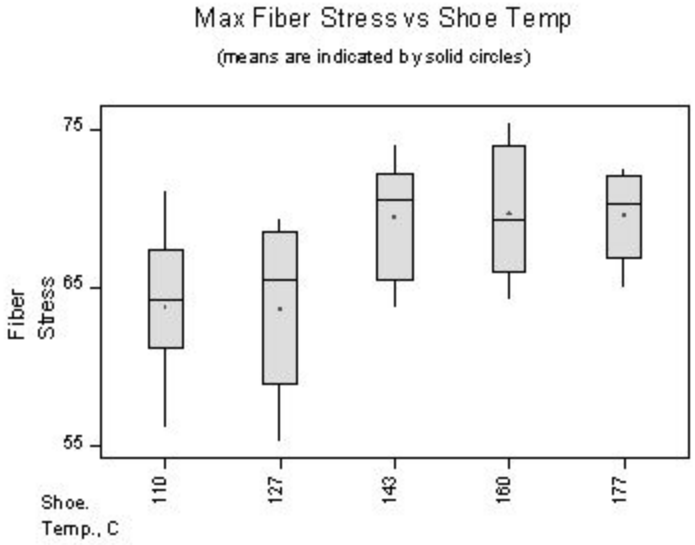

Analysis of Variance for Shoe Temp Max Fiber Stress

Source	DF	SS	MS	F	P
S.T., C	4	490.7	122.7	7.09	0.000
Error	55	951.1	17.3		
Total	59	1441.9			

S.T.	N	Mean	StDev
110	12	63.722	4.720
127	12	63.610	5.140
143	12	69.367	3.531
160	12	69.600	4.260
177	12	69.536	2.674

Pooled StDev = 4.158

Individual 95% CIs For Mean
Based on Pooled StDev

```
------+---------+---------+---------+
(-------*-------)
(-------*-------)
                  (-------*-------)
                   (-------*-------)
                   (-------*-------)
------+---------+---------+---------+
   63.0      66.0      69.0      72.0
```

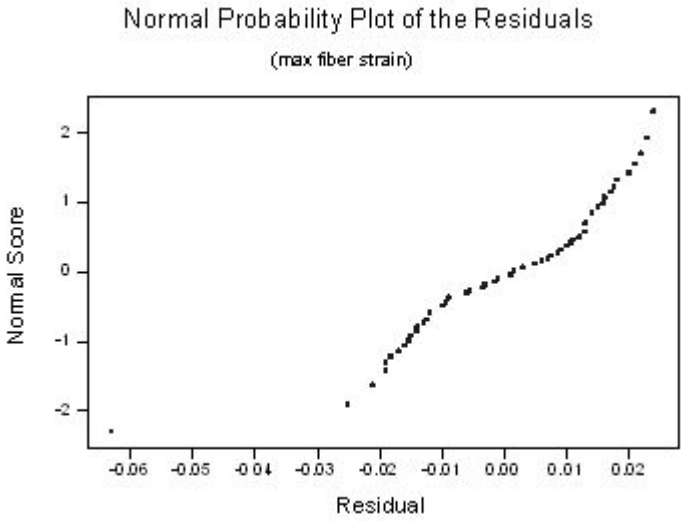

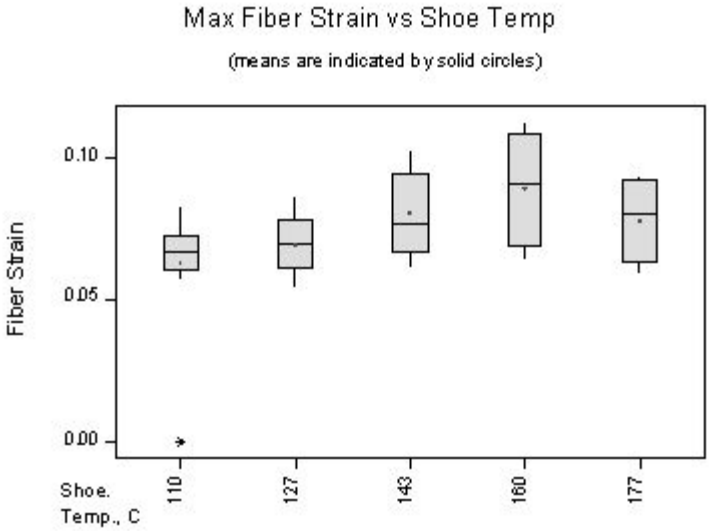


```
Analysis of Variance for Shoe Temp Fiber Strain
Source     DF      SS        MS        F        P
S.T., C     4  0.004837  0.001209     4.36    0.004
Error      55  0.015257  0.000277
Total      59  0.020094

                                    Individual 95% CIs For Mean
                                    Based on Pooled StDev
S.T.        N      Mean     StDev  -----+---------+---------+---------+-
110        12   0.06300   0.02133   (-----*-----)
127        12   0.06942   0.00991       (-----*------)
143        12   0.08000   0.01526              (-----*------)
160        12   0.08908   0.01955                    (-----*------)
177        12   0.07792   0.01479             (-----*-----)
                                    -----+---------+---------+---------+-
Pooled StDev =  0.01666               0.060     0.075     0.090     0.105
```

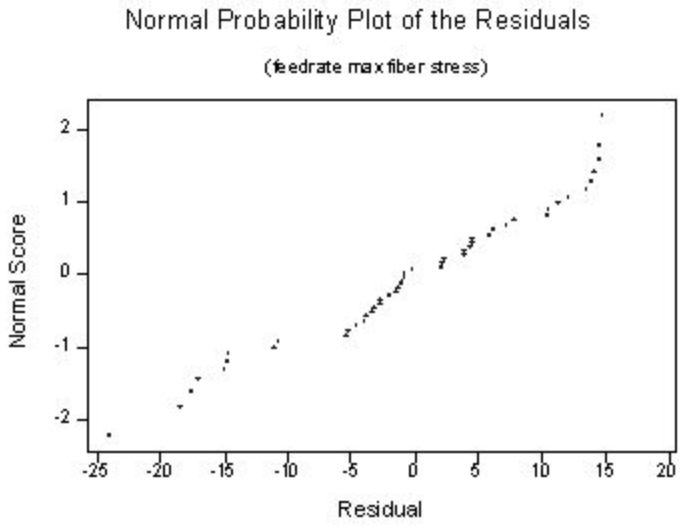

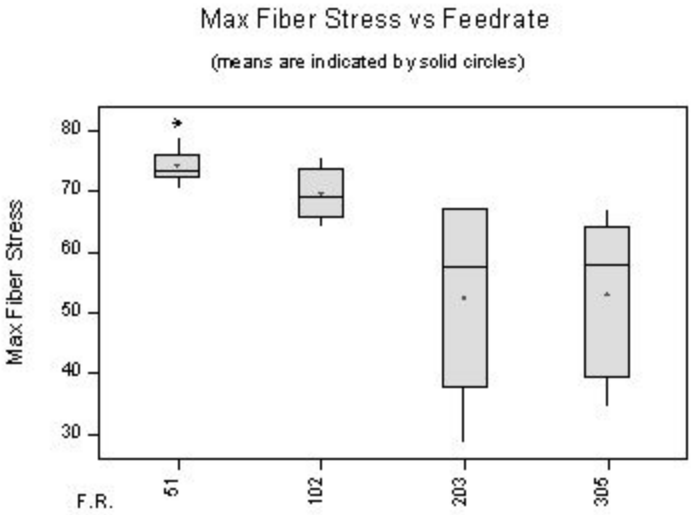

Analysis of Variance for Feedrate Max Fiber Stress

Source	DF	SS	MS	F	P
F.R.	3	4535	1512	14.51	0.000
Error	44	4585	104		
Total	47	9120			

F.R.	N	Mean	StDev	Individual 95% CIs For Mean Based on Pooled StDev
51	12	74.30	3.19	(-----*-----)
102	12	69.60	4.26	(-----*-----)
203	12	52.62	15.27	(-----*-----)
305	12	52.98	12.47	(-----*-----)

Pooled StDev = 10.21

50 60 70 80

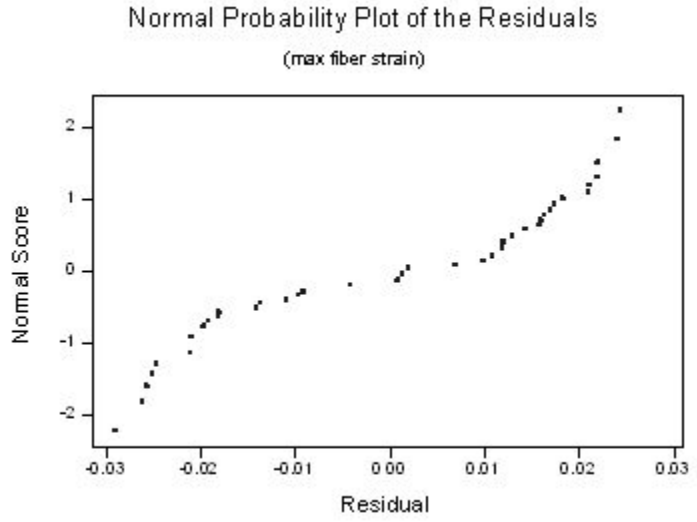

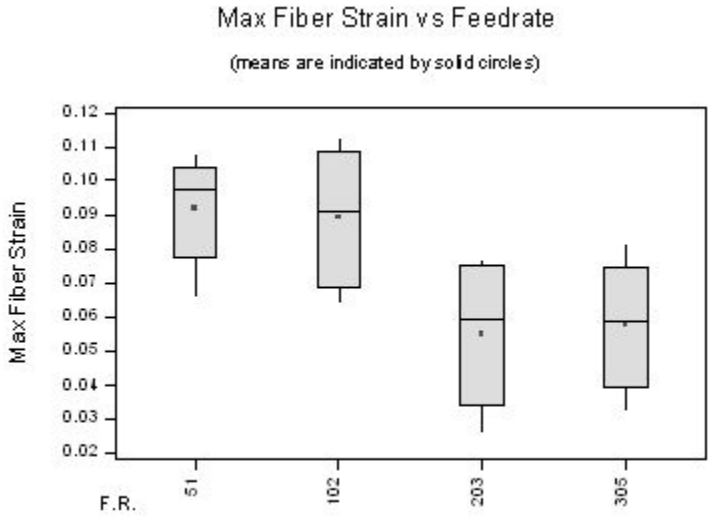

Analysis of Variance for Feedrate Max Fiber Strain

Source	DF	SS	MS	F	P
F.R.	3	0.014211	0.004737	14.57	0.000
Error	44	0.014301	0.000325		
Total	47	0.028512			

F.R.	N	Mean	StDev
51	12	0.09217	0.01440
102	12	0.08908	0.01955
203	12	0.05500	0.01949
305	12	0.05767	0.01819

Pooled StDev = 0.01803

Individual 95% CIs For Mean
Based on Pooled StDev

```
---+---------+---------+---------+---
                          (------*-----)
                        (------*-----)
(-----*------)
 (------*------)
---+---------+---------+---------+---
0.048     0.064     0.080     0.096
```

APPENDIX 6

Statistical Analysis: Weld Microstructure

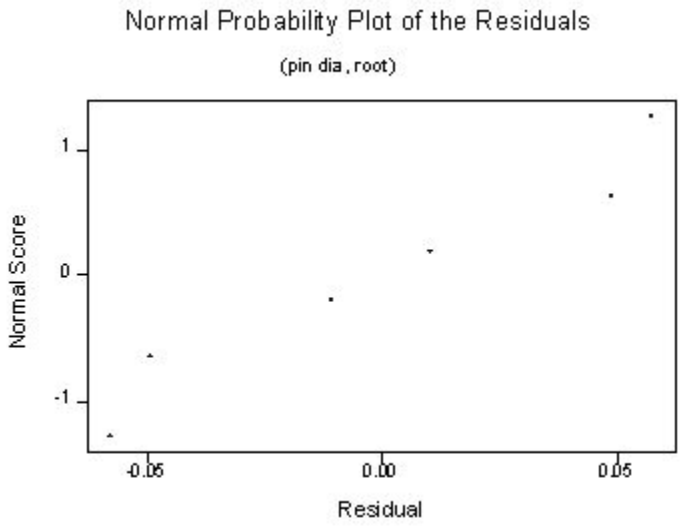

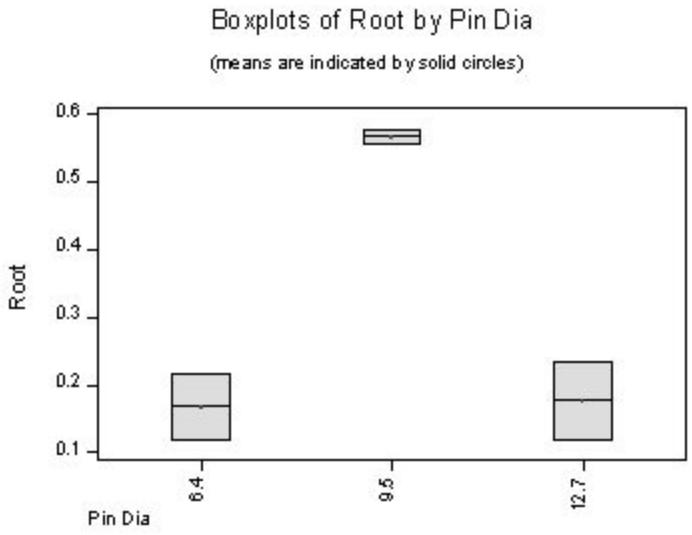


```
Analysis of Variance for Pin Dia, Root
Source     DF        SS        MS        F        P
pin dia     2   0.20587   0.10293    26.41    0.012
Error       3   0.01169   0.00390
Total       5   0.21756

                                 Individual 95% CIs For Mean
                                 Based on Pooled StDev
pin dia     N      Mean     StDev  ---------+---------+---------+-------
 6.4        2   0.16909   0.06943  (------*------)
 9.5        2   0.56624   0.01511                    (------*------)
12.7        2   0.17765   0.08153   (------*------)
                                 ---------+---------+---------+-------
Pooled StDev =  0.06244                 0.20      0.40      0.60
```

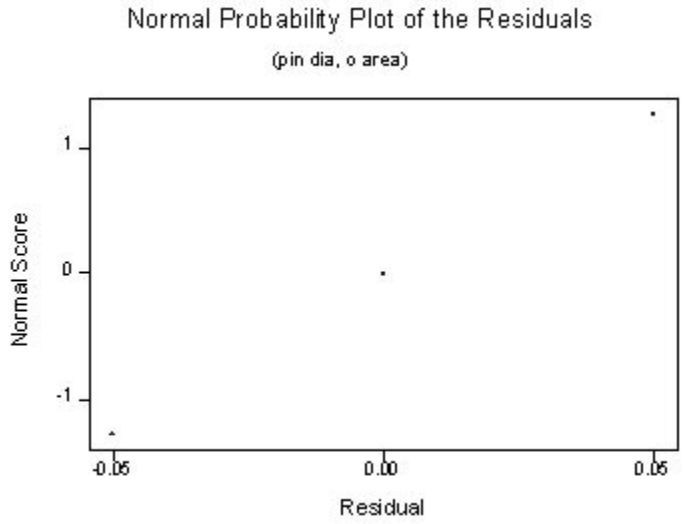

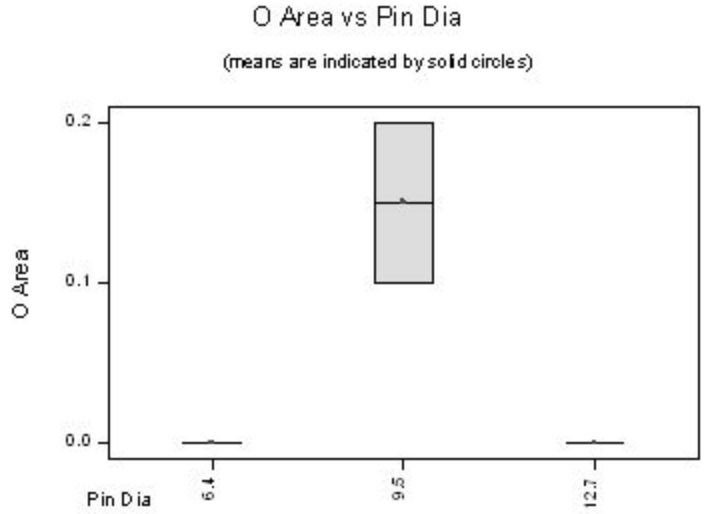


```
Analysis of Variance for Pin dia, O Area
Source     DF        SS        MS        F        P
pin dia     2   0.03000   0.01500     9.00    0.054
Error       3   0.00500   0.00167
Total       5   0.03500

                                 Individual 95% CIs For Mean
                                 Based on Pooled StDev
pin dia     N      Mean     StDev  ----------+---------+---------+------
 6.4        2   0.00000   0.00000   (--------*--------)
 9.5        2   0.15000   0.07071                    (--------*--------)
12.7        2   0.00000   0.00000   (--------*--------)
                                 ----------+---------+---------+------
Pooled StDev =  0.04082                  0.00      0.10      0.20
```

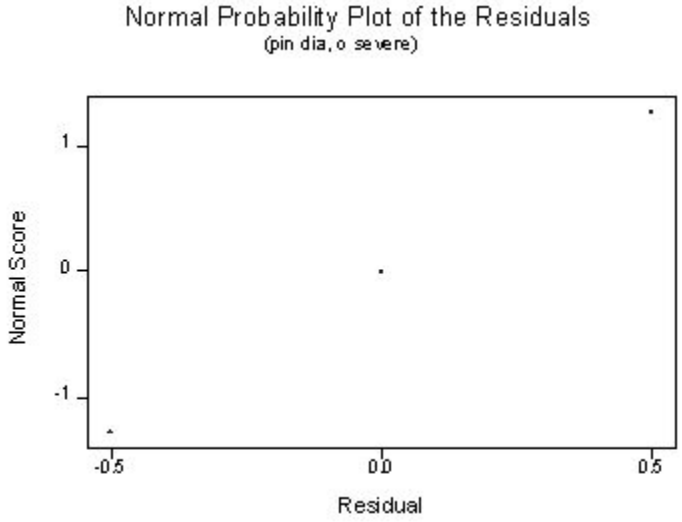

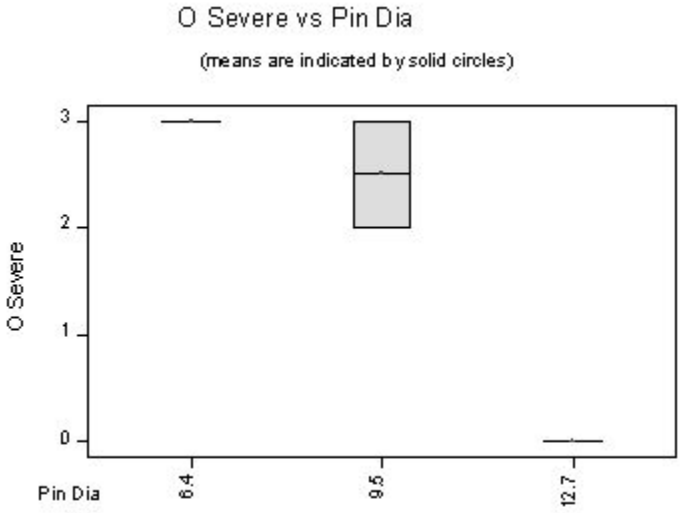


```
Analysis of Variance for Pin Dia, O Severe
Source     DF        SS        MS        F        P
pin dia     2    10.333     5.167    31.00    0.010
Error       3     0.500     0.167
Total       5    10.833

                                  Individual 95% CIs For Mean
                                  Based on Pooled StDev
pin dia     N      Mean     StDev  -------+---------+---------+---------
 6.4        2    3.0000    0.0000                       (-----*-----)
 9.5        2    2.5000    0.7071                  (-----*-----)
12.7        2    0.0000    0.0000   (-----*-----)
                                  -------+---------+---------+---------
Pooled StDev =   0.4082               0.0       1.5       3.0
```

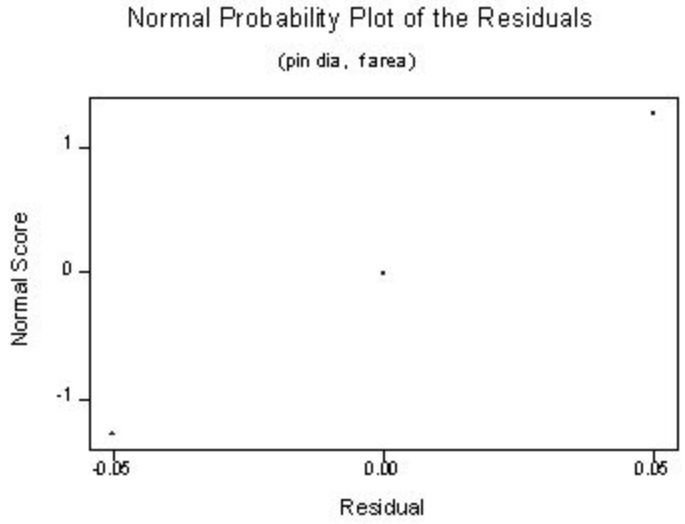

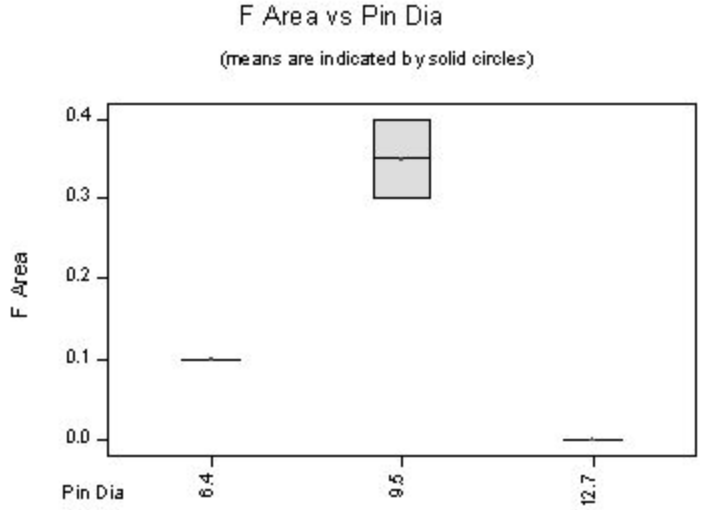


```
Analysis of Variance for Pin Dia, F Area
Source     DF        SS        MS        F        P
pin dia     2   0.13000   0.06500    39.00    0.007
Error       3   0.00500   0.00167
Total       5   0.13500

                                Individual 95% CIs For Mean
                                Based on Pooled StDev
pin dia     N      Mean     StDev  -------+---------+---------+---------
 6.4        2   0.10000   0.00000          (-----*-----)
 9.5        2   0.35000   0.07071                      (-----*-----)
12.7        2   0.00000   0.00000   (-----*-----)
                                -------+---------+---------+---------
Pooled StDev =  0.04082             0.00      0.15      0.30
```

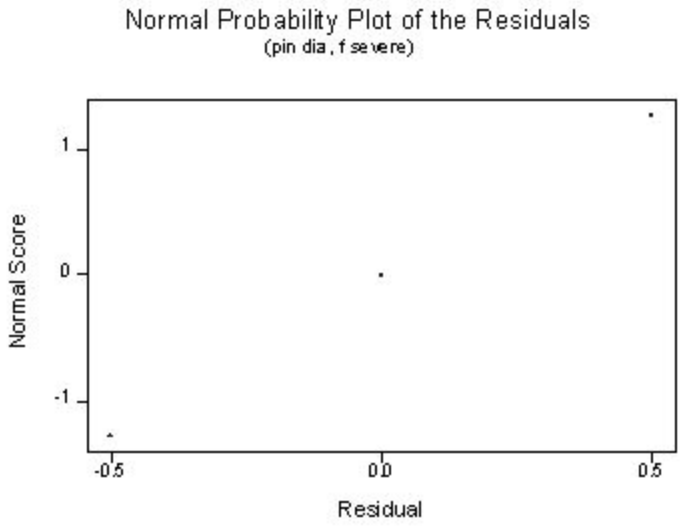

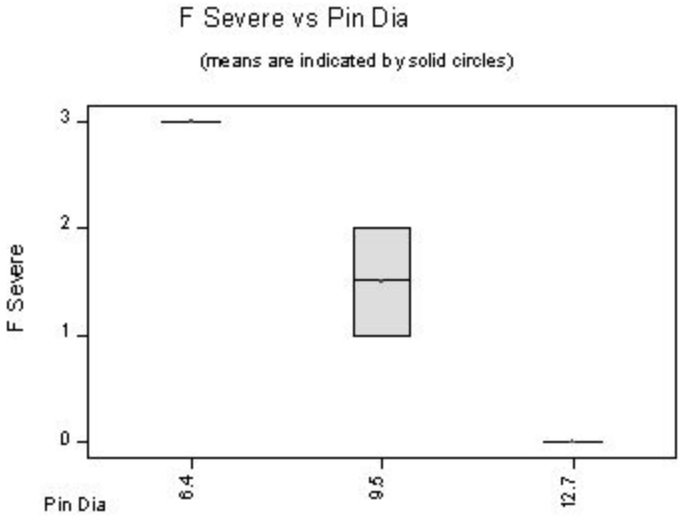


```
Analysis of Variance for Pin Dia, F Severe
Source     DF        SS        MS        F        P
pin dia     2     9.000     4.500    27.00    0.012
Error       3     0.500     0.167
Total       5     9.500

                                  Individual 95% CIs For Mean
                                  Based on Pooled StDev
pin dia     N      Mean     StDev  -------+---------+---------+---------
 6.4        2    3.0000    0.0000                       (-----*-----)
 9.5        2    1.5000    0.7071             (-----*-----)
12.7        2    0.0000    0.0000   (-----*-----)
                                  -------+---------+---------+---------
Pooled StDev =   0.4082               0.0       1.5       3.0
```

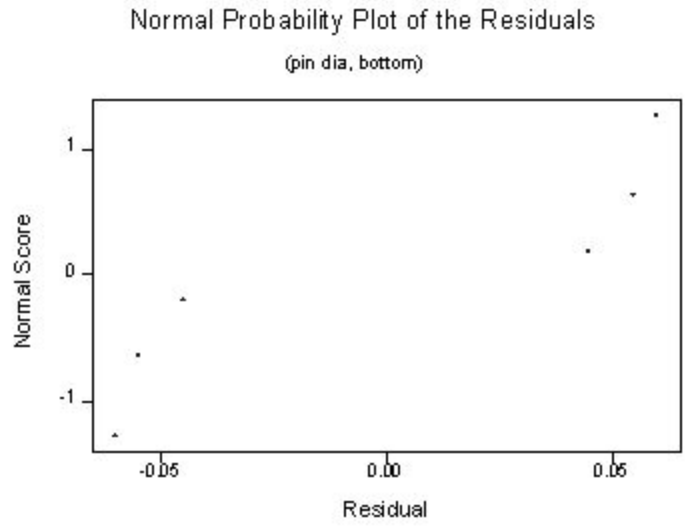

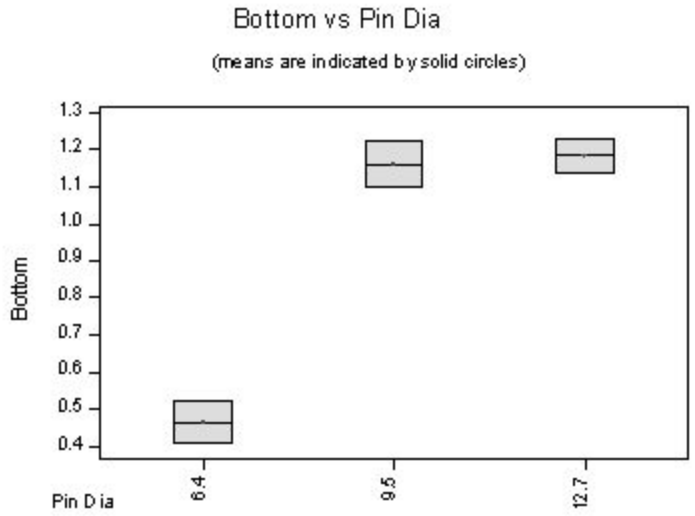


```
Analysis of Variance for Pin Dia, Bottom
Source     DF        SS        MS        F        P
pin dia     2   0.66803   0.33402    57.92    0.004
Error       3   0.01730   0.00577
Total       5   0.68533
                                  Individual 95% CIs For Mean
                                  Based on Pooled StDev
pin dia     N      Mean     StDev  -+---------+---------+---------+-----
 6.4        2    0.4650    0.0778   (-----*----)
 9.5        2    1.1600    0.0849                      (-----*----)
12.7        2    1.1850    0.0636                       (-----*----)
                                  -+---------+---------+---------+-----
Pooled StDev =   0.0759           0.30      0.60      0.90      1.20
```

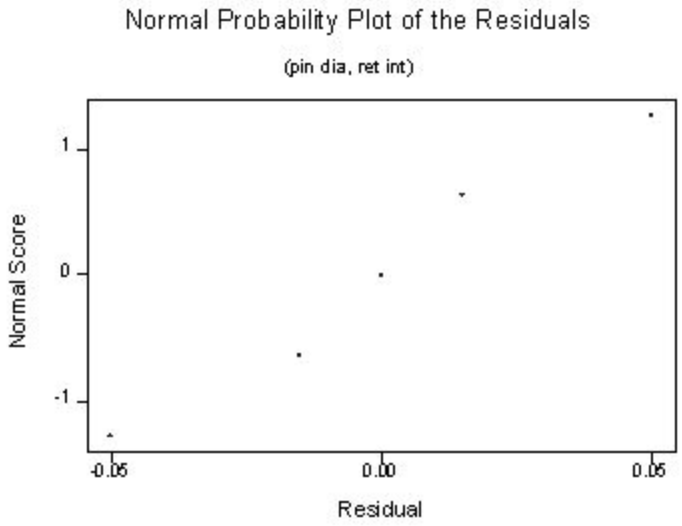

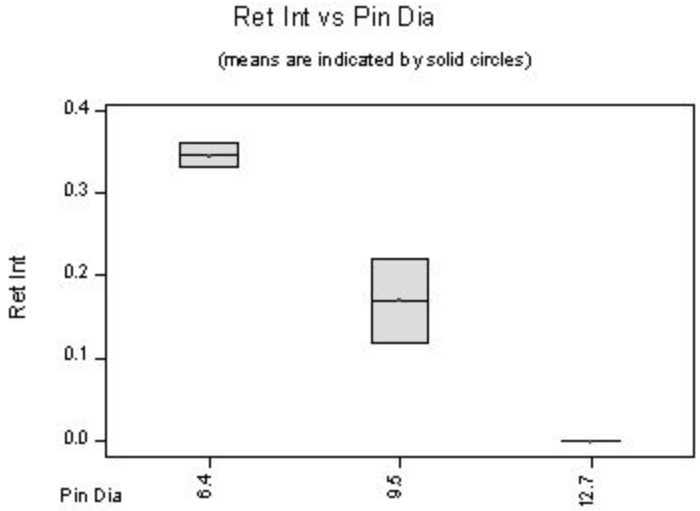


```
Analysis of Variance for Pin Dia, Ret Int
Source     DF        SS        MS        F        P
pin dia     2   0.11903   0.05952    32.76    0.009
Error       3   0.00545   0.00182
Total       5   0.12448

                                 Individual 95% CIs For Mean
                                 Based on Pooled StDev
pin dia     N      Mean     StDev  -------+---------+---------+---------
 6.4        2   0.34500   0.02121                          (-----*-----)
 9.5        2   0.17000   0.07071              (-----*------)
12.7        2   0.00000   0.00000   (-----*-----)
                                 -------+---------+---------+---------
Pooled StDev =  0.04262               0.00      0.15      0.30
```

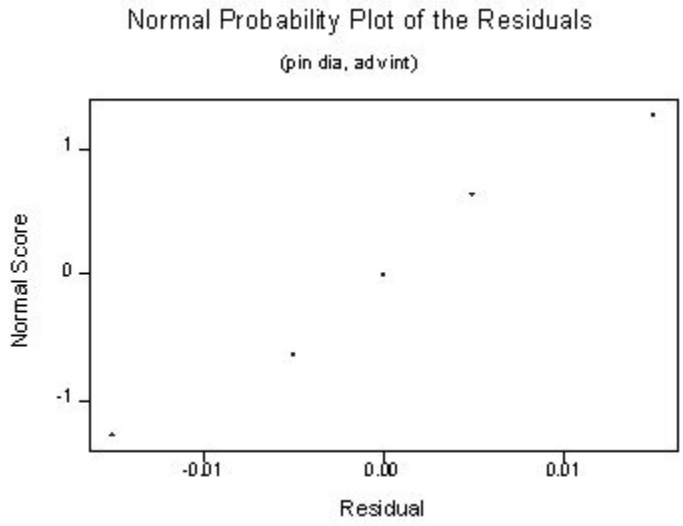

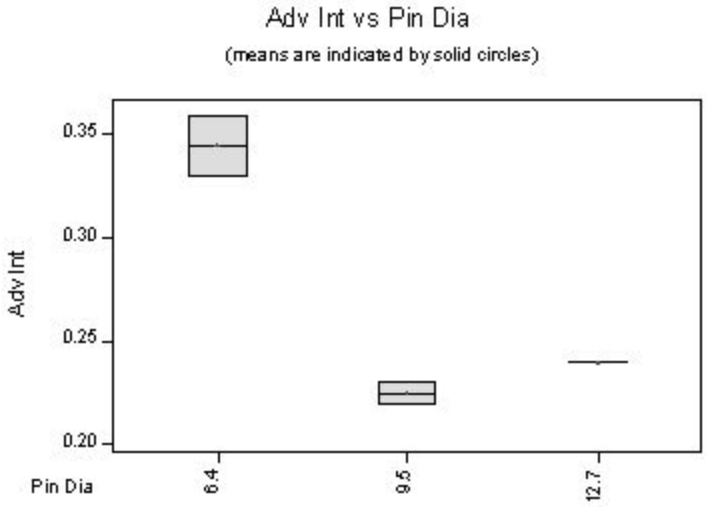


```
Analysis of Variance for Pin Dia, Adv Int
Source     DF        SS        MS        F        P
pin dia     2  0.017100  0.008550    51.30    0.005
Error       3  0.000500  0.000167
Total       5  0.017600

                                  Individual 95% CIs For Mean
                                  Based on Pooled StDev
pin dia     N      Mean     StDev  -+---------+---------+---------+-----
 6.4        2   0.34500   0.02121                           (-----*-----)
 9.5        2   0.22500   0.00707  (-----*-----)
12.7        2   0.24000   0.00000     (-----*-----)
                                  -+---------+---------+---------+-----
Pooled StDev =  0.01291          0.200     0.250     0.300     0.350
```

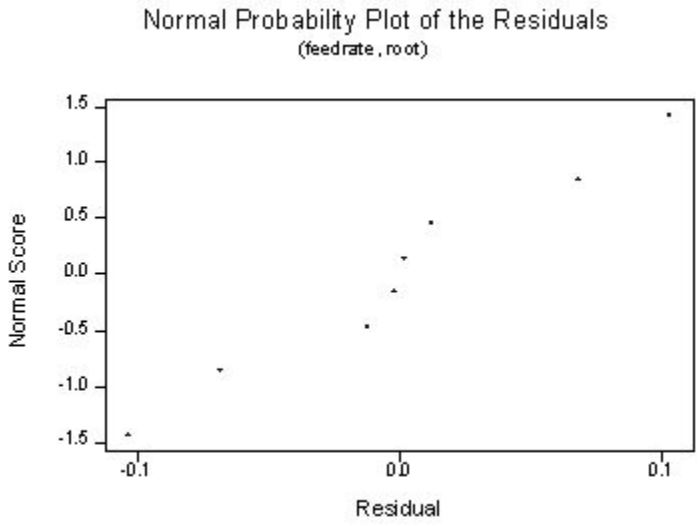

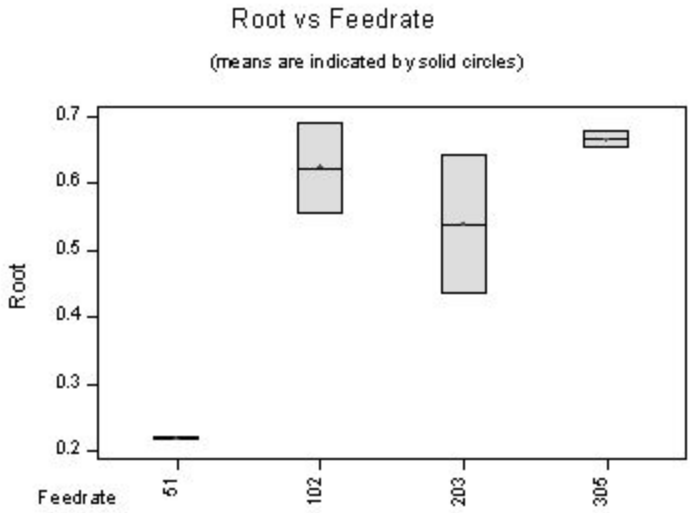

Analysis of Variance for Feedrate, Root

Source	DF	SS	MS	F	P
feedrate	3	0.24486	0.08162	10.54	0.023
Error	4	0.03098	0.00775		
Total	7	0.27584			

feedrate	N	Mean	StDev
51	2	0.22020	0.00286
102	2	0.62393	0.09670
203	2	0.53961	0.14601
305	2	0.66690	0.01747

Pooled StDev = 0.08801

Individual 95% CIs For Mean
Based on Pooled StDev

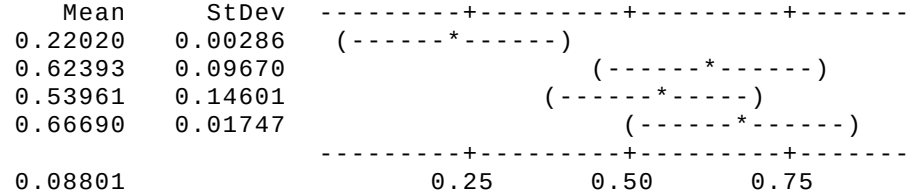

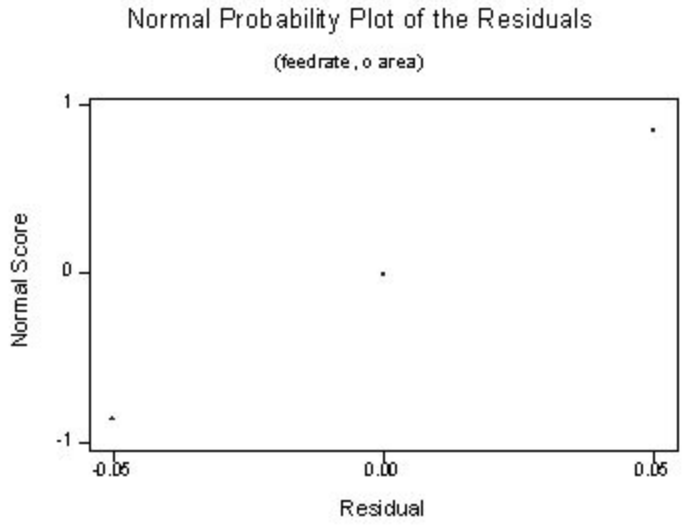

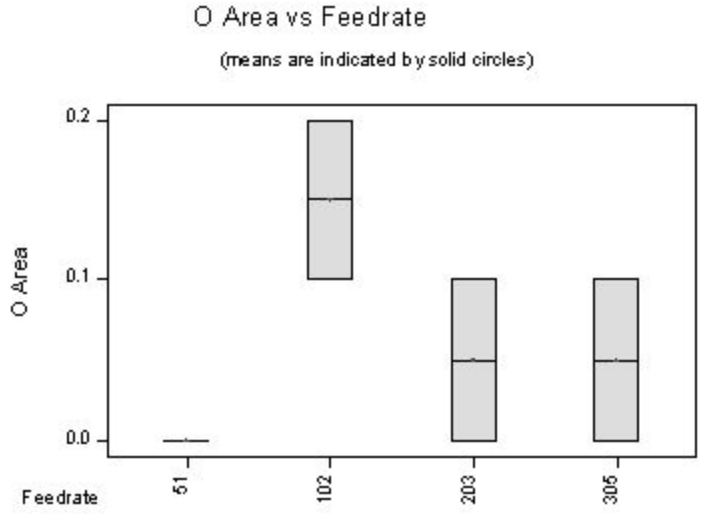


```
Analysis of Variance for Feedrate, O Area
Source     DF        SS        MS        F        P
feedrate    3   0.02375   0.00792     2.11    0.242
Error       4   0.01500   0.00375
Total       7   0.03875

                                  Individual 95% CIs For Mean
                                  Based on Pooled StDev
feedrate    N      Mean     StDev  -+---------+---------+---------+-----
 51         2   0.00000   0.00000   (---------*---------)
102         2   0.15000   0.07071             (---------*----------)
203         2   0.05000   0.07071       (---------*---------)
305         2   0.05000   0.07071       (---------*---------)
                                  -+---------+---------+---------+-----
Pooled StDev =  0.06124          -0.12      0.00      0.12      0.24
```

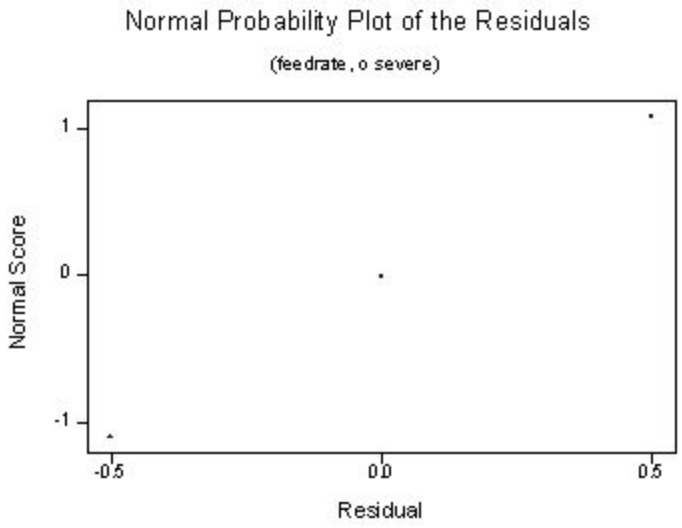

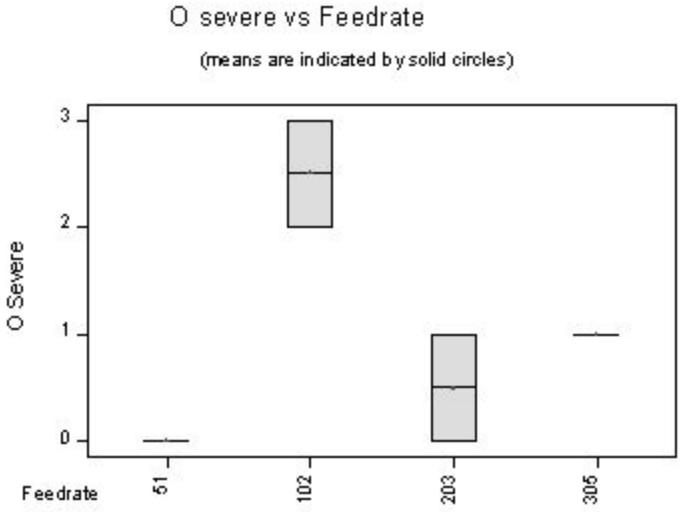


```
Analysis of Variance for Feedrate, O Severe
Source     DF        SS        MS        F        P
feedrate    3     7.000     2.333     9.33    0.028
Error       4     1.000     0.250
Total       7     8.000

                                  Individual 95% CIs For Mean
                                  Based on Pooled StDev
feedrate    N      Mean     StDev  -------+---------+---------+---------
 51         2    0.0000    0.0000  (------*------)
102         2    2.5000    0.7071                   (------*-----)
203         2    0.5000    0.7071      (-----*------)
305         2    1.0000    0.0000         (------*-----)
                                  -------+---------+---------+---------
Pooled StDev =   0.5000               0.0       1.5       3.0
```

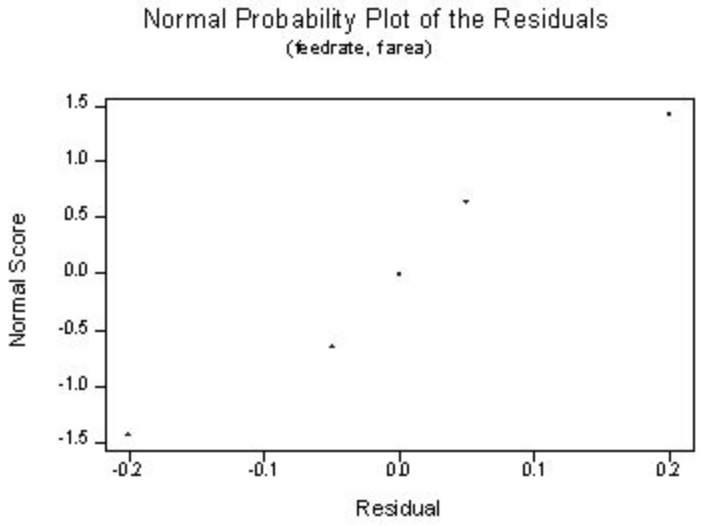

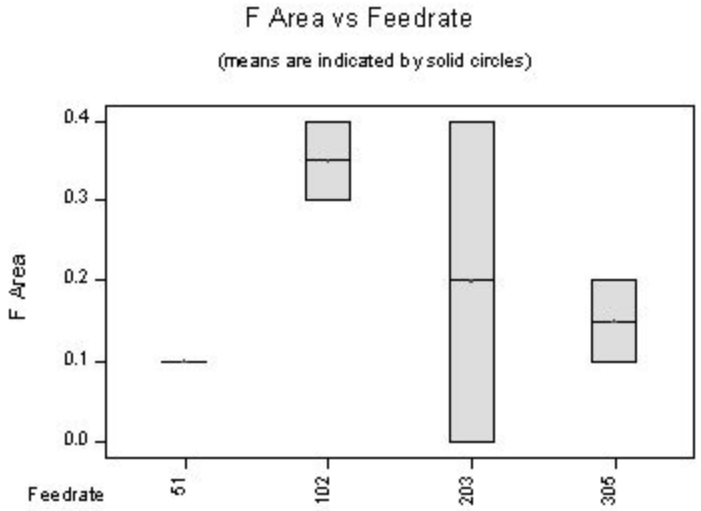

Analysis of Variance for Feedrate, F Area

Source	DF	SS	MS	F	P
feedrate	3	0.0700	0.0233	1.04	0.466
Error	4	0.0900	0.0225		
Total	7	0.1600			

feedrate	N	Mean	StDev
51	2	0.1000	0.0000
102	2	0.3500	0.0707
203	2	0.2000	0.2828
305	2	0.1500	0.0707

Pooled StDev = 0.1500

Individual 95% CIs For Mean
Based on Pooled StDev

```
--------+---------+---------+--------
(-----------*-----------)
          (-----------*-----------)
     (-----------*-----------)
  (-----------*-----------)
--------+---------+---------+--------
      0.00      0.25      0.50
```

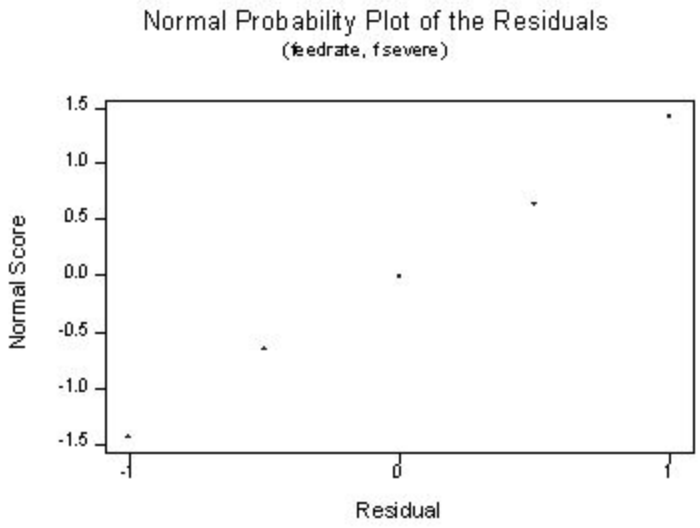

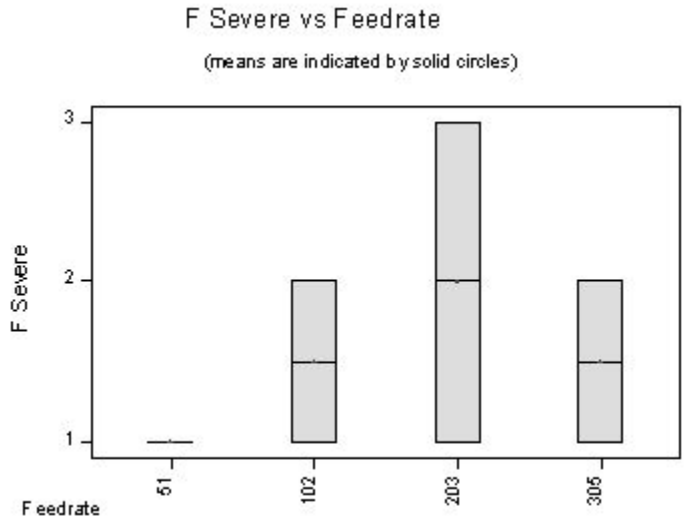


```
Analysis of Variance for Feedrate, F Severe
Source     DF        SS        MS        F        P
feedrate    3     1.000     0.333     0.44    0.734
Error       4     3.000     0.750
Total       7     4.000

                                  Individual 95% CIs For Mean
                                  Based on Pooled StDev
feedrate    N      Mean     StDev  ------+---------+---------+---------+
 51         2    1.0000    0.0000  (-------------*--------------)
102         2    1.5000    0.7071      (-------------*--------------)
203         2    2.0000    1.4142         (--------------*-------------)
305         2    1.5000    0.7071      (-------------*--------------)
                                  ------+---------+---------+---------+
Pooled StDev =   0.8660               0.0       1.2       2.4       3.6
```

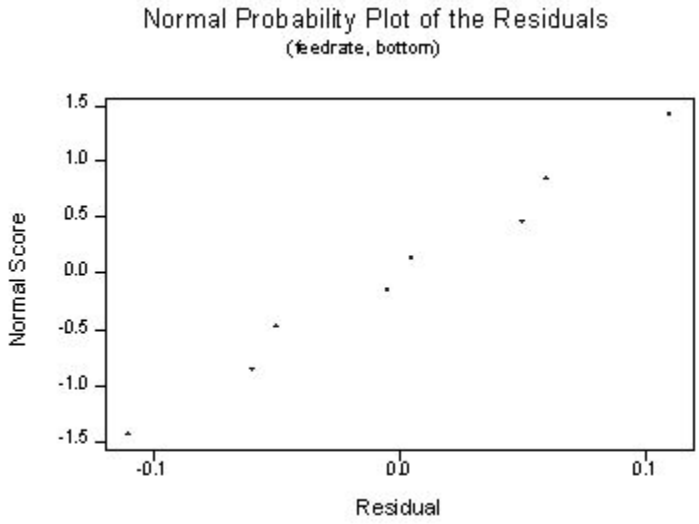

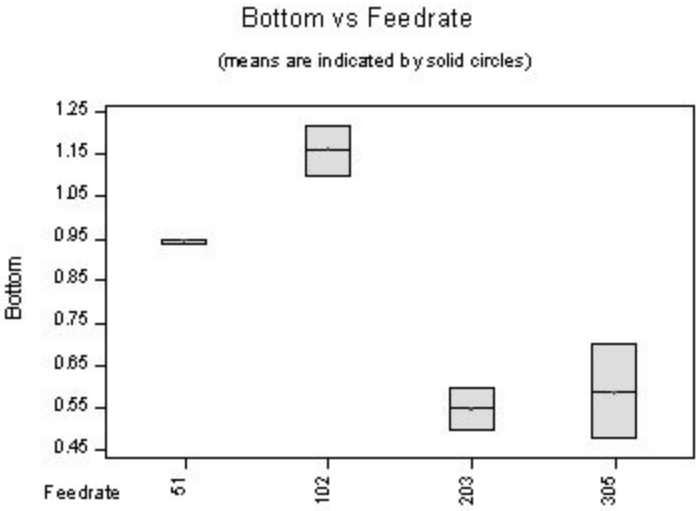

Analysis of Variance for Feedrate, Bottom

Source	DF	SS	MS	F	P
feedrate	3	0.51344	0.17115	18.78	0.008
Error	4	0.03645	0.00911		
Total	7	0.54989			

feedrate	N	Mean	StDev
51	2	0.9450	0.0071
102	2	1.1600	0.0849
203	2	0.5500	0.0707
305	2	0.5900	0.1556

Pooled StDev = 0.0955

Individual 95% CIs For Mean
Based on Pooled StDev

```
--------+---------+---------+--------
              (------*-----)
                     (------*-----)
(-----*------)
 (------*-----)
--------+---------+---------+--------
      0.60      0.90      1.20
```

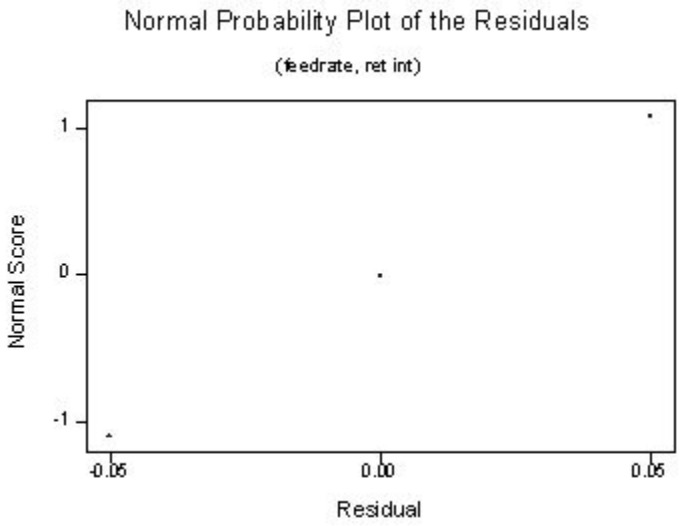

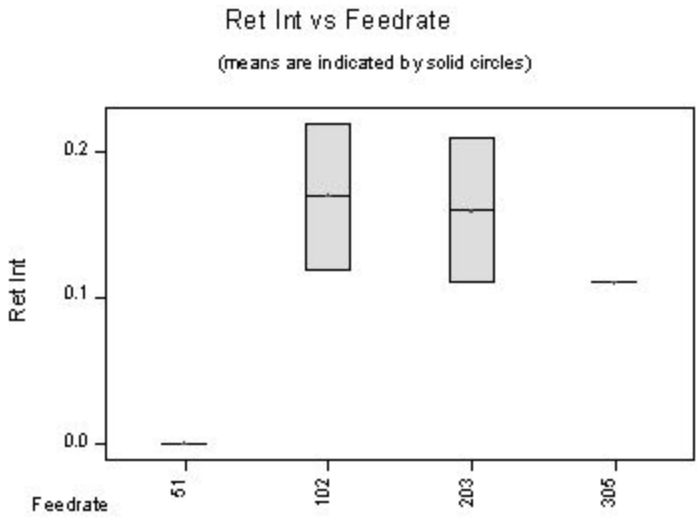


```
Analysis of Variance for Feedrate, Ret Int
Source     DF        SS        MS        F        P
feedrate    3   0.03640   0.01213     4.85    0.081
Error       4   0.01000   0.00250
Total       7   0.04640

                                 Individual 95% CIs For Mean
                                 Based on Pooled StDev
feedrate    N      Mean     StDev  ----------+---------+---------+------
 51         2   0.00000   0.00000  (---------*---------)
102         2   0.17000   0.07071                (---------*---------)
203         2   0.16000   0.07071                (---------*---------)
305         2   0.11000   0.00000           (---------*---------)
                                 ----------+---------+---------+------
Pooled StDev =  0.05000                  0.00      0.10      0.20
```

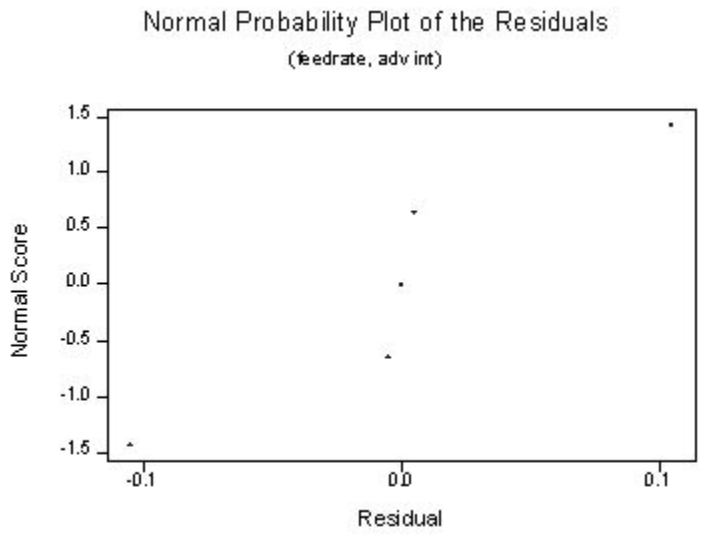

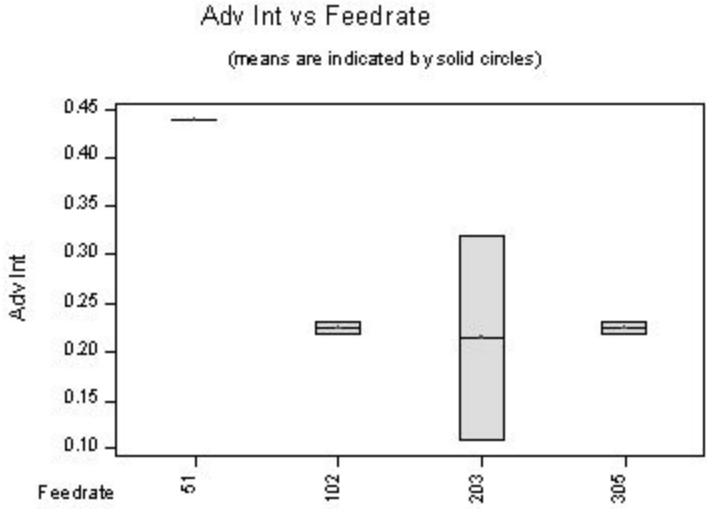

Analysis of Variance for Feedrate, Adv Int

Source	DF	SS	MS	F	P
feedrate	3	0.07164	0.02388	4.31	0.096
Error	4	0.02215	0.00554		
Total	7	0.09379			

feedrate	N	Mean	StDev
51	2	0.44000	0.00000
102	2	0.22500	0.00707
203	2	0.21500	0.14849
305	2	0.22500	0.00707

Pooled StDev = 0.07441

Individual 95% CIs For Mean
Based on Pooled StDev

```
------+---------+---------+---------+
                      (--------*---------)
       (---------*---------)
       (---------*---------)
       (---------*---------)
------+---------+---------+---------+
    0.15      0.30      0.45      0.60
```

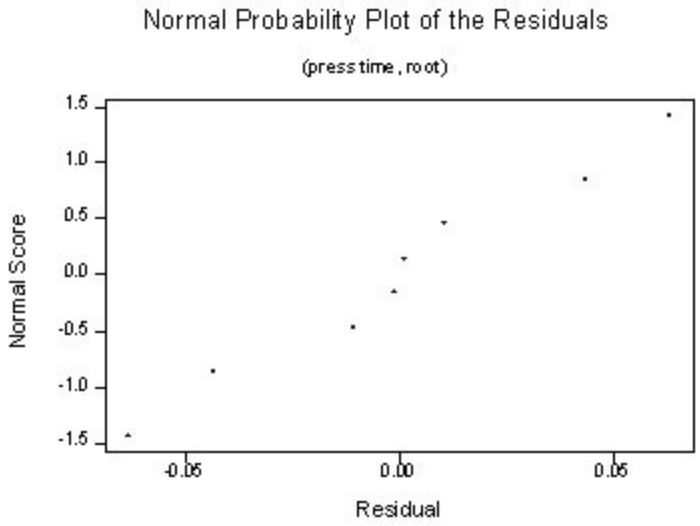

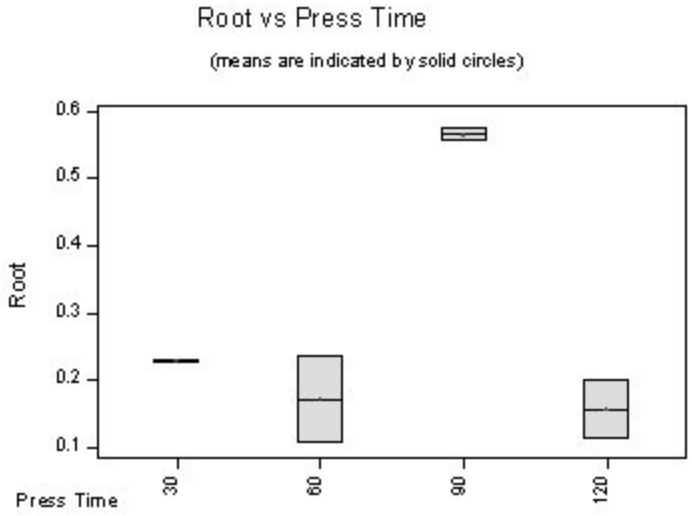


```
Analysis of Variance for Press Time, Root
Source     DF        SS        MS        F        P
Press. T    3   0.22262   0.07421    24.82    0.005
Error       4   0.01196   0.00299
Total       7   0.23458

                                 Individual 95% CIs For Mean
                                 Based on Pooled StDev
press time  N      Mean     StDev  --------+---------+---------+--------
 30         2   0.22967   0.00155      (----*-----)
 60         2   0.17219   0.08924   (-----*----)
 90         2   0.56624   0.01511                      (----*-----)
120         2   0.15660   0.06137  (-----*----)
                                 --------+---------+---------+--------
Pooled StDev =  0.05468               0.20      0.40      0.60
```

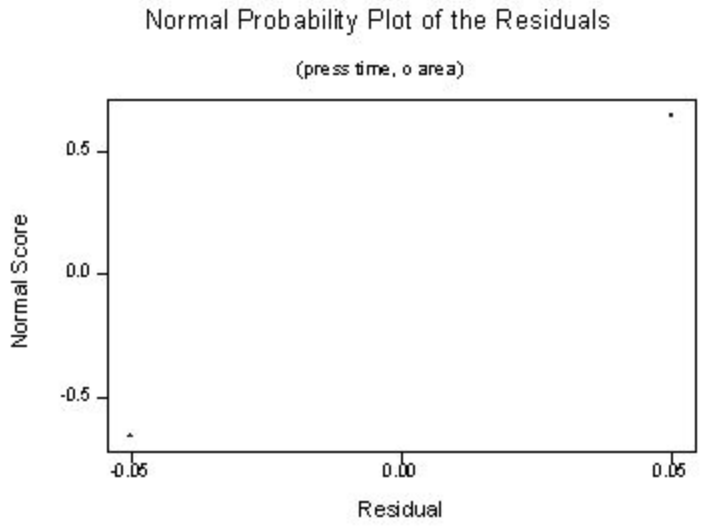

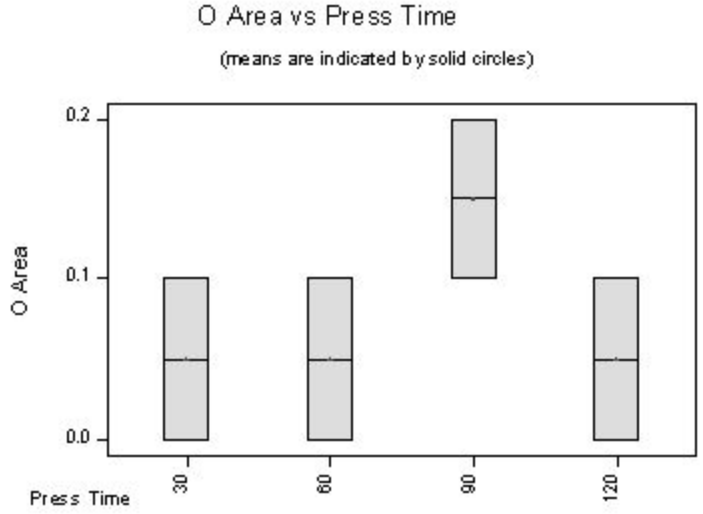

Analysis of Variance for Press Time, O Area

Source	DF	SS	MS	F	P
Press. T	3	0.01500	0.00500	1.00	0.479
Error	4	0.02000	0.00500		
Total	7	0.03500			

press time	N	Mean	StDev	Individual 95% CIs For Mean Based on Pooled StDev
30	2	0.05000	0.07071	(----------*----------)
60	2	0.05000	0.07071	(----------*----------)
90	2	0.15000	0.07071	(----------*----------)
120	2	0.05000	0.07071	(----------*----------)

Pooled StDev = 0.07071

0.00 0.12 0.24

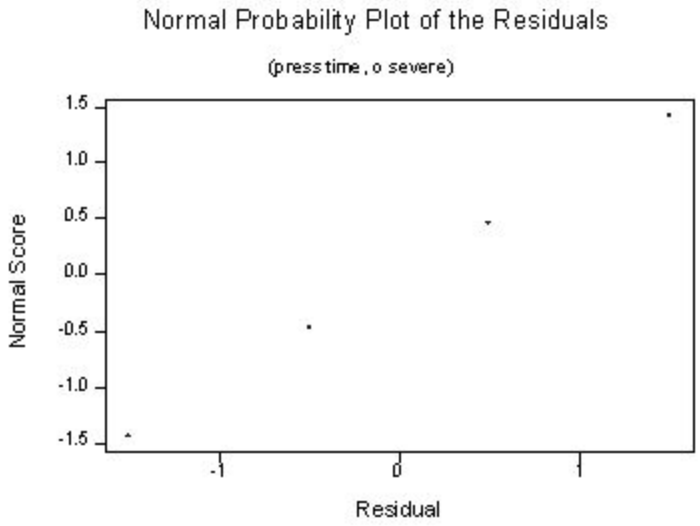

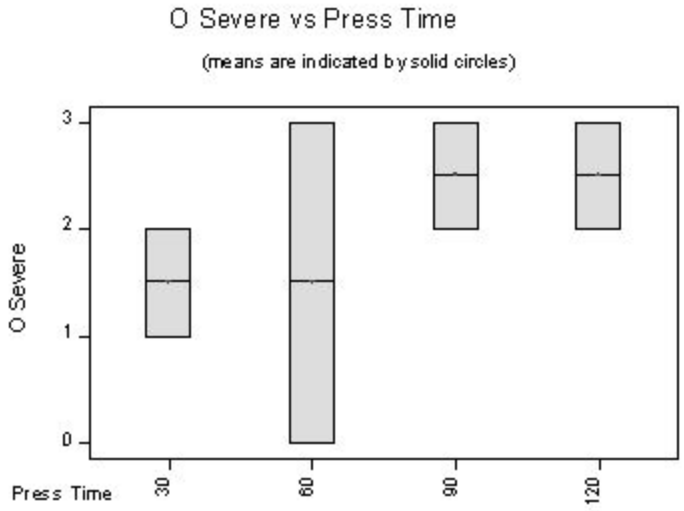


```
Analysis of Variance for Press Time, O Severe
Source     DF        SS        MS        F        P
Press. T    3      2.00      0.67     0.44    0.734
Error       4      6.00      1.50
Total       7      8.00

                                  Individual 95% CIs For Mean
                                  Based on Pooled StDev
press time  N      Mean     StDev  ------+---------+---------+---------+
 30         2     1.500     0.707  (--------------*--------------)
 60         2     1.500     2.121  (--------------*--------------)
 90         2     2.500     0.707        (--------------*--------------)
120         2     2.500     0.707        (--------------*--------------)
                                  ------+---------+---------+---------+
Pooled StDev =    1.225              0.0       1.6       3.2       4.8
```

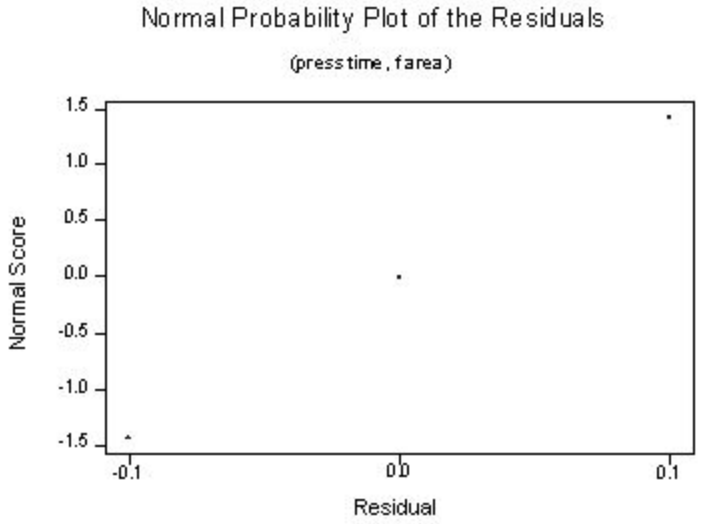

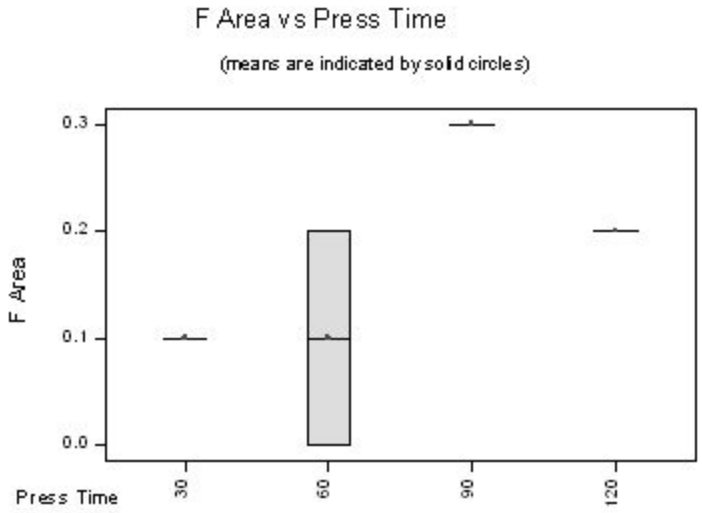

Analysis of Variance for Press Time, F Area

Source	DF	SS	MS	F	P
Press. T	3	0.05500	0.01833	3.67	0.121
Error	4	0.02000	0.00500		
Total	7	0.07500			

press time	N	Mean	StDev
30	2	0.10000	0.00000
60	2	0.10000	0.14142
90	2	0.30000	0.00000
120	2	0.20000	0.00000

Pooled StDev = 0.07071

Individual 95% CIs For Mean
Based on Pooled StDev

```
---+---------+---------+---------+---
(---------*--------)
(---------*--------)
          (--------*--------)
 (--------*---------)
---+---------+---------+---------+---
 0.00      0.15      0.30      0.45
```

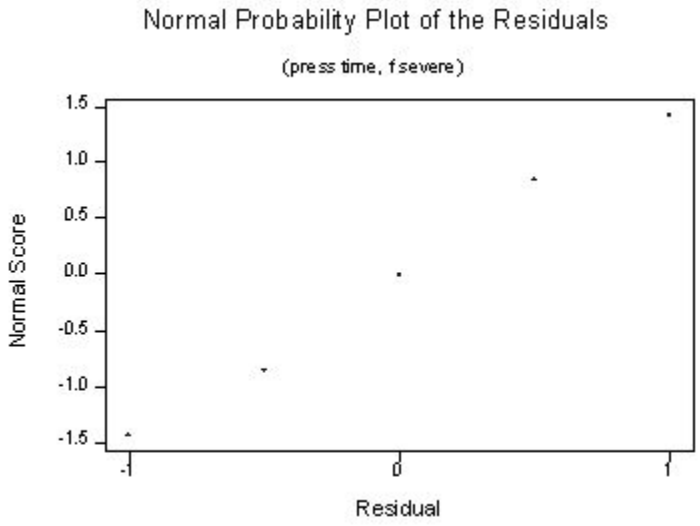

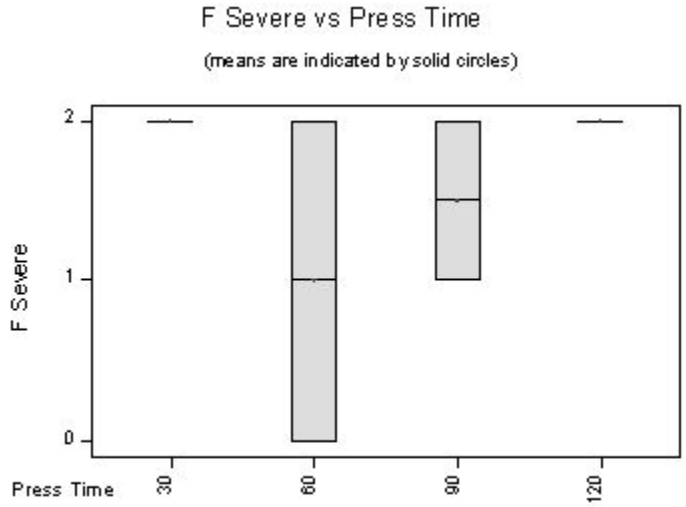


```
Analysis of Variance for Press Time, F Severe
Source     DF        SS        MS        F        P
Press. T    3     1.375     0.458     0.73    0.584
Error       4     2.500     0.625
Total       7     3.875

                                  Individual 95% CIs For Mean
                                  Based on Pooled StDev
press time  N      Mean     StDev  -----+---------+---------+---------+-
 30         2    2.0000    0.0000           (------------*------------)
 60         2    1.0000    1.4142  (------------*------------)
 90         2    1.5000    0.7071       (-----------*------------)
120         2    2.0000    0.0000           (------------*------------)
                                  -----+---------+---------+---------+-
Pooled StDev =   0.7906             0.0       1.2       2.4       3.6
```

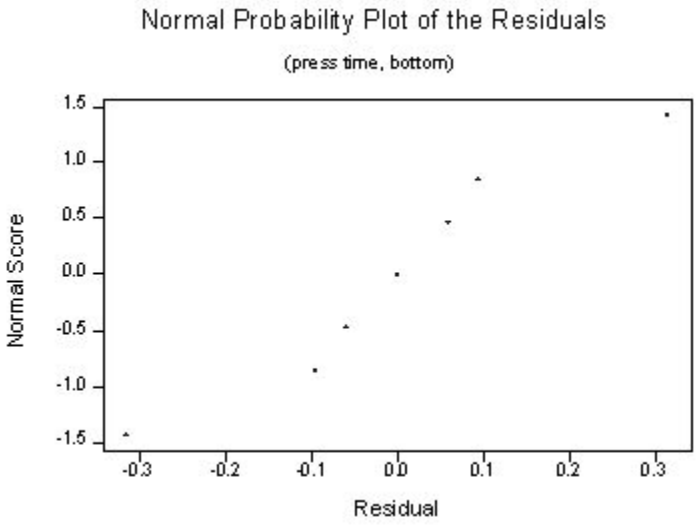

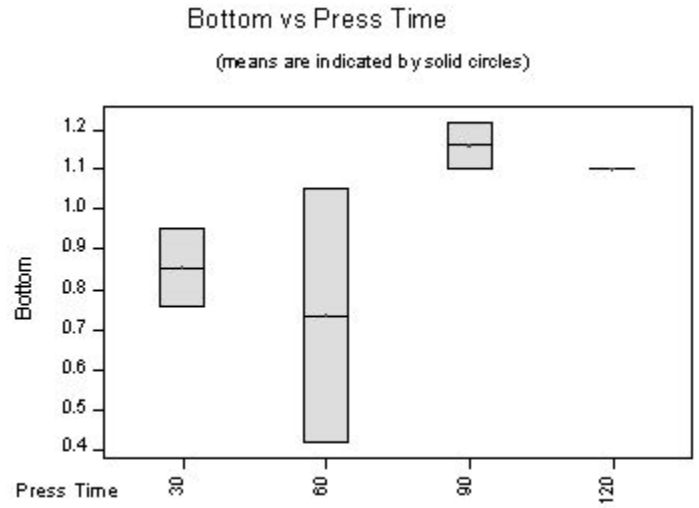

Analysis of Variance for Press Time, Bottom

Source	DF	SS	MS	F	P
Press. T	3	0.2424	0.0808	1.45	0.355
Error	4	0.2237	0.0559		
Total	7	0.4661			

press time	N	Mean	StDev
30	2	0.8550	0.1344
60	2	0.7350	0.4455
90	2	1.1600	0.0849
120	2	1.1000	0.0000

Pooled StDev = 0.2365

Individual 95% CIs For Mean
Based on Pooled StDev

```
----+---------+---------+---------+--
    (----------*----------)
  (----------*----------)
            (----------*----------)
           (----------*----------)
----+---------+---------+---------+--
  0.40      0.80      1.20      1.60
```

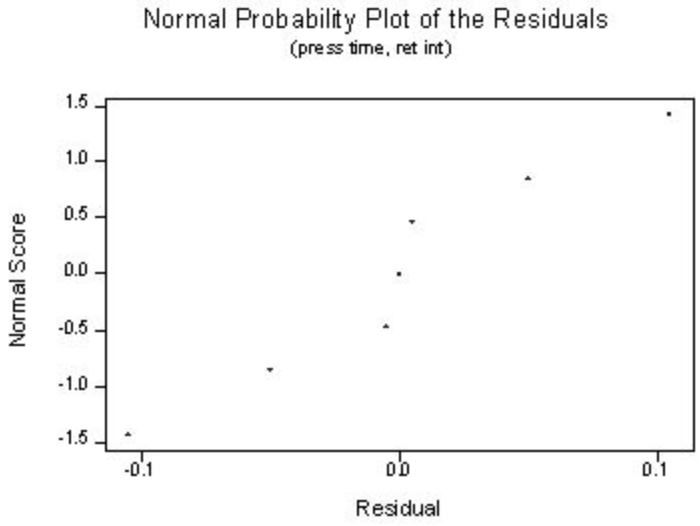

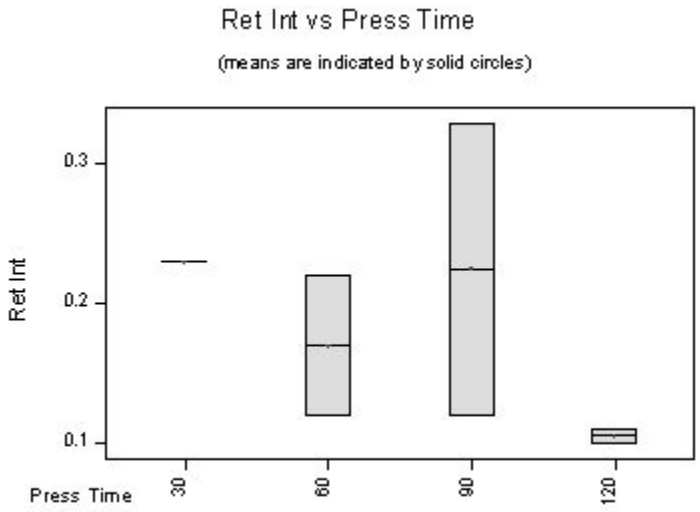

Analysis of Variance for Press Time, Ret Int

Source	DF	SS	MS	F	P
Press. T	3	0.02045	0.00682	1.01	0.477
Error	4	0.02710	0.00678		
Total	7	0.04755			

press time	N	Mean	StDev
30	2	0.23000	0.00000
60	2	0.17000	0.07071
90	2	0.22500	0.14849
120	2	0.10500	0.00707

Pooled StDev = 0.08231

Individual 95% CIs For Mean
Based on Pooled StDev

```
----+---------+---------+---------+--
          (---------*----------)
       (---------*----------)
          (----------*----------)
(----------*----------)
----+---------+---------+---------+--
  0.00      0.15      0.30      0.45
```

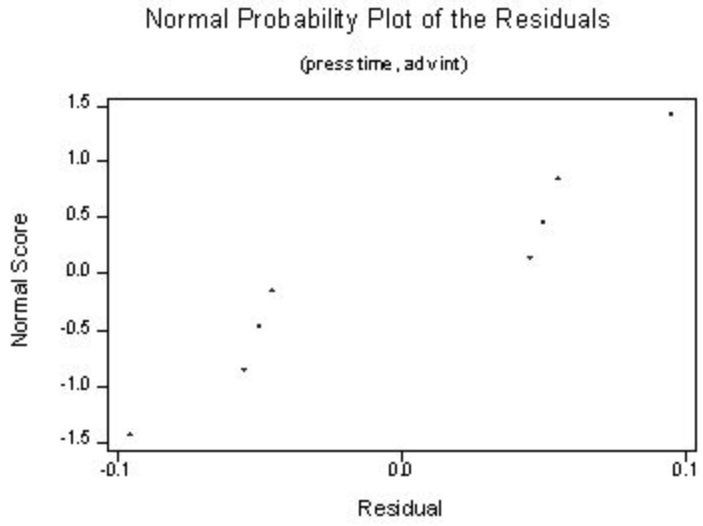

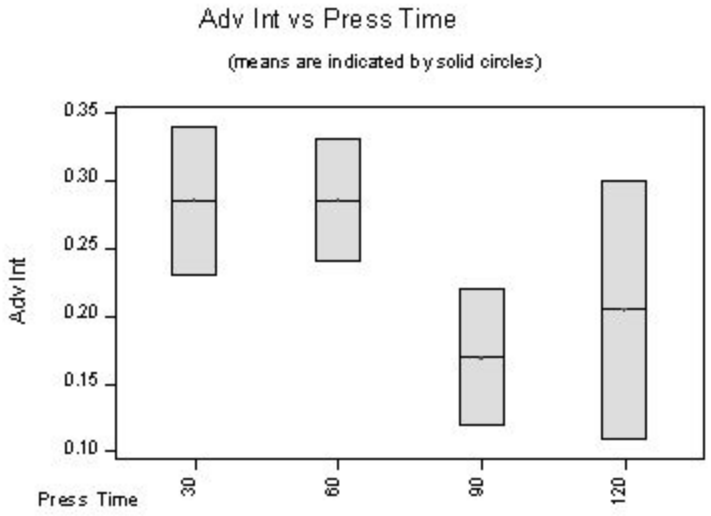


```
Analysis of Variance for Press Time, Adv Int
Source     DF        SS        MS        F        P
Press. T    3   0.02024   0.00675     0.81    0.549
Error       4   0.03315   0.00829
Total       7   0.05339

                                 Individual 95% CIs For Mean
                                 Based on Pooled StDev
press time  N      Mean     StDev  -+---------+---------+---------+-----
 30         2   0.28500   0.07778          (-----------*-----------)
 60         2   0.28500   0.06364          (-----------*-----------)
 90         2   0.17000   0.07071  (-----------*-----------)
120         2   0.20500   0.13435     (-----------*-----------)
                                 -+---------+---------+---------+-----
Pooled StDev =  0.09104           0.00      0.15      0.30      0.45
```

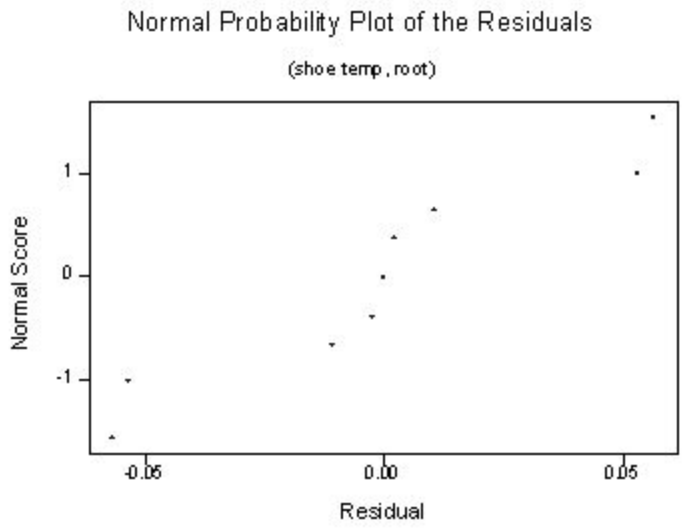

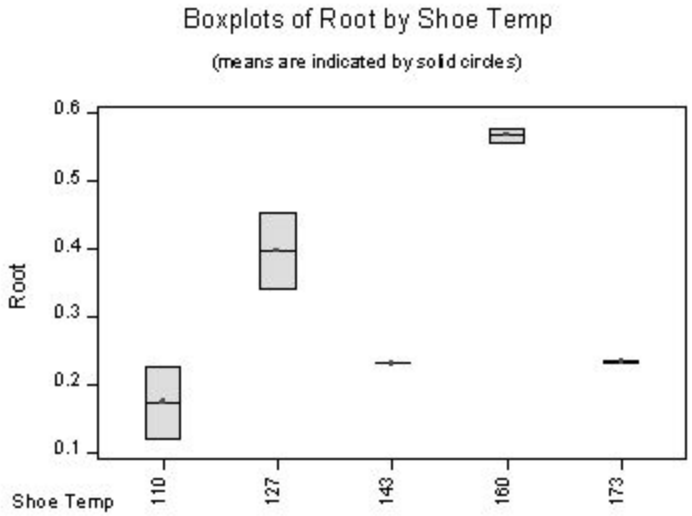


```
Analysis of Variance for Shoe Temp, Root
Source     DF        SS        MS        F        P
Shoe Tem    4   0.20704   0.05176    21.03    0.003
Error       5   0.01231   0.00246
Total       9   0.21934

                                  Individual 95% CIs For Mean
                                  Based on Pooled StDev
Temp        N      Mean     StDev  -----+---------+---------+---------+-
110         2   0.17321   0.07525  (-----*----)
127         2   0.39623   0.08005               (-----*----)
143         2   0.23077   0.00000     (----*-----)
160         2   0.56624   0.01511                          (----*-----)
173         2   0.23303   0.00320     (-----*----)
                                  -----+---------+---------+---------+-
Pooled StDev =  0.04962             0.16      0.32      0.48      0.64
```

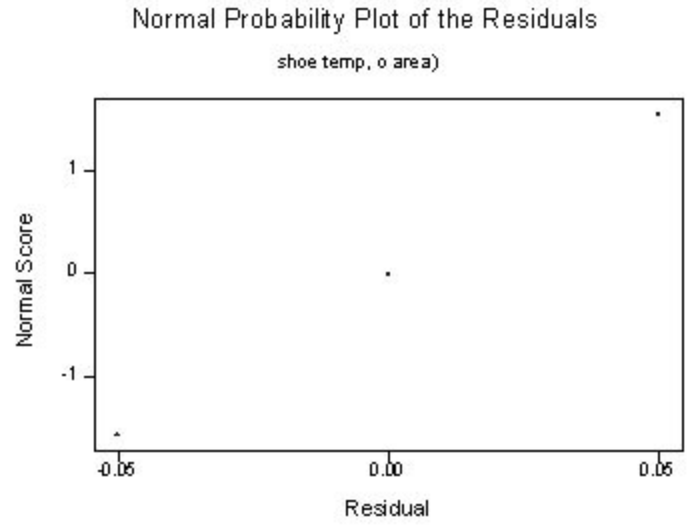

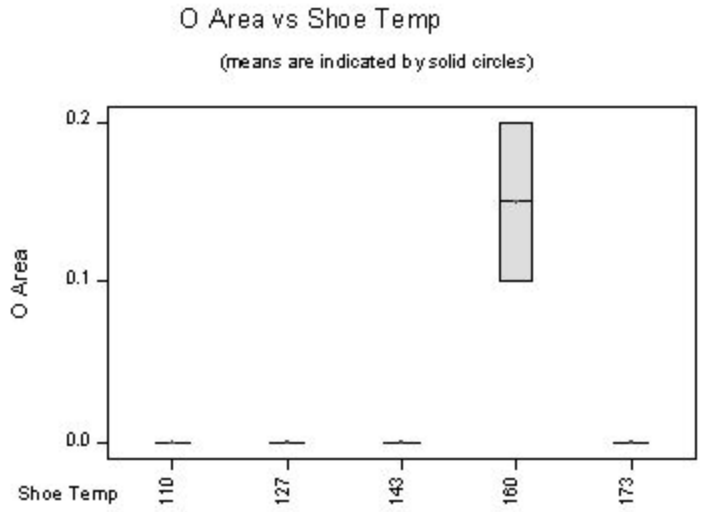


```
Analysis of Variance for Shoe Temp, O Area
Source     DF        SS        MS         F        P
Shoe Tem    4   0.03600   0.00900      9.00    0.017
Error       5   0.00500   0.00100
Total       9   0.04100

                                  Individual 95% CIs For Mean
                                  Based on Pooled StDev
Shoe temp   N      Mean     StDev  --------+---------+---------+--------
110         2   0.00000   0.00000   (------*------)
127         2   0.00000   0.00000   (------*------)
143         2   0.00000   0.00000   (------*------)
160         2   0.15000   0.07071                    (------*------)
173         2   0.00000   0.00000   (------*------)
                                  --------+---------+---------+--------
Pooled StDev =  0.03162             0.000     0.080     0.160
```

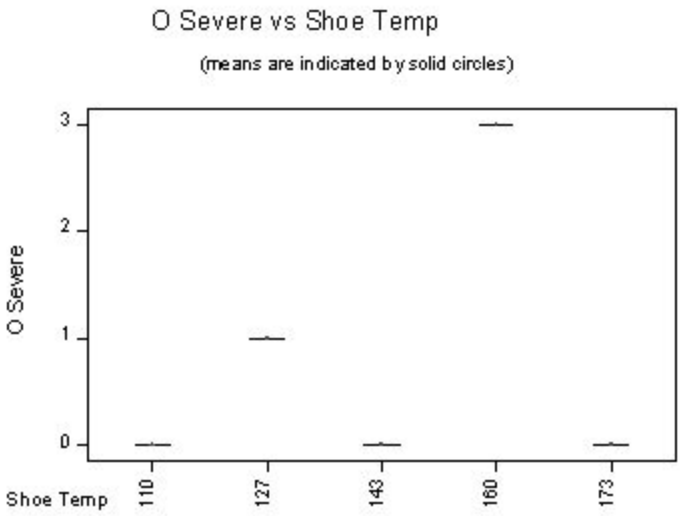


```
Analysis of Variance for shoe temp, O Severe
Source     DF        SS        MS        F        P
Shoe Tem    4  13.60000   3.40000        *        *
Error       5   0.00000   0.00000
Total       9  13.60000
                                  Individual 95% CIs For Mean
                                  Based on Pooled StDev
shoe temp   N      Mean     StDev  +---------+---------+---------+------
110         2   0.00000   0.00000  *
127         2   1.00000   0.00000            *
143         2   0.00000   0.00000  *
160         2   3.00000   0.00000                                    *
173         2   0.00000   0.00000  *
                                  +---------+---------+---------+------
Pooled StDev =  0.00000          0.0       1.0       2.0       3.0
* NOTE * Cannot perform the Normal Score plot with MSE=0
```

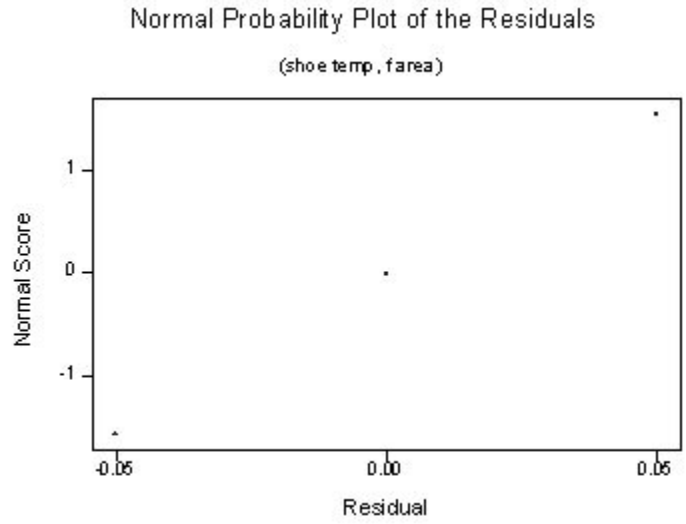

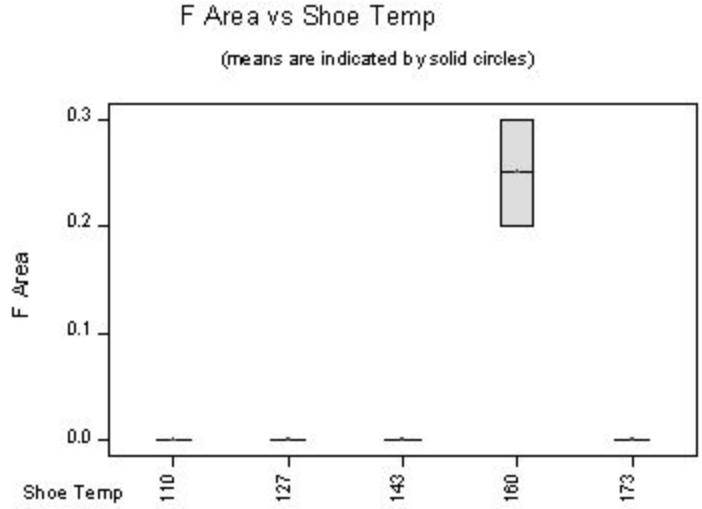


```
Analysis of Variance for Shoe Temp, F Area
Source     DF        SS        MS        F        P
Shoe Tem    4   0.10000   0.02500    25.00    0.002
Error       5   0.00500   0.00100
Total       9   0.10500

                                  Individual 95% CIs For Mean
                                  Based on Pooled StDev
shoe temp   N      Mean     StDev  ------+---------+---------+---------+
110         2   0.00000   0.00000  (-----*-----)
127         2   0.00000   0.00000  (-----*-----)
143         2   0.00000   0.00000  (-----*-----)
160         2   0.25000   0.07071                        (-----*-----)
173         2   0.00000   0.00000  (-----*-----)
                                  ------+---------+---------+---------+
Pooled StDev =  0.03162              0.00      0.10      0.20      0.30
```

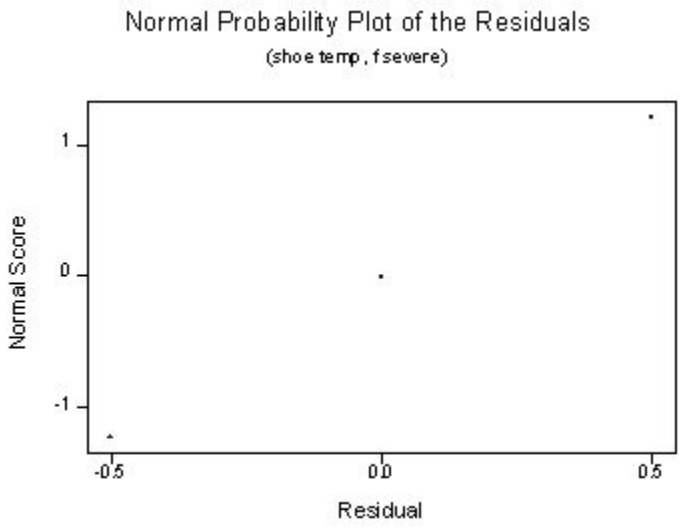

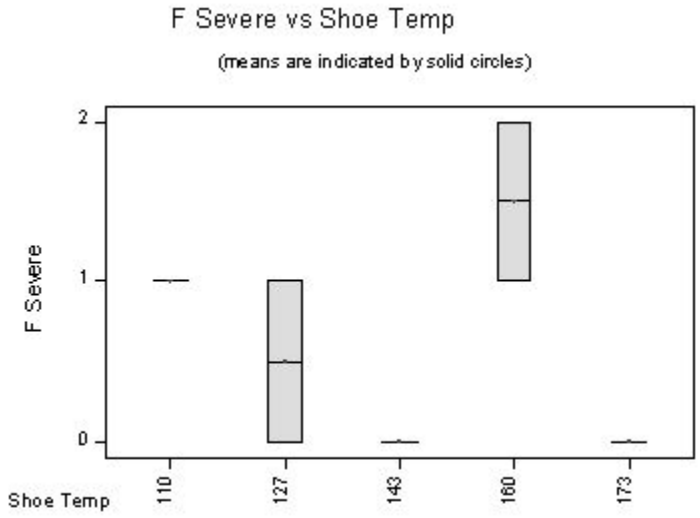

Analysis of Variance for Shoe Temp, F Severe

Source	DF	SS	MS	F	P
Shoe Tem	4	3.400	0.850	4.25	0.072
Error	5	1.000	0.200		
Total	9	4.400			

shoe temp	N	Mean	StDev
110	2	1.0000	0.0000
127	2	0.5000	0.7071
143	2	0.0000	0.0000
160	2	1.5000	0.7071
173	2	0.0000	0.0000

Pooled StDev = 0.4472

Individual 95% CIs For Mean
Based on Pooled StDev

```
---------+---------+---------+-------
          (-------*-------)
      (-------*-------)
 (-------*-------)
               (-------*-------)
 (-------*-------)
---------+---------+---------+-------
       0.0       1.0       2.0
```

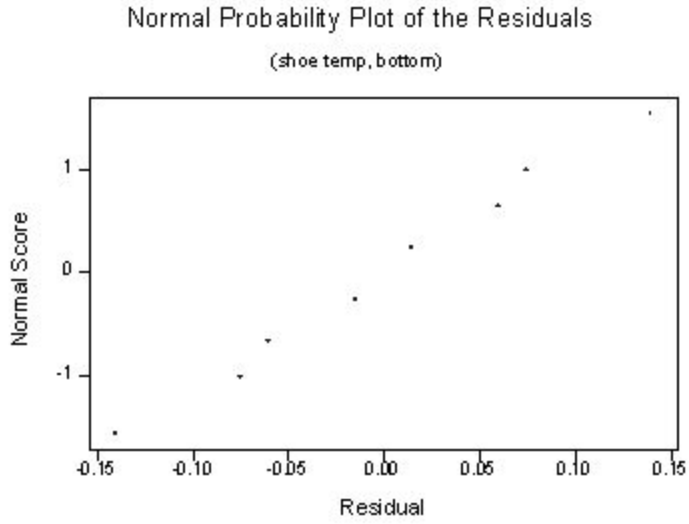

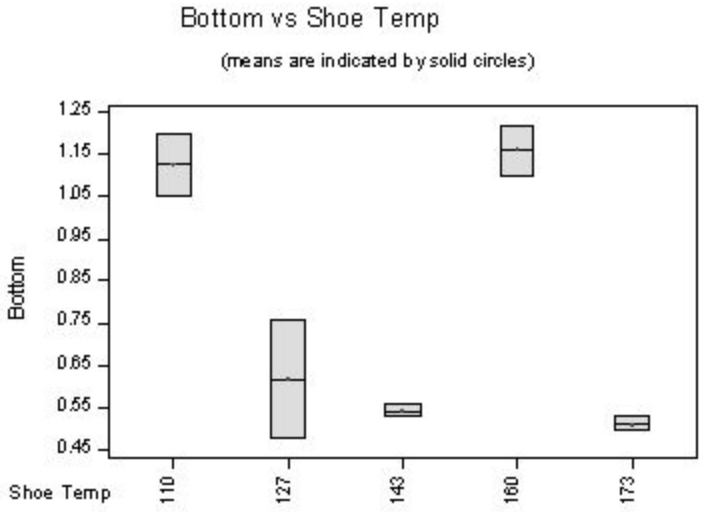


```
Analysis of Variance for Shoe Temp, Bottom
Source     DF        SS        MS         F        P
Shoe Tem    4    0.8273    0.2068    17.66    0.004
Error       5    0.0585    0.0117
Total       9    0.8858

                                  Individual 95% CIs For Mean
                                  Based on Pooled StDev
shoe temp   N      Mean     StDev  ----------+---------+---------+------
110         2    1.1250    0.1061                      (------*-----)
127         2    0.6200    0.1980        (------*-----)
143         2    0.5450    0.0212     (-----*------)
160         2    1.1600    0.0849                       (------*-----)
173         2    0.5150    0.0212   (-----*------)
                                  ----------+---------+---------+------
Pooled StDev =   0.1082                  0.60      0.90      1.20
```

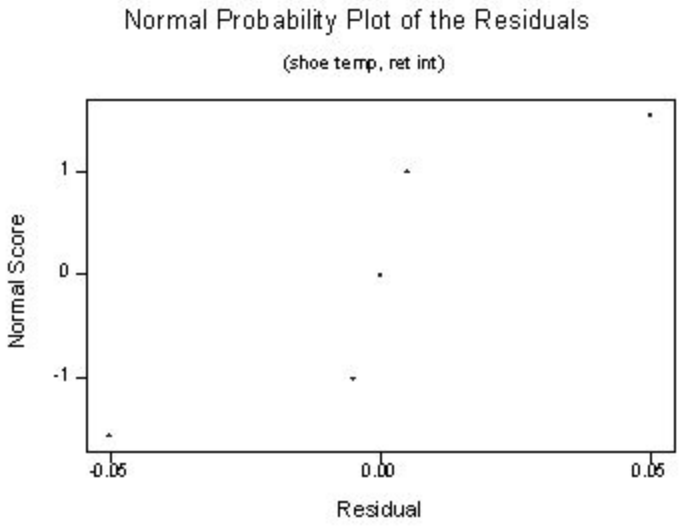

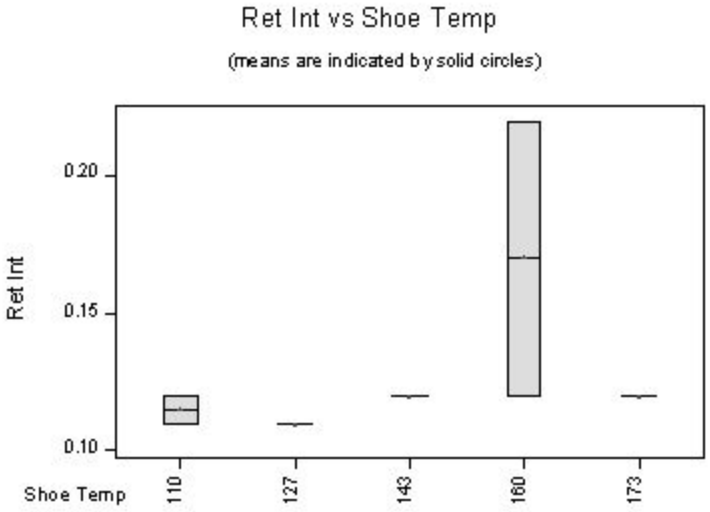


```
Analysis of Variance for Shoe Temp, Ret Int
Source     DF        SS        MS        F        P
Shoe Tem    4   0.00476   0.00119     1.18    0.421
Error       5   0.00505   0.00101
Total       9   0.00981

                                    Individual 95% CIs For Mean
                                    Based on Pooled StDev
shoe temp   N      Mean     StDev  ----------+---------+---------+------
110         2   0.11500   0.00707   (-----------*-----------)
127         2   0.11000   0.00000  (-----------*-----------)
143         2   0.12000   0.00000    (-----------*-----------)
160         2   0.17000   0.07071              (-----------*-----------)
173         2   0.12000   0.00000    (-----------*-----------)
                                    ----------+---------+---------+------
Pooled StDev =  0.03178                 0.100     0.150     0.200
```

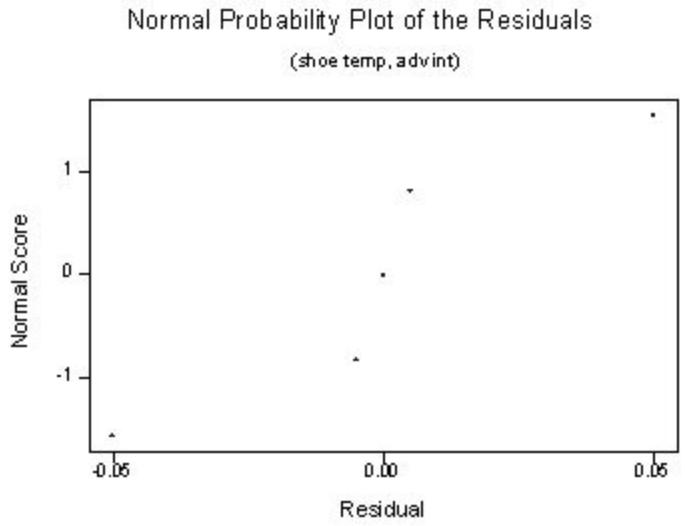

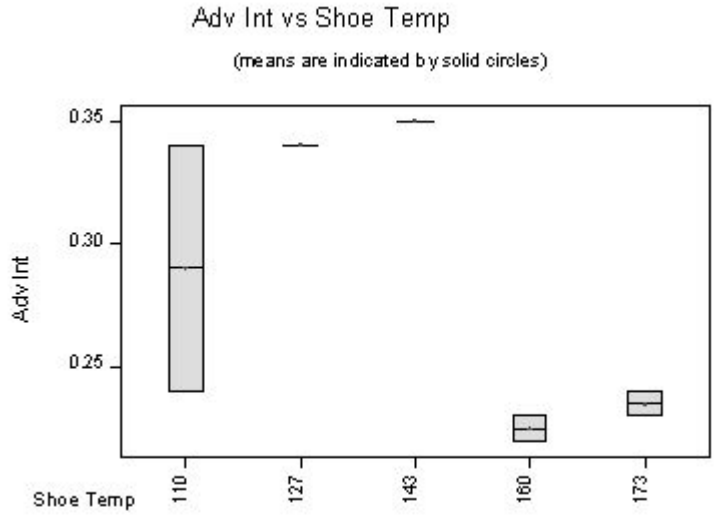


```
Analysis of Variance for Shoe Temp, Adv Int
Source     DF        SS        MS        F        P
Shoe Tem    4   0.02666   0.00667     6.53    0.032
Error       5   0.00510   0.00102
Total       9   0.03176

                                  Individual 95% CIs For Mean
                                  Based on Pooled StDev
shoe temp   N      Mean     StDev  -------+---------+---------+---------
110         2   0.29000   0.07071            (-------*--------)
127         2   0.34000   0.00000                   (--------*-------)
143         2   0.35000   0.00000                     (-------*-------)
160         2   0.22500   0.00707   (-------*-------)
173         2   0.23500   0.00707    (--------*-------)
                                  -------+---------+---------+---------
Pooled StDev =  0.03194               0.210     0.280     0.350
```

Works Cited

1. Stokes, Vijay K. 1989. Joining methods for plastics and plastic composites: An overview. Polymer Engineering and Science 29 (October) : 1310-1318.

2. Bauer, Lori.1990. Joining plastics. Welding Design & Fabrication (April) : 72-75.

3. ASM International. 2000. Reciprocating friction stir welding joins thermoplastics. Advanced Materials & Processes 158 (September) : 27.

4. Nelson, T.W., et al. 2000. Joining of thermoplastics with friction stir welding. Provo, Utah: Brigham Young University.

5. Johns, Clark.1999. *Friction stir welding of polymeric materials*. Brigham Young University: Brigham Young University Press.

6. Sorensen, Carl D., et al. 2001. Joining of thermoplastics with friction stir welding. Provo, Utah: Brigham Young University.

7. Deutscher Verband für Schweissen und Verwandte Verfahren E.V. 1999. Testing of welded joints of thermoplastics plates of tubes: Technological bend test. Düsseldorf, Germany.

8. Menges, G., J. Zohren. 1967. Untersuchungen zum heizelementschweissen von polyolefinen. Der Pastverarbeiter 18 : 165-171

9. Barber, P., J. R. Atkinson. 1972. Some microstructural features of the welds in butt-welded polyethylene and polybutene-1 pipes. Journal of Material Sciences 7 : 1131-1136.

10. Atkinson, J.R., D. R. DeCourcy. 1981. The assessment of fusion joint quality and some evidence for the presence of molecular orientation in butt-fusion welds in polyethylene pipes. Plastics and Rubber Processing and Applications 1 : 287-292.

11. DeCourcy, D. R. PhD. 1976. Thesis. Department of Metallurgy, University of Leeds : University of Leeds Press.